UNIVERSITY OF TURKU

# Exploring the Potential of Machine Learning in Hand Motion Recognition Through Forearm EMG and IMU Data

Master's thesis
University of Turku
Department of Mechanical and Materials Engineering
May 2024
Lukas Martin Zehner
Examiners:
Wallace Moreira Bessa
Salma Salimi

The originality of this thesis has been checked in accordance with the University of Turku quality assurance system using Turnitin Originality Check service.

UNIVERSITY OF TURKU
Department of Mechanical and Materials Engineering

Zehner, Lukas Martin

Exploring the Potential of Machine Learning in Hand Motion Recognition Through Forearm EMG and IMU Data
Master's thesis, 147 pp.
May 2024

---

Machine learning and pattern recognition is an ever-evolving domain where major technological breakthroughs have occurred in recent times. This study aims to research the implementability of an innovative framework for hand motion recognition using forearm EMG and IMU recordings performed on real-life subjects. The literature review focuses on the background of those signals and on the characteristics that must be considered to measure and analyse them. The current status of hand motion recognition and its use within the control industry are also covered. The full process is then detailed, from the presentation of the material to the recording of the hand motions and data obtention. The establishment of models for the classification processes is presented and thorough analysis is performed. The main findings of this research are the great accuracy levels which are obtained as well while using full forearm recordings as measurement limited to the sole wrist area. These findings make it possible to imagine and suggest a future implementation of the technology in the shape of an innovation which could have a significant impact on the way systems are controlled. This research allows the opening of a new scope of study within the motion recognition world and may support future investigations that could result in breakthroughs and have a considerable impact on the relationship that humans have with the always more complex systems that surround them.

All the codes used for the purpose of this thesis and that are detailed throughout this document are available online at: https://github.com/LukasZehner/Exploring-the-Potential-of-ML-in-Hand-Motion-Recognition-Through-Forearm-EMG-and-IMU-Data

Keywords: Machine Learning, Hand Motion Recognition, Electromyogram (EMG), Inertial Measurement Unit (IMU), Human-System Interaction, Classification Models

# Contents

# List of Abbreviations

**AI** Artificial Intelligence

**AR** Auto-regressive coefficients

**CARD** Cardinality

**Ch** Channel

**DAMV** Difference absolute mean value

**DASDV** Difference absolute standard deviation value

**ECG** Electrocardiogram

**EMG** Electromyogram

**EMI** Electromagnetic interference

**ESD** Electrostatic discharge

**fig** figure

**GNB** Gaussian Naive Bayes

**IMU** Inertial Measurement Unit

**kNN** k-Nearest-Neighbours

**MAV** Mean Absolute Value

**MAVS** Mean absolute value slope

**MYOP** Myopulse percentage Rate

**NN** Neural Network

**NN-1** Neural Network with one hidden layer

**NN-2** Neural Network with two hidden layers

**OVO** One-Versus-One Regression

**OVR** One-Versus-Rest Regression

**PGA** Programmable-gain amplifier

**PSD** Power spectral density

**Ref** Reference

**RF** Random Forest

**RMOM** Reduced spectral moment

**RMS** Root Mean Square

**SampEnt** Sample entropy

**SSI** Simple square integral

**tab** table

**VAR** Variance

**WAMP** Wilison Amplitude

**WL** Waveform Length

**ZCR** Zero Crossing Rate

# Legal Background

Before presenting the research work, it is necessary to add a detailed explanation of the legal background which must be considered when working with biosignals and especially when the project involves recording biosignals on human subjects. The main idea of this disclaimer is to allow transparency towards the legal point of view that was considered for this project.

The legal requirements towards a project such as this research considering the Finnish law may consist of two main parts: an ethical review and a data protection impact assessment (DPIA). The following section will detail both of those requirements.

Firstly, an ethical review consists of a full review of the methods and processes used in a research project and must be accepted by the regional medical ethics committee prior to the project: "Prior to the commencement of any research referred to in the Medical Research Act, the research must have been given a favourable statement by the regional medical ethics committee" (*Ethical review in medical research* 2023). Nonetheless, not all studies involving biosignals require such ethical review. Indeed, as mentioned by the legal department and mentioned in the previously provided quote, only "research referred to in the Medial Research Act" require such review. Further, the definition provided by the Medical Research Act is very explicit as to which studies fulfil the needs: "medical research means research involving intervention in the integrity of a person, human embryo or human foetus for the purpose of increasing knowledge of health, the causes, symptoms, diagnosis, treatment and prevention of diseases or the nature of diseases in general" ("Medical Research Act" n.d.).

Based on the definition given by the Medical Research Act mentioned previously. This research does not involve intervention on the integrity of any person, as everything hap-

pens as noninvasive and non-hindering. Additionally, it should be noted that this research does not serve any of the aforementioned purposes. In fact, the goal of the study is to develop a device which does not include an increase in the knowledge of the health condition of the subject nor trying to gain knowledge of any sickness of any kind.

According to the fact that non-medical research that is invasive would still need to be evaluated by the ethics committee, it was further suggested to explicitly mention that the methods used in this research are surface EMG and surface IMU recordings which implies that no puncture, incision, or intrusion within the body occurs. The measuring is based on external sensors which do not enter the body, which means that they are non-invasive.

The conclusion based on those observations is that considering all the previously mentioned information, no ethical review is required, as the definition of medical research does not apply in the case of this study. This conclusion was further supported by the legal department of the University of Turku (legal@utu.fi).

Secondly, the data protection impact assessment (DPIA) is required when personal data is being handled, which is further defined as data including any criteria which allow identifying individuals directly or indirectly (as defined by the legal department of UTU, legal@utu.fi). Hence, applied to this research, it can be mentioned that the recorded EMG and IMU data themselves do not allow direct or indirect identification of any kind for the individual subjects. Hence these signals are not considered to be personal data and do in turn not require a DPIA.

However, it can be mentioned that it was considered to ask subjects for some personal information such as their gender, weight, height or whether they perform any physical activity. Linking the signals with such information would make it personal, increase the

required administrative work considerably and while reducing the possible scopes and implementations of the research. Past research illustrated that the impact of gender, height and weight is minimal on the results (Kim, Mastnik, and André, 2008). Further, it can be questioned how strongly those features are related to each other. In fact, taller people may very likely weigh more than smaller people. In addition to the non-consequent result of past studies, the scale in which this research is carried out would not allow to conclude that any observable difference could be linked to the mentioned features. Indeed, many other factors could have an impact on the quality of the measured data and resulting pattern recognition such as moisture level, temperature, subject's ability to reproduce the motion, electrode placement, etc.

For all these reasons, it was concluded that asking subjects for personal information and making the data personal was not beneficial for the scope of this study. Hence, the data is kept non-personal and there is no requirement for filling a DPIA.

Additionally, all the subjects from which IMU and EMG data was recorded were informed of all of the previously mentioned and discussed elements and have been explained what the scopes and objectives of this study are and how the recorded data will be used.

# 1 Introduction

Controlling increasingly complex mechanisms has always been one of the biggest challenges of humanity. Early examples of control technology trace back to ancient Greece, where gears were used to measure lunar cycles (Edmunds, 2024). The Industrial Revolution marked another breakthrough, introducing control applications for machines like steam engines. James Watt's centrifugal governor in 1788 regulated machine speed (Navathale, Paralkar, and Ghorade, 2017). The spread of electricity and telegrams in the early 19th century initiated electrical control systems, evolving into feedback control theory. The digital revolution in the late 20th century popularised computer-based control systems, leading to widespread automation. The current world is experiencing rapid changes and with the swift evolution of artificial intelligence and virtual reality, it becomes crucial to adapt the way systems and mechanisms can be controlled.

In the recent past, controlling systems and robotic processes from a distance has become a major wish and objective of industrial application and most likely one of the most important technological breakthroughs of the upcoming decade. In fact, such an implementation allowing people to control their surrounding world in a simple and contactless way, without the presence of any hindering and space-consuming hardware would be an advancement comparable to the removal of the physical keyboard on phones in the past decade which was one of the main elements to lead to the worldwide breakthrough and emergence of the smartphone. Indeed, over the past recent decades, the introduction of the technology of tactile or touch-sensitive screens has been a major breakthrough that thoroughly changed the lives of most people. This innovation now plays a constant and omnipresent role in society. It became so natural that its presence is often not even acknowledged. With the rising widespread of augmented and virtual reality, the disappearing of physical screens appears as a challenge. How could these new systems and mechanisms that occur in a non-physical world be controlled? This research aims to

present the adaptability of an EMG/IMU-based application that would allow a new and innovative versatile approach to the control of complex systems.

By measuring biosignals in the forearm area, it might be possible to obtain relevant information which in turn would allow understanding which hand motion is performed by a subject. The idea of this research is hence to measure electrical signals from the forearm and wrist muscles and the acceleration induced by specific motions and use a variety of machine learning algorithms while building different approaches of feature extractions from those signals and obtain clear statements on the possible implementation of such technology within various possible employments.

This study starts by explaining the backgrounds of the application by going through the methods of recognition of hand motions and detailing the nature and methods of acquisition of EMG and IMU signals. After which the methodology of data acquirement used within the research is detailed, followed by the process of the establishment of the proposed framework. The final analysis details the implementability and suggestion of applications based on the obtained results.

# 2 Literature Review

The literature review aims to cover a wide range of topics and provide a deep and thorough understanding of several aspects. The literature review opens with a discussion of approaches that have been used in previous research or introduced within the industrial world to implement hand motion recognition, detailing the main methods currently in use and introducing certain innovations suggested in recent studies. Following this brief summary, the main part of the literature review discusses the two main biosignals which will be used in this study: the EMG and the IMU. Their nature and origin are detailed, describing the entire processes of acquisition suggested in the literature by covering the approaches, possible and usual issues, pre-processing methods and post-processing feature extraction. The main objective is to give a thorough and complete understanding of the needs and requirements that such methods may include and further develop the steps and variations of those methodologies to obtain a global point of view and suggestion of approaches which can then be used in a later stage within this study to obtain own results and optimise the process to try and fulfil the goals and objectives of the project in an adequate manner.

## 2.1 Methods of hand motion capture

Over the past decade, many innovative technologies allowing the remote control of complex systems based on hand motions have been introduced. The main concepts include gesture recognition, motion-sensitive devices, and simple wearable or depth-sensing technologies.

The most commonly implemented technology has been gesture recognition which based on a camera identifies the hand motion performed by the person trying to control the system. Examples of products using this technology are for example smart TVs such as

certain Neo QLED TVs introduced by Samsung in 2022, which allowed motion recognition control, yet only in the USA and in Korea (samsung, 2022). This technology allows the person watching the TV within others to zoom on the screen, enable subtitles, or move the captions by performing pre-defined hand motions while in front of their TV.

Another example of an implementation of gesture recognition-based control is the *Spark* drone first introduced by DJI in 2017 and has constantly been improved since. The main idea of this drone is that it can be controlled using predefined hand gestures which are captured by the camera of the drone (dji, 2024). The possible controls include within other the possibility to take a picture, record a video, ask the drone to follow oneself, or move following the motion of the hand, etc.

Another common approach to controlling the system remotely using hand motions is the motion-sensing device. This method requires the use of an additional device which is used as an emitter of a signal which is in turn captured and analysed to control a system. If this method has the negative aspect of requiring an additional piece of equipment compared to gesture recognition, it has usually proved to be more robust. A very popular implementation of such a technology is the remote-control system for the Nintendo Wii Controllers, where players could mimic a motion while holding the controller in their hand which is in turn used as input signal to control a wide range of actions.

If those methods have shown their implementability and robustness for some, the main issue is the constant requirement hindering components or conditions for the controlling to work. For example, motion-sensitive control devices require the person to hold a remote controller in their hand, while gesture recognition technologies require the person willing to control the system to stand in front of the device to be controlled and so allow the system to capture their motion. All of those issues are still considerable limitations

towards unobstructed remote control.

To improve these methods or find new technologies that would allow the reduce those limitations, many studies focused on hand motion recognition have been conducted. This section summarises the main approaches that are used to recognise hand motion, and how those have been implemented and used within different contexts. It can firstly be mentioned that the main methods in use currently can be summarised within two major categories: methods based on computer vision, and methods based on instrumented gloves (Oudah, Al-Naji, and Chahl, 2020).

The methods based on computer vision are approaches involving a camera which captures visual data of a hand motion, which in turn is recognised through appropriate classification methods (Oudah, Al-Naji, and Chahl, 2020). Many studies have shown the capacities that using simple cameras such as a webcam can already provide when it comes to recognising hand motion.

One of the main issues with this approach is described as the background issue, which occurs when the computer struggles to identify the hand within the environment. This can be partly explained by the fact that the skin colour does not always stand out.

An approach that was suggested to counter the background issue involves the use of a glove coloured in specific and outstanding colours as shown in fig. 2.1a. A colour-sensitive camera is then used to record the hand motion (R. Y. Wang and Popović, 2009). This study then used two of such cameras to obtain a 3D model of the hand, which in turn allowed them to obtain information on the performed motion. If this approach provided a robust and simple way to recognise hand motions, the use of two external cameras and the requirement of wearing a colourful glove makes it not well adapted to the needs of

most sectors.

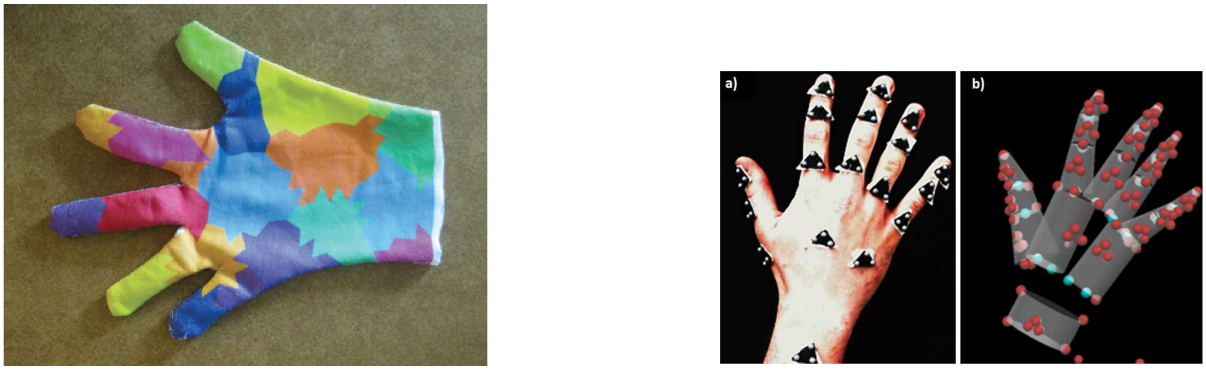


(a) (b)

Figure 2.1: Experimental setup: (a) Coloured glove used for motion recognition (R. Y. Wang and Popović, 2009), (b) Hand motion capture using reflecting markers (Vignais et al., 2013)

A major implementation of a system using computer vision-based motion recognition was made when Microsoft launched the Kinect technology within their Xbox in 2010. A combination of cameras and sensors captures depth and colour information of the motion of the player. This allows it to create a 3D map of the player's body which can in turn be used to control various aspects of games or other implementations. The active range from which a motion could be recognised with satisfying accuracy is from 0.8m to 4.2m (sell). Nonetheless, despite a great launch and rapid sales at first, the Xbox Kinect did not meet any breakthrough and Microsoft stopped manufacturing its technology in 2017 (Lee, 2023). Some explanations were suggested for this failure. The main one was the fact that the abilities of the Kinect technology were limited and difficult to implement. Another element that surely played a role was the additional cost for little added benefit (Lee, 2023). These elements can explain the failure from the marketing point of view.

Another popular implementation of camera-based motion recognition is performed in the cinema industry, especially with the emergence of 3D and computer-animated movies,

or additional platforms (Wendong and Changjun Wang, 2021). It became important to attach real motion to characters generated artificially. This could be performed by analysing the motion of real actors. This method is not directly based on motion recognition from computer vision, but rather on the capture of visual sensors which stand out from the rest of the image and are hence easy to recognise for the computer. This technology has proven to be very robust and has hence become one of the major approaches (Wendong and Changjun Wang, 2021). A great illustration of such a process is provided in fig. 2.1b (Vignais et al., 2013). In that research, several reflective markers were set on the hands of the subjects to in turn obtain information on the occurring motion and allow additional analysis of the data (Vignais et al., 2013). This approach shows great robustness and accuracy when it comes to capturing hand motions. However, the implementation of such a method requires considerable hardware and preparation. Hence, it can be concluded that no simple and light use of this technology could be made for other utilisation which would require the system to be discrete and non-hindering for the wearer.

Despite its robustness, it can be questioned how well-suited a system based on external vision can be used within the industrial world as well as within society. The breakthrough of the smartphone using fingers as the main control scheme is the perfect illustration that systems relying on simple control methods have a great chance of success compared to systems requiring external sensors.

## 2.2 Background on EMG and IMU

The two types of signals which will be used throughout this research are EMG (Electromyogram) and IMU (Inertial Measurement Unit). The first part of this literature review aims to provide detailed information on both of these signal types.

**EMG**

An EMG signal, short for electromyogram signal, is an electrical biosignal generated by neuromuscular activity (Rangayyan, 2015). To understand the background of this biosignal, it is necessary to acknowledge the functioning process of muscles. Muscles are made out of a large number of muscle units. Muscle units (MU) are the smallest segment of the muscle that can be activated by intentional effort. These MU are made of three main parts: the motor neuron, the axons, and the muscle fibres. The information which the muscle must follow is provided by the motor neuron. This signal is then transferred through the axons towards the muscle fibres which then contract according to the received instruction. Each motor unit generates a contraction. A contraction of a single motor unit is known as a single-motor-unit action potential (SMUAP). When a muscle enters into action, a vast amount of its single motor unit contracts simultaneously. The resulting electrical signal is the summation of the single-motor-unit action potentials.

**IMU**

Inertial Measurement Unit (IMU), is a system of sensors very popular for several applications especially in navigation and in motion tracking. This technology is based on inertial sensors and is commonly composed of an accelerometer and a gyroscope (Zhao, 2018). Certain more advanced IMU sensor systems can further be expanded by additional sensors such as magnetometer and altimeter (Zhao, 2018).

The main purpose behind an IMU is to obtain 6-axis information on the motion of a system performing a certain motion. The accelerometer records the acceleration of the system on a 3 dimensional basis. Further speed and position of the system of interest can be obtained following known relations between acceleration, speed and position. Theses relations are given in eq. (2.1). Further, angular velocity sensors allow to have information on the angular velocity of the system on a further 3 dimensional basis. The combination

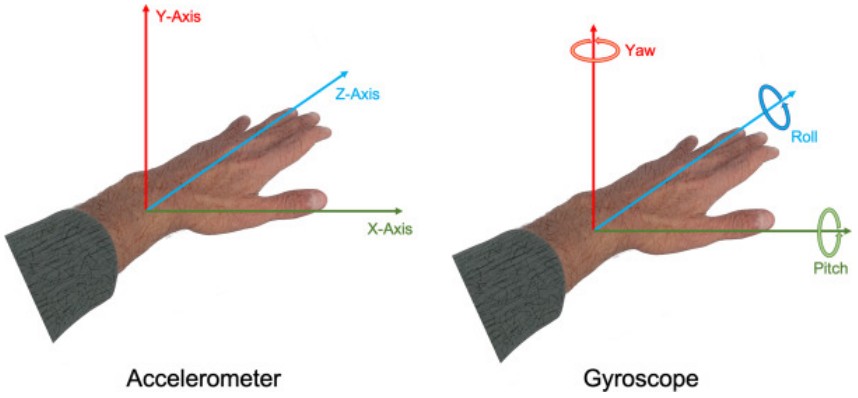


Figure 2.2: Illustration of the function of a 6-axis IMU sensoring for hand motions (Constant et al., 2021)

of both measuring devices allow obtaining a 6-axis model of the system.

$$\begin{bmatrix} x \\ y \\ z \end{bmatrix} = \int \begin{bmatrix} v_x \\ v_y \\ v_z \end{bmatrix} dt = \iint \begin{bmatrix} a_x \\ a_y \\ a_z \end{bmatrix} dt^2 \tag{2.1}$$

IMUs are usually utilised in systems including moving vehicles or objects as they allow obtaining precise information on the trajectory followed by such. However, growing interest in the use of IMU in the medical domain and especially in the sector of telemedicine can be observed (Constant et al., 2021). Such systems would require recording of live (bio-)signals to obtain information on health status or activity. In fact, IMU recording devices are commonly found in systems such as smartwatches or other devices worn at the wrist which aim to record body motions (Constant et al., 2021). An illustration of the 6 IMU axis for hand motions is provided in fig. 2.2.

## 2.3 EMG signal acquisition

This section initially aims to describe the two main methods to detect EMG signals and understand which method may be the best suited for the purpose of this research. Subse-

quently, the general method of EMG data recording will be expanded through additional necessary methods including pre-processing, segmentation and feature extraction.

### 2.3.1 Overview of the general process of EMG recording

The general process which is followed to work with EMG data acquisition and further utilisation within classifier applications is given in fig. 2.3. To give an overview a brief summary can first be given. At the beginning of the process, the input is the motion of the arm which induces an electrical signal labelled as EMG signal which, captured by an electrical sensor, results in a raw electrical signal. This electrical signal must then be segmented to obtain the information of a single and specific motion and then pre-processed adequately. These steps allow the raw signal to become easier to read and understand for the next steps of the process. These can be compared to the polishing of a stone after its excavation from a mine, allowing it to be smoother and easier to appreciate. Once the segmentation and pre-processing are performed, elevant features are extracted from the processed signal and stored in a data dictionary for use in the classification process. In the following subsections, these steps are detailed, their exact usability and functions are explained and the possible upcoming challenges are elaborated.

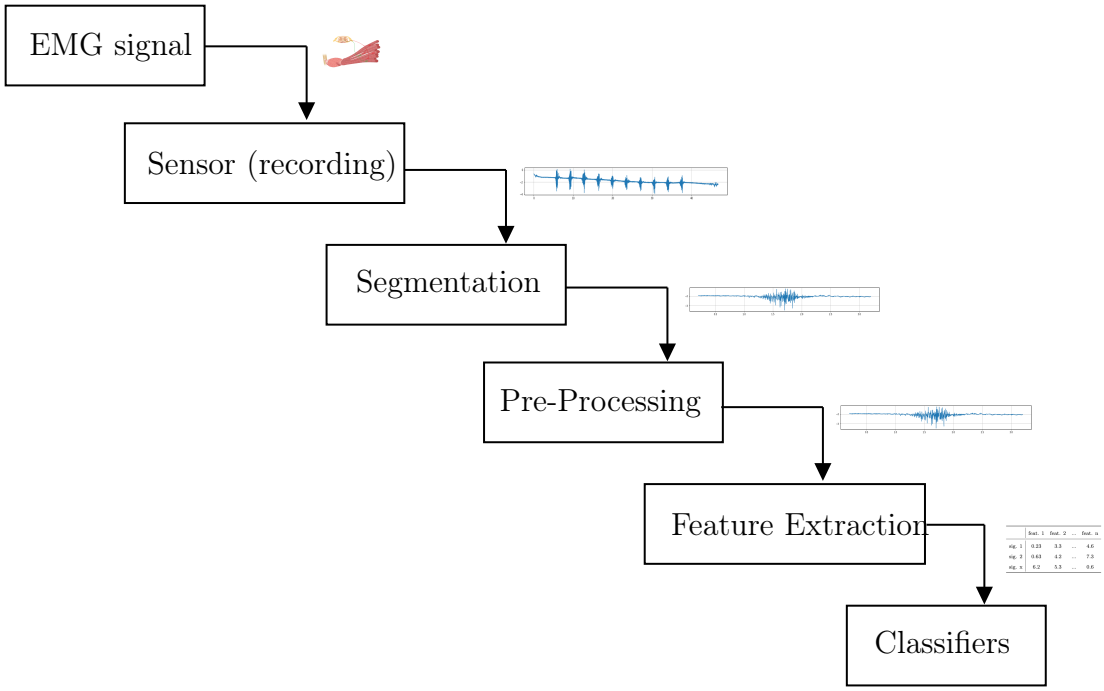


Figure 2.3: General process of acquisition of EMG signals (adapted from Parajuli et al., 2019, Bangaru, Chao Wang, and Aghazadeh, 2022 and Shoemaker, 2016)

### 2.3.2 EMG detection approaches

A first method used to record EMG is the use of intramuscular electrodes. This process is also known as intramuscular EMG recording (iEMG). This is an invasive recording approach that uses needle electrodes to record EMG signals. This method of detection is usually described as very beneficial for neurophysiologists to diagnose diseases as it allows a very precise and incisive insight into the EMG signals generated by the muscle (Chan et al., 2021).

In fact, the iEMG approach has several advantages such as fast recording of the EMG signal of an individual SMUAP, and clearer recorded signals with a usually better signal-to-noise ratio (Chan et al., 2021). For these reasons, the intramuscular method is especially beneficial and well-adapted to situations in which the objective is to identify disorders within precise and specific muscle areas. Nonetheless, despite these positive

points, iEMG has several down points. In addition to requiring complex installation due to the invasive nature of the method, the collected signals are focused on the specified muscle area and hence only target selected motor units which is not as well suited for a wider analysis of muscle activity (Chan et al., 2021). In fact, in order to obtain simultaneous information on various muscle units when the overall EMG of a muscle is of interest, the number of needle electrodes must be enhanced (Chan et al., 2021).

Another widely used method to record EMG signals, also known as surface EMG (sEMG), consists of recording muscle activity from electrodes set on the skin. This method has the benefit of being non-invasive and simple to implement, based on the principle of electrolytic conduction to sense and record the electrical signal generated by muscular activity (Chan et al., 2021). The electrodes used to record sEMG are usually silver-silver chloride (Ag-AgCl) electrodes (Jamal, 2012). To further reduce the occurring resistance between the electrodes and the skin and ensure swift and more reliable data collection, a gel consisting of an electrically conducting substance is applied (Chan et al., 2021).

The main benefit of the surface EMG is its non-invasive approach. This makes this method very easy to implement and further straightforward to use (Chan et al., 2021). It can additionally be mentioned that from the point of view of the patient, the surface approach provides considerably more comfort. Nonetheless, it has been mentioned that surface EMG is usually limited to the research environment (Felici and Del Vecchio, 2020). This is mainly because sEMG is harder to calibrate on single muscle units and hence usually of less interest for medical and clinical purposes (Felici and Del Vecchio, 2020). Despite this eventual inaccuracy, surface EMG is especially well suited for sport and activity monitoring and research. Its non-invasive approach allows for a wider area in which muscle activity can be observed simultaneously while allowing the subject to

behave in a normal and comfortable way. It can further be mentioned that surface EMG is usually more cost-effective than intramuscular needle electrodes (Felici and Del Vecchio, 2020).

To conclude, for the purpose of this study, the use of the surface EMG recording method appears to be better suited than intramuscular EMG recording. Indeed, the objective is to obtain information on the activation of several muscles and hence a vast number of single motor units over the forearm. While further emphasising the will to be non-hindering for the subjects which hence requires a non-invasive approach.

### 2.3.3 Possible issues and interferences occuring during EMG recordings

Detailed information on the two main existing ways to acquire EMG signals: intramuscular and surface EMG were obtained and detailed previously. It became clear that the surface EMG method is better suited for the purpose of this research. However, simply sensing data will not allow or ensure that the data will be readable due to various factors which may hinder the signal. Indeed, various research has shown that EMG signals are in most cases very fuzzy and noisy signals (Kim, Mastnik, and André, 2008 Parajuli et al., 2019). A wide range of interferences may occur througout the process of signal recording when measuring EMG signals.

#### Noise

The most common cause for unclean signals is noise, which can be arise from various causes such as electromagnetic radiations, motion artefacts of the electrodes and the cables, noise coming from the equipment, or the simple interaction with the different tissues (Kim, Mastnik, and André, 2008). And further through the instability and constant variation of the signal of interest (Parajuli et al., 2019). Therefore, the first step of most

research always consisted of using pre-processing techniques which aim to reduce the impact of the noise on the data and obtain a clearer and more intelligible signal.

The impact of noise on a signal can be described through the signal-to-noise ratio (SNR) of the signal. The SNR represents a ratio between the strength of the signal of interest towards the strength of the unwanted noise (Nadipally, 2019). It is a powerful tool to describe and understand the clarity of the signal, higher SNR values link to clearer and better understandable signals. A clear mathematical definition of the SNR was suggested in a study (Yuan et al., 2019). This definition can be adapted by defining two signals: $s_{ideal}$, the signal as it would be without noise, and $s_{real}$, the signal as it is measured with the impact of the noise. The noise signal $n$ can then be defined as $n = s_{real} - s_{ideal}$. By using the understanding derived from another study (Dicker, 2014), describing the SNR as the ratio between the variance of the ideal signal to the noise signal, the SNR can be defined as done in eq. (2.2) (Yuan et al., 2019). With this definition, the exact understanding of the role of the signal-to-noise ratio becomes clearer.

$$SNR = \frac{s_{ideal}}{n} \tag{2.2}$$

An equivalence to the previously given definition was suggested in a further study, using the power of both signals (González-Mendoza et al., 2018). Hence leading to the corresponding definition given in eq. (2.3).

$$SNR = 10 \cdot \log \frac{P(s_{ideal})}{P(n)} \tag{2.3}$$

### Baseline drift

Another issue that can commonly occur when recording biosignals including surface electrodes, as is the case when recording sEMG is the so-called phenomenon of baseline drift. This occurrence can be characterised as an inaccuracy or shifting from the actual value (Malwade et al., 2013). Several factors can lead to such baseline drift. Firstly, environmental factors such as temperature, moisture level or external interferences which vary between the calibration of the instruments and the recording or throughout the recording process can have an impact on the recording, when conditions in which a signal is being measured (Grover and Lall, 2020). Secondly, equipment issues, also known as equipment drift, can have an influence and is explainable through the ageing of the devices which can further accumulate a deposition of unwanted material on the sensing edge and hence hinder the precision of the device (Grover and Lall, 2020). And lastly, physiological changes can have an impact on the resulting measured signals (Grover and Lall, 2020). Such factors could, for example, be biological variations such as respiration or simple alteration in the position of the electrodes over the course of the experiment (Samuel et al., 2019). Overall, it can be mentioned that baseline-drift usually occurs in low frequencies (Samuel et al., 2019).

### Power-line interferences

A further common issue that has been observed in the process of measuring biosignals such as EMG signals is the concept of power-line interference. Powerline interference can be summarised as a type of noise which may arise in an environment where within other electrical disturbances occur (Sörnmo and Laguna, 2005). In fact, as mentioned previously, the human body is rich in such electrical signals which emerge within others around the various muscle activities which constantly happen amidst the body (Sörnmo and Laguna, 2005). Further electrical disturbances can also occur during the measuring

process, such as instrumentation noise (Sörnmo and Laguna, 2005). Those impeding electrical signals generate a noise which has been labelled as power-line interferences. This noise has the specificity to usually occur around a frequency of 50Hz to 60Hz (Sörnmo and Laguna, 2005).

**Aliasing**

Aliasing is an issue which occurs when the sampling frequency is not chosen adequately with the signal that is to be measured. If this phenomenon cannot be labelled as an interference, it is however crucial to consider this occurrence when working with signal recording as shown in a previous study (Samuel et al., 2019). A more detailed understanding of aliasing can be obtained when considering a simple example. Consider a study which would have as objective to record a simple ideal sinusoidal signal. Then, an adequate way to sample this signal could be performed as shown in fig. 2.4 (a). On the other hand, if the sampling frequency were chosen differently, then another sinusoidal may seem to fit the recorded values as shown in fig. 2.4 (b). Hence, the obtained signal has a new frequency. This phenomenon can be described as the aliasing of the original frequency (Hasegawa-Johnson, 2021). To avoid such aliasing, it is usual to follow the Nyquist theorem, which states that the highest frequency of the measured signal that can accurately be recorded is half of the sample frequency $f_S$ (Hasegawa-Johnson, 2021). This highest measurable frequency is known as Nyquist frequency $f_N$ and is further defined in eq. (2.4).

$$f_N = \frac{f_S}{2} \tag{2.4}$$

Additionally, further study mentioned that aliasing usually occurs in environments in which there is a considerable number of high-frequency signals within the recorded data

(a) Well sampled signal

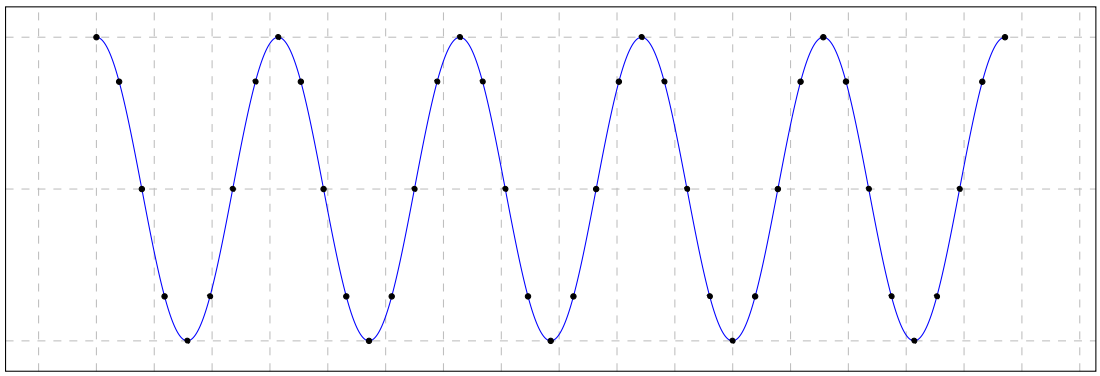

(b) Aliasing

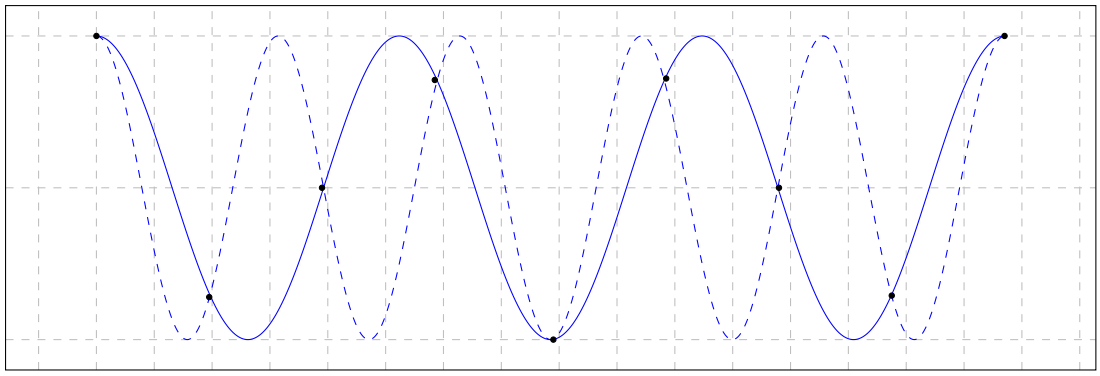

Figure 2.4: Example of aliasing which can occur due to undersampling, based on understanding from Hasegawa-Johnson, 2021

(Samuel et al., 2019). This can be understood through the fact that with higher frequencies within the flow of signals, the chance that the Nyquist theorem may be disregarded increases. Indeed, it becomes more likely that some recorded frequencies surpass half of the sample frequency. Following this observation, it was suggested that a high-frequency cutoff filter may be used as to filtrate those high frequencies and lower the impact of possibly occurring aliasing (Samuel et al., 2019).

### 2.3.4 EMG pre-processing and filtering

According to the understanding obtained on the many issues that may occur during the recording of EMG data, it becomes clear that certain measures must be considered. Indeed, to enhance the quality of the recorded EMG data, it becomes crucial to increase the

SNR and reduce the impact of any other factor hindering the quality and intelligibility of the signal of interest (Parajuli et al., 2019).

Firstly, certain measures can already be taken into account during the recording of the EMG data. In fact, the fixating of the surface electrodes can be optimised to reduce the issue of powerline interferences occurring due to instrumentation noise caused by unwell-attached electrodes (Sörnmo and Laguna, 2005). Further study also suggested to include an electromagnetic shield within the recording environment (Samuel et al., 2019). Such a mechanism would help reduce the influence and impact of possible external electromagnetic radiation which in turn would enable reducing the occurring noise and enhancing the quality of the recorded signal (Parajuli et al., 2019). However, such a system may prove to be challenging in terms of manageability and add great complexity to the whole recording process, while no clear result on the actual benefit was mentioned (Parajuli et al., 2019 & Samuel et al., 2019).

**Bandpass filter**

Therefore, to fulfil this objective, past research on EMG signals supports the use of filtering processes as a following step to the data recording of the data, known as pre-processing. Many previous studies in the recording of EMG signals agree on the idea of suggesting the use of band-pass filters (Simao et al., 2019 & Samuel et al., 2019 & Yuan et al., 2019). Band-pass filters consist of a frequency-based filtering method which includes a low-pass and a high-pass filter. The concept of such frequency-based filters can be understood as systems or algorithms that block or reduce signals within certain range frequencies. In fact, a low-pass filter allows signals below a specified cutoff frequency to pass through, reducing frequencies above this cutoff. A high-pass filter works analogously, allowing frequencies above its cutoff frequency to pass through, blocking frequencies below the defined

cutoff. Consequently, a band-pass filter consisting of a low-pass and a high-pass filter has two cutoff frequencies and allows only a band of frequencies between both of those cutoff frequencies to pass and blocks any frequencies outside of the scope defined by those two cutoff frequencies (Bretherton, 2014).

The reason why such band-pass filtering is useful when it comes to increasing the SNR can be explained by the fact that the high-frequency noise can be reduced (Samuel et al., 2019). Additionally, as mentioned previously, a past study has revealed that aliasing is more likely to occur when high-frequency signals are present within the data. Hence, the use of this high-frequency cutoff filter also helps prevent aliasing from occurring (Samuel et al., 2019). Further, findings have illustrated that the low-pass filter is often enough to eliminate the unwanted impact of baseline drift which usually occurs in a low-frequency environment (Samuel et al., 2019).

It has been shown that EMG frequencies containing information of interest usually range from 20Hz to 500Hz (González-Mendoza et al., 2018). Hence it can be expected that the frequencies outside of this scope are not relevant to the study of EMG. Consequently, the bandpass filter cutoff frequencies may be chosen according to the suggested range.

Several studies working with EMG signals have supported the idea of using a bandpass filter and illustrated its effectiveness (Afsharipour et al., 2016 & Niegowski et al., 2015 & Phinyomark et al., 2014 & Botter and Vieira, 2015 & Giannini et al., 2020). In fact, a summary of the found studies that used such a bandpass filter as a pre-processing method in a process of EMG recording is shown in table 2.1 in which the low-cutoff frequency, the high-cutoff frequency and the sampling frequency are provided if mentioned by the corresponding author.

| Author | Low-cutoff | High-cutoff | Sampling frequency |
|---|---|---|---|
| Afsharipour et al., 2016 | 10Hz | 750Hz | 2048Hz |
| Niegowski et al., 2015 | 10Hz | 500Hz | 2048Hz |
| Botter and Vieira, 2015 | 10Hz | 500Hz | 2048Hz |
| Phinyomark et al., 2014 | 20Hz | 500Hz | 1024Hz |
| Giannini et al., 2020 | 20Hz | 250Hz | n/a |
| Yuan et al., 2019 | 30Hz | n/a | n/a |

Table 2.1: Summary of some cutoff frequencies used for the bandpass filtering in past EMG related research.

This summary shows that most of the previous research working with a band-pass filter in the context of EMG recording used a low cutoff of around 10Hz and a high cutoff of around 500Hz. In addition to this observation, previous literature research on EMG pre-processing concluded that the low-frequency cutoff should range between 5Hz to 20Hz, and that the high-frequency cutoff should range between 20Hz to 450Hz (Samuel et al., 2019). However, they further mentioned that the exact value of the used cutoff frequencies should be chosen to fit with the precise condition in which the data collection occurred. In other words, the filtering should be adapted to the level of interferences occurring within the recorded signal in such a way as to obtain an adequate level of intelligibility and allow further analysis of the obtained data.

### Notch filter

In addition to the previously mentioned band-pass filtering, an additional frequency-based filter is usually used to lower the influence of the power-line interferences (Samuel et al., 2019). This is a notch filter. Notch filters are filters that can be understood as a blocking

| Author | Cutoff | Sampling frequency |
|---|---|---|
| Phinyomark et al., 2014 | 50Hz | 1024Hz |
| Giannini et al., 2020 | 50Hz | n/a |
| Niegowski et al., 2015 | 50-60Hz | 2048Hz |
| Samuel et al., 2019 | 50-60Hz | n/a |

Table 2.2: Summary of some cutoff frequencies used for the notch filtering in past EMG related research.

filter which filters out a very narrow band of frequencies (Liu and Blaabjerg, 2021). It is usually used to reduce the impact of frequency-specific interferences, which is why it appears to be especially effective when lowering the influence of the power-line interferences occurring during the recording of EMG signals (Samuel et al., 2019).

To understand which cutoff frequency is of interest for the notch filtering, several previous research linked to the recording of EMG which used such a notch filter and mentioned the utilised cutoff frequency were identified and are summarised in table 2.2. Following this observation, it becomes obvious that the notch cutoff is usually set around 50Hz. A similar conclusion was also found by a previous literature research on EMG preprocessing which concluded that the notch cutoff is usually around 50Hz to 60Hz (Samuel et al., 2019). It can further be mentioned that such a notch frequency is in adequation with the previously mentioned frequency at which the power-line interferences usually occuring between 50Hz to 60Hz (Sörnmo and Laguna, 2005).

**Other suggestions**

In addition to using a bandpass filter and a notch filter, some studies also included further kinds of filtering approaches in their process of EMG data acquisition. In fact, methods

such as independent component analysis (ICA) and common spatial pattern (CSP) were suggested as possible ways to filter EMG data (Parajuli et al., 2019). Independent component analysis (ICA) is a method which makes it possible to separate a signal of mixed frequencies into its different signals of origins (Calabrese, 2019). This method is hence no filtering, but rather a signal analysis method which can be useful to understand the patterns of a signal made up of a range of sub-signals. Common spatial pattern (CSP) is an algorithmic method which enables finding patterns within multichannel signals and is usually used for EEG applications (W. Wu et al., 2014). EEG (Electroencephalography) is the recording of electrical biosignals occurring due to brain activity. However, the study which mentioned using ICA and CSP as preprocessing methods for the process of EMG recording did not specify additional details or parameters used for those filters and further, no clear outcome or analysis was provided (Parajuli et al., 2019). Nonetheless, a further study suggested that CSP could be implemented into a process of multi-channel EMG recordings as a method that would improve the consistency and reliability of the resulting measured signals, especially in environments in which the muscle force would vary (Li et al., 2017).

To conclude, filtering methods must be considered and implemented to increase the SNR and the intelligibility of the recorded signal. The main filters would consist of a bandpass filter with cutoffs around 10Hz and 500Hz and a notch filter with a cutoff around 50Hz (**??** & table 2.2). Nonetheless, the cutoff frequencies should be adapted to the circumstances of recording and tuned to fit best with the context. Further, additional filters can be added to fit the needs and requirements of the research.

### 2.3.5 EMG signal segmentation

Following the filtering of the EMG signal, the influence of possible noise and non-desired interferences would be reduced. The next objective is to extract features from this cleansed data, on which a later pattern recognition model would be based to classify the data back to the original motion. However, this pre-processed EMG signal would generally not be considered as a relevant input for the feature extraction due to the randomness of its nature (Parajuli et al., 2019). In fact, irrelevant and non-informative segments were also captured during the data measuring. For example, it is likely that a time delay was recorded between the start of the measuring process and the start of the actual motion. Such delays are random non-controllable elements which are not relevant and would have a significant impact on the features if not taken into account. Indeed, for the example of a time delay prior to the motion, the mean value of the signal would vary considerably depending on the duration of this delay. For this purpose, it is imperative to segment the data and isolate the information-carrying sections of the signal (Samuel et al., 2019).

The segmentation method usually used to isolate the relevant sections of the signal is the adjacent segmentation approach (Parajuli et al., 2019). This procedure usually uses a pre-defined length of consecutive window segments (Samuel et al., 2019). An illustration of this method is given in fig. 2.5 (a). In this illustration, the adjacent consecutive segments can clearly be observed. The relevant sections are obtained and can be isolated to then extract the features based solely on the EMG-relevant segments.

A further suggestion to perform data segmentation with the idea of isolating relevant sections was further suggested as a process based on the amplitude of the EMG signals which would recognise the relevant segments (Simao et al., 2019). This method uses an amplitude threshold to establish the start and end of the informative sections of the signal. This approach also provided great results (Simao et al., 2019).

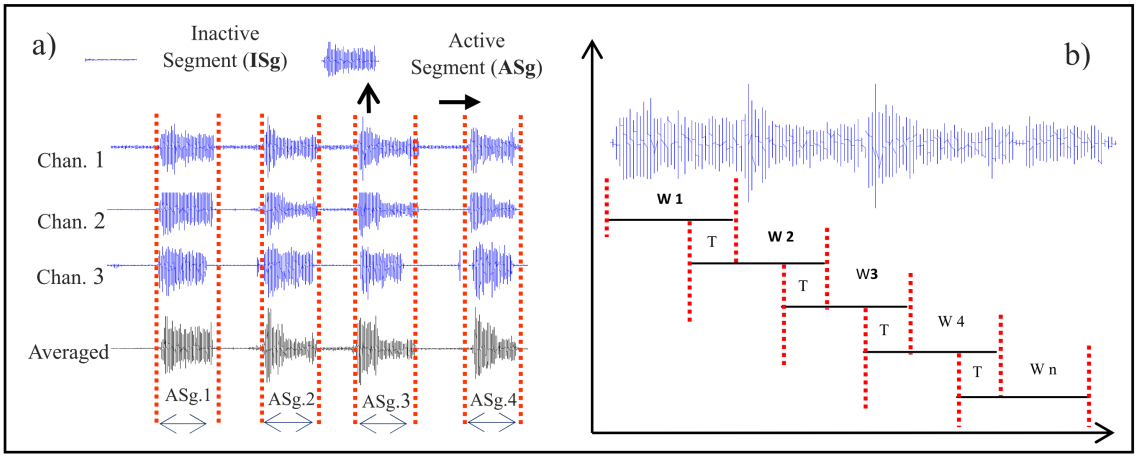


Figure 2.5: Illustration of the segmentation of EMG signal from randomly selected channels during a hand close task (Samuel et al., 2019)

Furthermore, an additional reason to consider segmentation is the computing capacity of the system when the overall process is performed in real time. In fact, it may prove unadapted if the processor had to consider the entire time signal that has been recorded, which leads to a great number of data being handled simultaneously. Indeed, previous study has shown a certain delay between the motion and the recognition of the motion by the system (Samuel et al., 2019). This is especially an issue when the controller is expected to make decisions fast, such as in the case of prosthesis control (Samuel et al., 2019). To reduce this phenomenon, another type of segmentation known as overlapping segmentation can be implemented. This method makes use of the idle time to optimise full utilisation of the resource available within the processor. The obtained windows of segments are hence overlapping with each other by an increment time which is shorter than the window length (Samuel et al., 2019). This process is illustrated in fig. 2.5 (b).

For overlapping segmentation, the size of the set windows is very relevant as it determines the amount of EMG data being considered simultaneously by the model of pattern recognition (Samuel et al., 2019). Indeed, larger windows would mean that more data

would be handled which may lead to more accurate results. Nonetheless, it is crucial to consider the occurring delay due to computing speed. Hence, it is suggested to optimise the window length based on the maximal computing capacity of the system so as to keep an optimised stream of data in real-time implementation (Samuel et al., 2019). A first example of an optimal window length was given as ranging from 150ms to 250ms by research in the context of EMG recordings in post-amputation circumstances (Smith et al., 2010). Another research related to the study of myoelectric signals suggests a window length of 250ms (Englehart and Hudgins, 2003). Nonetheless, the window length may highly vary on the computing capacity of the system and must be optimised to fit with the exact needs of the application (Samuel et al., 2019).

To conclude, two main types of segmentation can be implemented. Adjacent segmentation will ensure that the data considered for feature extraction is made out of the informative and relevant segments. And further, the second type of segmentation, overlapping segmentation, can be implemented to ensure a more reliable and robust overall system, especially if the process performs in real-time conditions (Samuel et al., 2019).

### 2.3.6 EMG feature extraction

Following the signal pre-processing and segmentation, relevant features must be extracted from the data. These features will in a further step serve as the input for the pattern recognition algorithms which will classify the provided data back to the original motion from which the data was created. Several past studies were involved in the process of feature extraction of EMG signals. As in any other kind of application, those features can be divided into three main categories: time-domain features, frequency-domain features, and time-frequency-domain features. The features from the time domain are based on the simple signal as such, observed as a time signal. The features from the frequency domain

will consider the signal as transformed to the frequency domain. Several methods can be used to observe a signal from the frequency domain as the Fourier transform, or more usually in such applications, the fast Fourier transform (FFT) (Kim, Mastnik, and André, 2008). Analysing a signal within the frequency gives additional information on the signal features. In fact, a signal such as the EMG signal is made of a wide band of sub-signals which may all have different frequencies and hence an evaluation of features obtained from those various frequency bands may be of interest. And lastly, the time-frequency domain will consider features that take into account both the time and the frequency domains. The following sections will detail the use of those domains in past studies.

### Time Domain features

The first domain from which features could be extracted is the time domain. The time domain features that were obtained from EMG signals in past studies are summarised in table 2.3. A total of 22 different time features could be found in the analysed literature and are shown in the table. The features are ordered from the most used to the least used. In the following segments, the main features from the time domain will be detailed to provide a deeper understanding of those.

**MAV :** Usually described as the most popular and one of the most information-carrying features of EMG, the mean absolute value (MAV) describes the mean of the absolute value of the signal (Chan et al., 2021). The MAV is defined in eq. (2.5) (Chan et al., 2021).

$$MAV = \frac{1}{N}\sum_{t=1}^{N}|x(t)| \tag{2.5}$$

| **Time domain features** | [1] | [2] | [3] | [4] | [5] | [6] | [7] | [8] |
|---|---|---|---|---|---|---|---|---|
| Mean absolute value (MAV) | X | X | X | X | X | X | X | X |
| Waveform length (WL) | X | X | | | X | X | X | X |
| Root mean square (RMS) | X | | X | | X | X | | X |
| Zero crossing rate (ZCR) | X | X | X | | | | X | |
| Willison amplitude (WAMP) | | X | | | X | | X | X |
| Slope sign change | X | X | | | | | X | |
| Variance (VAR) | | | X | | | | | X |
| Maximum & minimum values | | | X | X | | | | |
| Standard deviation | | | | X | | | | |
| Difference absolute mean value (DAMV) | | | | | | | | X |
| Difference absolute standard deviation value (DASDV) | | | | | | | | X |
| Simple square integral (SSI) | | | | | | | | X |
| Myopulse percentage Rate (MYOP) | | | | | | | | X |
| Sample entropy (SampEnt) | | | | | | | X | |
| Reduced spectral moment (RMOM) | | | | | | | X | |
| Irregularity factor | | | | | | | X | |
| Sparseness | | | | | | | X | |
| Cepstral Coefficients | | | | | | | X | |
| Signal length | | | | | | X | | |
| Auto-regressive coefficients (AR) | | | | | X | | | |
| Cardinality (CARD) | | X | | | | | | |
| Mean absolute value slope (MAVS) | X | | | | | | | |

Table 2.3: Summary of various **time domain features** used in previous research in context of pattern recognition related to EMG signal recordings.

Used articles: [1] : Parajuli et al., 2019 ; [2] : Mendez et al., 2017 ; [3] : Kim, Mastnik, and André, 2008 ; [4] : Bangaru, Chao Wang, and Aghazadeh, 2022 ; [5] : Simao et al., 2019 ; [6] : Chan et al., 2021 ; [7] : Samuel et al., 2019 ; [8] : Phinyomark et al., 2014

**WL :** The waveform length describes the cumulative length of the EMG wave and is defined in eq. (2.6) (Chan et al., 2021).

$$WL = \sum_{t=1}^{N-1} |x(t+1) - x(t)| \tag{2.6}$$

**RMS :** The root-mean square (RMS) quantifies the overall magnitude of the data while considering the squares of the value. In EMG studies, it is usually used to obtain information on the muscle force and observe levels of fatigue (Chan et al., 2021). The definition of the RMS is given in eq. (2.7) (Phinyomark et al., 2014).

$$RMS = \sqrt{\frac{1}{N} \sum_{t=1}^{N} x(t)^2} \tag{2.7}$$

**ZCR :** The zero-crossing rate describes the number of times the signal crosses the zero-axis within the signal length (Torres-Garcıa et al., 2022). It can be otbained by counting how many times both following conditions given in eq. (2.8) and eq. (2.9). In real applications, the ZCR is usually defined using a threshold $\epsilon$ to avoid overcounting noise, as shown in eq. (2.9) (Torres-Garcıa et al., 2022).

$$\{x(t) < 0 \text{ and } x(t+1) > 0\} \text{ or } \{x(t) < 0 \text{ and } x(t+1) > 0\} \tag{2.8}$$

$$|x(t) - x(t+1)| \geq \epsilon \tag{2.9}$$

**WAMP :** The Willison amplitude is a feature that describes a measure of the changes within the signal and is obtained by establishing the number of times that the difference of two consecutive points exceeds a certain threshold (Xi et al., 2017). The WAMP is defined in eq. (2.10) (Phinyomark et al., 2014).

$$WAMP = \sum_{t=1}^{N-1} [f(|x(t+1) - x(t)|)]$$
$$\text{with : } f(a) = \begin{cases} 1, \text{ if } a > \epsilon \\ 0, \text{ otherwise} \end{cases} \tag{2.10}$$

**Slope Sign Changes :** The slope sign changes feature is a count of the number of times that the sign of the slope of the EMG signal changes (Torres-Garcıa et al., 2022). The slope sign changes feature increases by one every time that both conditions defined in eq. (2.11) and eq. (2.12) are fulfilled (Torres-Garcıa et al., 2022). The threshold $\epsilon$ was also introduced to avoid capturing sign changes due to noise interferences.

$$([x(t) > x(t-1) \text{ and } x(t) > x(t+1)] \text{ or } [x(t) < x(t-1) \text{ and } x(t) < x(t+1)]) \tag{2.11}$$

$$(|x(t) - x(t+1)| \geq \epsilon \text{ or } |x(t) - x(t-1)| \leq \epsilon) \tag{2.12}$$

**VAR :** The variance (VAR) is described as the measure of the average power of the signal (Xi et al., 2017). It is defined in eq. (2.13) (Phinyomark et al., 2014).

$$VAR = \frac{1}{N-1}\sum_{t=1}^{N} x(t)^2 \tag{2.13}$$

**Minimum and Maximum :** The minimum and maximum values feature simply represent the highest and lowest value contained in the EMG signal (Bangaru, Chao Wang, and Aghazadeh, 2022).

### Frequency-Domain features

The second kind of features that can be extracted from the signal are features from the frequency domain. To be able to obtain those features, the signal must first be transformed into a frequency signal which is performed using Fourier transformation or more typically fast Fourier transformation (Kim, Mastnik, and André, 2008). The frequency domain features that were extracted in the past studies are summarised in table 2.4. In total, only six different frequency-based features were used throughout the analysed past research. Further, it was mentioned that the features obtained from the frequency domain did not lead to any significant improvement for the following pattern recognition system as it appeared that those features did not represent the classes of motions properly (Simao et al., 2019 & Samuel et al., 2019). In addition, the feature extraction based on the frequency domain required a significantly higher computing capacity compared to the feature extraction from the time domain which significantly reduced the implementability of such (Samuel et al., 2019).

| **Frequency domain features** | [1] | [2] | [3] | [4] | [5] | [6] | [7] | [8] |
|---|---|---|---|---|---|---|---|---|
| Mean frequency | | | | | | X | | |
| Median frequency | | | | | | X | | |
| Frequency ratio | X | | | | | X | | |
| Power spectral density (PSD) | X | | | | | | | |
| Fundamental frequency (f_0) | | | X | | | | | |
| Fourier variance | | | X | | | | | |

Table 2.4: Summary of various **frequency domain features** used in previous research in context of pattern recognition related to EMG signal recordings.
Used articles: [1] : Parajuli et al., 2019 ; [2] : Mendez et al., 2017 ; [3] : Kim, Mastnik, and André, 2008 ; [4] : Bangaru, Chao Wang, and Aghazadeh, 2022 ; [5] : Simao et al., 2019 ; [6] : Chan et al., 2021 ; [7] : Samuel et al., 2019 ; [8] : Phinyomark et al., 2014

The following section goes over the main frequency domain features mentioned in the analysed past literature.

**Mean frequency :** The mean frequency represents the average frequency contained within the signal (Chan et al., 2021). It is defined in eq. (2.14) (Chan et al., 2021), where $L$ represents the length of the power spectrum and $p_k$ represents the power spectrum.

$$f_{mean} = \sum_{k=1}^{L} \frac{p_k}{L} \tag{2.14}$$

**Median frequency :** The median frequency represents the midpoint of the frequency distribution, it is the frequency above which half of the total power and below which the

remaining half lies (Davis, Parbrook, and Kenny, 1995). The median frequency is defined in eq. (2.15) (Chan et al., 2021).

$$f_{med} = \frac{1}{2}\sum_{k=1}^{L} p_k \tag{2.15}$$

**Power Spectral Density :** The power spectral density is a feature from the frequency domain. It describes the power held in the signal as a function of the frequency (Maral, 2003). As shown in past study, obtaining information on the PSD and clear ways for its calculation can end up as a tedious task which has led to several possibilities of approximation processes for the PSD (Andren, 2006). In fact, the EMG-related study mentioning the use of the PSD as a feature in pattern recognition did not specify the method used to obtain the PSD (Maral, 2003).

**Frequency ratio :** The frequency ratio is sometimes used as a tool to obtain information on the activity of muscles and has proven helpful to identify whether a muscle is in a state of relaxation or contraction (Chan et al., 2021). Past study defined the frequency ratio considering: $f_{ucl}$ and $f_{lcl}$, the upper and lower cutoff frequencies of the muscle signals at low-frequency band, and $f_{uch}$ and $f_{lch}$ the upper and lower cutoff frequencies of the muscle signals at high-frequency band, and this definition is given in eq. (2.16) (Chan et al., 2021).

$$f_{ratio} = \frac{\sum_{k=f_{lcl}}^{f_u cl} p_k}{\sum_{k=f_{lch}}^{f_{uch}} p_k} \tag{2.16}$$

### 2.3.7 Conclusion process of EMG data extraction

To conclude the acquisition of EMG signals it can be said that the process of acquisition is complex but usually follows a certain pattern. The main step that must be taken into account are the correct conditions and considerations of the issues and interferences which can occur during the recording process. The post-processing steps are also crucial to ensure the correct readability of the signal and a better result of the feature extraction by removing interfering and non-informative signals which would reduce the informativeness of the extracted features. The choice of the features has been shown to be crucial. Different studies were reviewed, illustrating the possibility of using a varied range of features. Hence, all these elements must be taken into account when building the process of EMG signal acquisition and analysis for this research.

## 2.4 IMU signal acquisition

Compared to the numerous research including EMG signals, the use of inertial measurement units (IMU) has not been as vastly detailed in past literature. Especially for medical applications and for research aiming to identify specific motions. Nonetheless, it is interesting to understand which process is usually followed to acquire IMU data accurately to then allow a relevant feature extraction on which the pattern recognition systems will, in a later step, be based to identify the motion from which the IMU signal was generated.

As an overview, it can however be understood that the overall process of IMU data acquiring is similar to the previously detailed process of EMG data acquiring. Thus following the step of measuring, pre-processing and extraction of features.

### 2.3.1 Possible interferences and issues occuring during IMU recordings

In order to apply filters smartly, understanding which interferences can usually occur when recording IMU signals is relevant. It has been shown by past studies that good results can already be obtained when extracting features from IMU signals without first applying any filter or preprocessing technique (Bangaru, Chao Wang, and Aghazadeh, 2022). Nonetheless, certain interferences may still occur.

Firstly, the most likely interference to occur is noise. The main concept of noise can be understood in the same way as presented previously for the EMG. However, due to the nature of the IMU sensors, the reasons why noise would occur in this case could be related to ultrasound, radio or electromagnetic waves (Hellmers et al., 2013). Further, it was shown that other influencing factors could also have an impact on the quality of the measured IMU signals. Such factors could for example be temperature or humidity fluctuations (Hellmers et al., 2013). Hence, this illustrates that many interfering factors may hinder the measuring of IMU signals and cause a certain noise.

In addition to noise, in a similar way to the process of EMG acquirement, the issue of aliasing should also be considered. For this matter, it is crucial to choose the sampling frequency appropriately, in such a way as to ensure the correct acquiring of the signal (Hasegawa-Johnson, 2021).

### 2.3.2 IMU pre-processing and filtering

Following the established understanding of the interferences that can occur within IMU signals, appropriate filters were found throughout the literature. A common way to reduce

the impact noise was given as the use of Butterworth filters. As an example, one research which measured three-dimensional kinematic motions of surgical tasks with the objective to obtain statements on the possibility to measure such motions accurately used a 6Hz $4^{th}$ order Butterworth filter to filter their signals (Morrow et al., 2017). Nonetheless, this study was the only found example of research explicitly mentioning the use of such a filter. It can however be expected that the use of such a filter is most likely implicitly understood when research only mentions the use of *filtering* as its effectiveness towards noise reduction has been shown multiple times (Simao et al., 2019 & Samuel et al., 2019 & Yuan et al., 2019).

**Extended Kalman-Filter**

Nonetheless, a very common filter used when it comes to IMU recording is the extended Kalman-Filter (EKF). IMU signals are usually six-dimensional signals which describe the three-dimensional translational acceleration and the three-dimensional rotational speed. Hence, the IMU sensor measures the translational accelerations ($\ddot{x}$, $\ddot{y}$ and $\ddot{z}$) and the angular speed ($\dot{\phi}$, $\dot{\theta}$ and $\dot{\psi}$). When the objective of the study is to obtain information on the position of the measured system at a certain time, the translational acceleration or the rotational speed would be integrated to obtain the desired information on the position. In fact, this can be visualised through eq. (2.17) and eq. (2.18). Nonetheless, as shown in previous studies, the use of such linear integration leads to a propagating error which may greatly affect the result (Hellmers et al., 2013).

$$\text{Translational Position} = \begin{bmatrix} x \\ y \\ z \end{bmatrix} = \int \begin{bmatrix} \dot{x} \\ \dot{y} \\ \dot{z} \end{bmatrix} dt = \iint \begin{bmatrix} \ddot{x} \\ \ddot{y} \\ \ddot{z} \end{bmatrix} dtdt \tag{2.17}$$

$$\text{Angular Position} = \begin{bmatrix} \phi \\ \theta \\ \psi \end{bmatrix} = \int \begin{bmatrix} \dot{\phi} \\ \dot{\theta} \\ \dot{\psi} \end{bmatrix} dt \tag{2.18}$$

To avoid this effect, a process known as the Extended Kalman Filter (EKF) was developed. It can be described as an adaptative method which continuously updates an adequate estimate of the current state of the system (Hellmers et al., 2013). This method was used by several studies which aimed to obtain information on the current position of a system based on IMU signal recordings (Hellmers et al., 2013 & Constant et al., 2021 & Zhao, 2018).

# 3 Data Acquisition

## 3.1 Requirements

Based on the previously established understanding, it became clear that in order to establish a control system based on recordings, adequate sensors would be needed. Those sensors should allow a swift acquisition of the required EMG and IMU signals, and allow the subject from which the data will be collected to perform the pre-defined easily.

Further, in order to acquire data, those sensors would have to be linked to a sensor-control unit which would allow the recording of the signals in such a way that the obtained data can be used for the post-processing and pattern recognition processes. In fact, simply setting sensors such as electrodes for EMG on the skin would not be sufficient to record any signal as the sensoring system would lack any data acquisition process. For this reason, to effectively record EMG and IMU signals, the sensor system must include electrodes which would be set on the forearm, a recording unit and a storage unit.

Nonetheless, to fulfil the purpose of this study, it must be kept in mind that the sensoring system cannot hinder the subject from performing the motion. Indeed, the objective is to record EMG and IMU signals of non-hindered and naturally performed hand gestures. If the system of recording is restricting the subject due to its size, weight or configuration, the hand motion cannot be considered natural anymore and the following conclusions that may be obtained would hence become limited to the sole scale of this purpose. Hence, it is crucial to keep the recording material as discrete and non-hindering for the subject as possible.

## 3.2 Presentation of the material

As established during the review of previous studies and research, several possibilities exist when it comes to selecting material for EMG and IMU recordings. Nonetheless, for this study, three main options are considered and evaluated: material from two different companies *Open-BCI*, *Shimmer*, as well as non-branded materials available in online stores. In the end, it is the equipment by *Shimmer* that is selected as the main material for this study. This equipment and the reasons for its selection are detailed in the following section. The other pieces of material are briefly summarised in the next section, and their benefits and negative points are presented and described.

### 3.2.1 Shimmers3 EMG Unit

The material selected to record EMG signals in the forearm region is the Shimmers3 EMG Unit by *Shimmers*. The main reasons why this particular piece of equipment is chosen are its usability and implementability which allows a swift and reliable EMG data recording, its non-hindering aspect allowed through its lightweight and small dimensions, and the ease of acquiring made possible as the company is easily reachable, with convenient delivery options to Finland. The following section presents the specifications and components of the device and provides an overview of the functioning of the unit.

Firstly, several specifications of the EMG recording units can be described. In fact, the device considered especially easy to implement due to its small dimensions (65 x 32 x 12 mm) and lightweight (31g) which are considered to make the device "ultralightweight" and "compact" (Shimmer, 2023b). The device has a total of five different input connections. Two pairs of negative/positive inputs as well as a reference connection are available. It can further be mentioned that the ground used is a Wilson-type driven ground (Shimmer, 2023b). Additionally, more detailed information is provided in table 3.1.

| | |
|---|---|
| Weight | 31g |
| Dimensions | 65 x 32 x 12 mm |
| Input differential dynamic range | approx 800 mV |
| Bandwidth | 8.4 kHz |
| Ground | Wilson Type Driven Ground |
| EEPROM memory | 2048 bytes |
| Input Protection | ESD and RF/EMI filtering;<br>Current limiting;<br>inputs include defibrillation protection |
| Connections | Input Ch1N, Input Ch1P, Input Ch2N, Input Ch2P,<br>Reference (Ref) |
| Jack types | 1mm Touchproof IEC/EN 60601-1 DIN42-802 jacks |

Table 3.1: Specifications of Shimmer3 EMG Unit (Shimmer, 2023f & Shimmer, 2023b)

The Shimmers3 EMG Unit is delivered with an elastic strap optimised to fixate the sensor around the arm or leg of a subject (Shimmer, 2023f). The five wires which can be used to connect the input channels to electrodes are also provided with the unit. The sensor device works on an included battery which can be recharged by plugging the device to the *Shimmer dock* which is sold separately by the company and shown in fig. 3.1e. The dock can further be used to program the parameters of the unit such as the sample frequency, the gain of the amplifier or what signals are to be measured by the device (Shimmer, 2023e).

The internal structure of the Shimmers3 EMG unit as given in the manual provided by *Shimmer* is shown in section 3.2 (Shimmer, 2023b). The five electrode inputs on the left side respectively connect to the channels labelled as Ch1N (in red), Ch1P (in brown), Ch2N (in white), Ch2P (in black) and Ref (in green). The mentioned colours are referred

from the block diagram shown in section 3.2, and the same colour code is being used in the physical EMG unit as is visible in fig. 3.1a. Following the inputs, defibrillation protection is applied. This component protects the measuring device in case of too high incoming electrical signals. The exact functioning of the defibrillation protection is however not provided (Shimmer, 2023b).

The two channels Ch2P and Ch2N are then connected to an EMI filter which is described by the company as reducing electromagnetic interferences (Shimmer, 2023b). In fact, the literature describes MEI as a simple noise interference which is caused by external electromagnetic waves (Taranovich, 2021). It has additionally been shown that EMI can hence lead to undesired effects on measuring devices, inducing unexpected currents and voltages into the electrical circuit and thus significantly reducing the performance of the equipment (Taranovich, 2021). For these reasons, the use of an EMI filter seems beneficial, nonetheless, the exact details of the IMU filter are not provided.

The signals are further amplified using two programmable gain amplifiers (PGA), before being transformed into digital data using a delta-sigma analogue-to-digital converter ($\Delta Sigma$ ADC). The amplifier ensures that the data will have a sufficient amplitude to be read correctly by the ADC. The $\Delta Sigma$ ADC transformed signal is made of 24-bit signed integer values for each sample (Shimmer, 2023b). Its functioning can be understood as a constant and continuous measuring between a reference signal and the predicted actual signal. Those usually use oversampling and noise-shaping methods to achieve a higher resolution of the resulting digitalised signal (Z. Tan et al., 2020). Hence, the presented EMG unit can measure electrical biosignals from the body such as EMGs and obtain a digitalised signal from it.

The Ag/AgCl electrodes to which the EMG unit connected are the ones sold by Shim-


(a)


(b)


(c)


(d)


(e)

(f)

Figure 3.1: Illustrations of the material : (a) EMG sensor ; (b) IMU sensor ; (c) EMG sensor attached to the wrist band ; (d) IMU sensor attached to wrist band ; (e) EMG to the charging/programming dock ; (f) electrodes

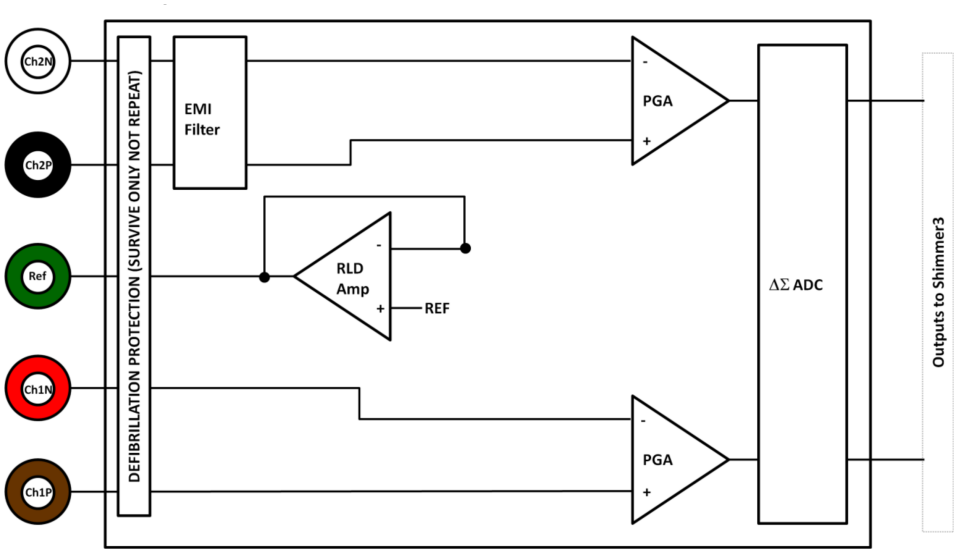


Figure 3.2: Block diagramm illustrating the inner structure of the Shimmers3 EMG Unit (Shimmer, 2023b)

mers and shown in fig. 3.1f. Those ECG/EMG snap-on electrodes are pre-gelled and feature an adhesive side with non-irritating gel to ensure that the electrodes will remain firmly fixated to the skin of the subject while minimising the risk of skin inflammation or allergic reaction (Shimmer, 2023c). It further mentioned that those electrodes are made of latex-free material which is meant to make them suitable for every type of skin.

### 3.2.2 Shimmer3 IMU Unit

The IMU sensor utilised in this research is the Shimmer3 IMU Unit. This sensor combines a variety of subsensors which include an accelerometer, gyroscope, magnetometer, and altimeter (Shimmer, 2023g). However, relevant for this study are only the accelerometer and the gyroscope. The accelerometer measures the three-dimensional acceleration how the sensor, while the gyroscope measures the rotational speed. The implementation of the IMU is thought of as a combination with the EMG to help make the resulting system more robust and capture additional information on the motion performed by the subject.

## 3.3 Additional material consideration

As mentioned previously the selected materials for the scope of this study are sensors sold by the company *Shimmer*. Nonetheless, before making the decision to use this equipment, additional measurement units are considered. It can be beneficial for future studies on similar topics to mention the result obtained from the material research which preceded the application study. This section will give a brief introduction and summary on similar material by the company *OpenBCI* as well as on unbranded sensing material.

### 3.3.1 Material by OpenBCI

OpenBCI is a well-known and established company in the sensing domain. The first item from that firm that is analysed is the *all-in-one emotibit bundle* by *Open-BCI* (OPEN-BCI, 2023a). This is shown in fig. A.1a. Although this kit of sensors is very effective, it is rather suitable for EDA and PPG measurements, which is hence not ideal for the purpose of this study.

Another device sold by *Open-BCI*, is of more interest: the *low-cost biosensing starter bundle* (OPEN-BCI, 2023b). This measuring device shown in fig. A.1b has been designed to record most kinds of electrical biosignals such as EEG, ECG and EMG. Hence, this device may have been of interest. However, the company states that although this kit includes a 4-channel Ganglion Board, a Headband Kit, plus the recommended set of electrodes and accessories, no battery is included. This is why batteries and chargers should be ordered separately. As suggested by *open-bci* is a *Lithium Ion Rechargeable Battery (500mAh)* from *adafruit* (adafruit, 2023b), shown in fig. A.1c, and its charger from the same company (adafruit, 2023a) and shown in fig. A.1d.

Despite the promising quality and possibilities that seemed acquirable with the pre-

viously presented equipment by *Open-BCI*, the fact that the shipment occurred from America, and that several pieces of independent equipment would be required to process with this equipment made it not ideal for the purpose of this study, especially when compared to the material used in the end.

### 3.3.2 Other material

Further research is also conducted towards non-branded material. Several various equipment options are studied. An example is the *Grove EMG detector* sold on *Digi-Key electronics* (DigiKey, 2023b). This equipment is shown in fig. A.2

Those elements are, for most, considerably cheaper than the equipments provided by well-established companies such as *Shimmer* or *OpenBCI*. Yet it is hard to know beforehand how well they will perform or how challenging it may be to connect them to a computer in such a way as to obtain coherent EMG/IMU data. Hence, making it difficult to imagine how well those may work in the end, or to prefer one over another. Additionally, buying basic equipment will not suffice to record the desired signal in an adequate way. As shown previously, accurate and precise recording equipment requires additional programming and a more complex structure. And further, as building a measuring device would be time and effort-consuming and outside the scope and objectives of this research, it is decided to avoid such a solution and prefer fully assembled and working sensing devices.

## 3.4 Presentation of the hand motions

The objective of this research is to use classifiers to predict which predefined hand motion has been performed by a subject based on the EMG/IMU recordings measured from the

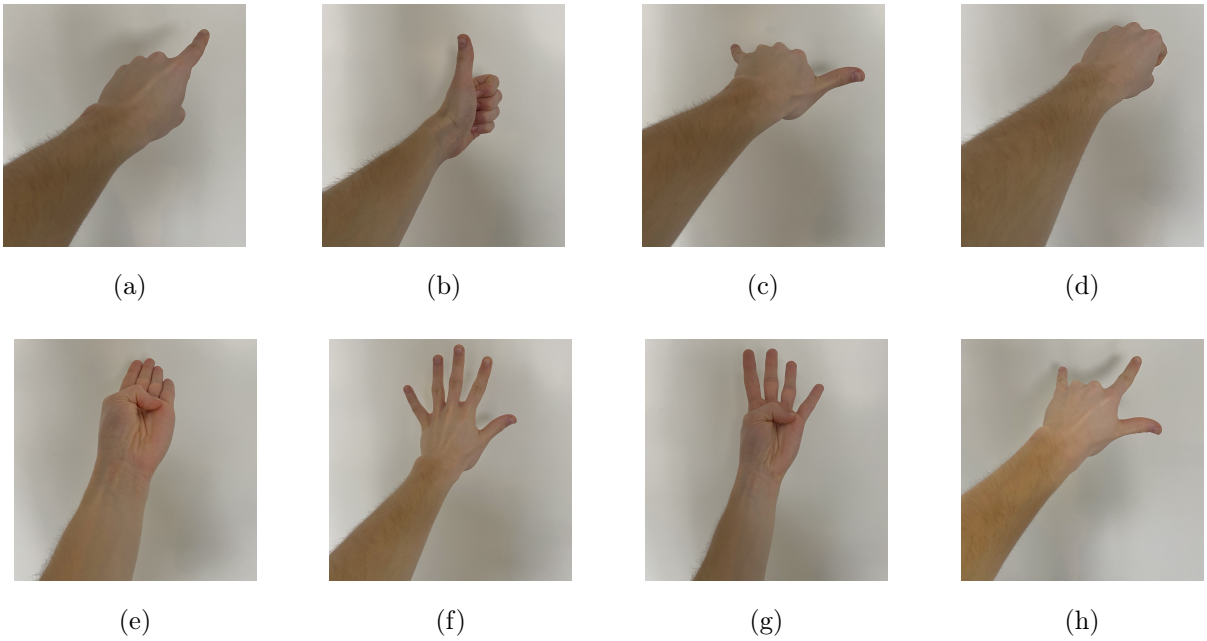

(a) (b) (c) (d)

(e) (f) (g) (h)

Figure 3.3: Hand motions : (a) EMG sensor ; (b) IMU sensor ; (c) EMG sensor attached to the wrist band ; (d) IMU sensor attached to wrist band ; (e) EMG to the charging/programming dock ; (f) electrodes

forearm and wrist areas. Hence, an important step is to define clearly which hand motions are to be performed, so that each subject can perform the motions as similarly and clearly as all the other subjects in order to keep consistency within the dataset.

For this purpose, eight distinct hand motions are defined. Those hand motions are provided in fig. 3.3. These hand motions are for some inspired by previous studies (Mendez et al., 2017). The main idea is to observe different kinds of hand motions while also having certain hand motions that share certain similar aspects.

The first hand motion (fig. 3.3a) consists of extending the arm and pointing the horizon with the index while the rest of the hand is firmly closed into a fist. The second hand motion (fig. 3.3b) represents a thumbs up with an extended arm. The other fingers are grouped into a tight fist. The third motion (fig. 3.3c) consists of extending the arm with

a closed fist while extending the thumb and the pinky towards the outside of the fist. The fourth hand motion (fig. 3.3d) is a simple closed tight fist while expanding the arm. The fifth hand motion (fig. 3.3e) consists of turning the arm around and extending all the fingers towards the horizons while the thumb is tightly held back within the fist area. The sixth hand motion (fig. 3.3f) consists of extending the arm towards the front and expanding all the fingers widely. The seventh hand motion (fig. 3.3g) is made by bending the arm at a 90-degree angle and rotating the hand so that the nail side of the fingers shows towards the horizon. All the fingers are then extended but the thumb is kept close to the inner hand. And the eighth hand motion (fig. 3.3h) consists of extending the arm while holding the hand into a fist but with the extension of the thumb, the index and the pinky.

It can be observed that certain of these motions share similarities. For example, the third and the eighth hand motions solely differ in the extension of the index finger, while all the other fingers maintain identical positions. The fifth and the seventh positions are also similar in the sense that the main difference is the rotation of the hand while all the fingers are in a similar position. These similarities are of great interest for the purpose of the research as they represent a challenge for the classifiers which will have to differentiate between those hand positions. Hence, including similarities allows observing whether the misclassification between certain specific motions is more common than for others.

The hand motions each occur from the rest position which is given in fig. 3.4. The rest position consists of a non-tight extended arm with released fingers. The process of measuring will then alternate between the rest position and the position of interest which is being recorded at the specific instant during the recording process.

Figure 3.4: Rest position

## 3.5 Recording Process

After defining the hand motions, the recording process could be detailed. The two sensors (IMU and EMG) were first placed on the forearm area of the subject using the straps to which they could easily be fixated using the snap clips. The IMU sensor placed on top of the forearm so that the positive direction of the y-axis would always face the front of the hand. The EMG sensor placed similarly on the side of the forearm. The placement of the EMG electrodes would then occur in the following way, based on the understanding obtained from section 3.2. The reference electrode placed on the top side of the hand. Following the information included in the user manual provided by the company the two electrodes forming each of the two electrode pairs would then be placed roughly a few centimetres apart (Shimmer, 2023b). The first electrode pair connected to the signals Ch1N and Ch1P, as labelled in section 3.2 are placed in the inner elbow region, this area is also known as the *anticubital fossa*. This area seemed of interest as many flexor muscles are entwined in this region, and past research has shown that the flexor muscles of the forearm are responsible within others for the motion of the hand (Bremer et al., 2006). The second pair of electrodes connected to the channels Ch2N and Ch2P and put in the wrist area. Many of the flexor muscles are further connected to this region which makes it of interest. Further, the aim of this research includes the study of the possible implementation of a pattern recognition process in a subtle way, hence it is of interest to measure

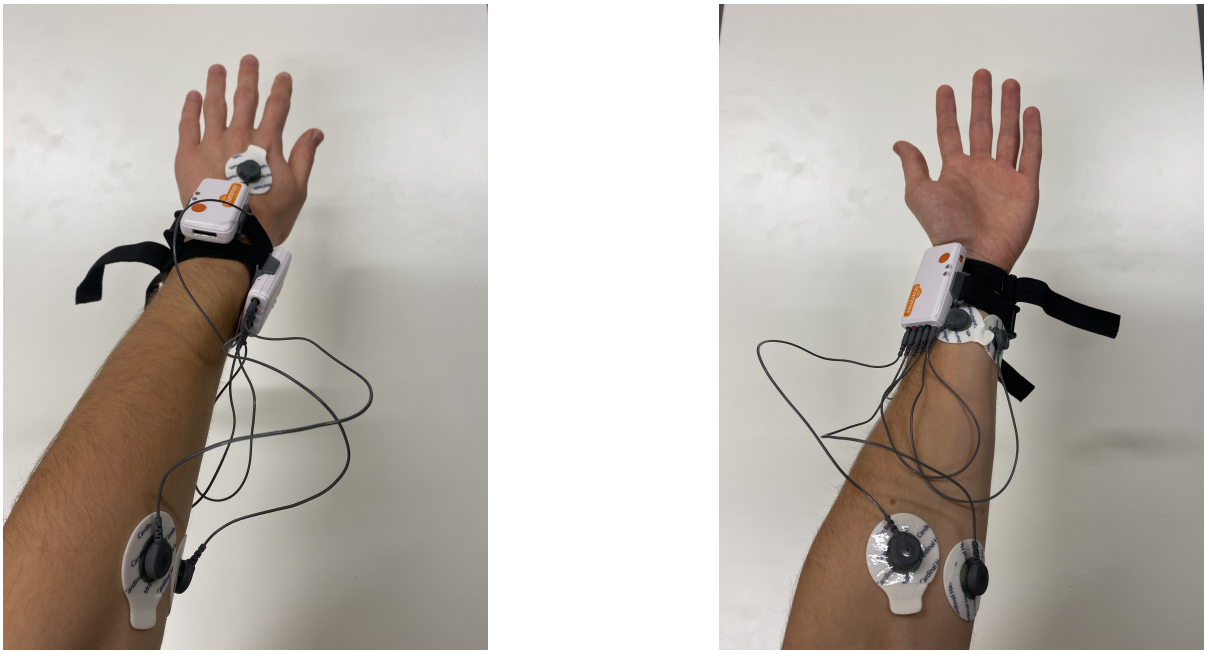

(a) (b)

Figure 3.5: Experimental setup: (a) upper view, (b) lower view

the EMG signals from the wrist area to analyse whether motions can be classified with only signals from the wrist section. The entire experimental setup is shown in fig. 3.5. The sample frequency used for both devices 512Hz.

The goal of this research is to record signals from those sensors for the eight previously defined hand motions. Each motion is recorded ten times on each side, resulting in a total of 160 motions recorded per subject. As recording every single motion individually would have required great time investment, a solution found. Instead of measuring each motion individually, the movements are recorded in sets. Hence, one set would represent a single motion repeated ten times. This allowed reducing the number of sets from 160 to 16 and made it considerably more convenient for the subjects. However, the issue that arises from this approach is that the motions are now recorded as sets and not as individual motions, which is not the intended input for the system. For this reason, pre-processing would be required to extract each single motion. For this purpose, it necessary to include sufficient

time between the motions to make it easier to isolate each motion from the overall segment.

Based on these requirements, the experimental process of data acquisition can then be defined. Once the sensors start recording, the subject sets their hand in the rest position. This position is then held for five seconds. Then, a pattern of four seconds is repeated ten times: on the second one, the hand goes into the desired position. On the second two, the hand returns to the rest position. On the second three and four, the hand remains in the rest position. After having repeated this pattern ten times, and hence recorded the motion of interest ten times, the hand remains in the rest position for an additional five seconds before the recordings are ended. This process is shown in fig. 3.6.

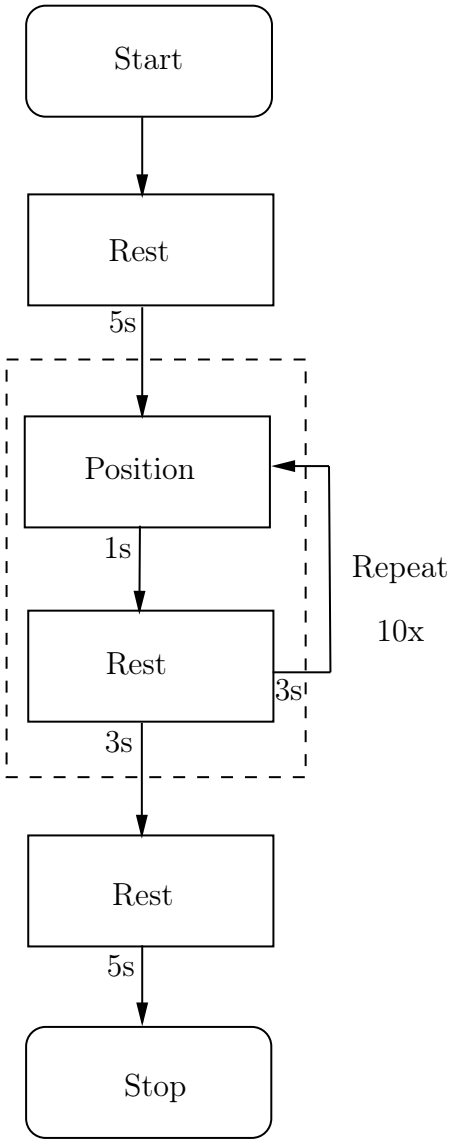


Figure 3.6: Recording Process

## 3.6 Isolation process

Following the recording of the data, one of the major challenges of this study emerged with the need to extract a single movement from sets containing ten individual motions. This section details the process of movement isolation and aims to provide a thorough understanding of the methods and approaches used to extract the data of a single movement from the recorded data.

First, it is crucial to remind why the process of data isolation is a necessary step for the correct fulfilment of this research. In fact, the main objective is to use algorithms of pattern recognition to classify the measured datasets back to one of the eight types of motion that are performed. However, the data to be classified must represent a single movement and not a signal comprising ten individual movements as is the case with the raw data obtained from the recording. An illustration of such a raw signal is shown in fig. 3.7 for the example of one of the EMG channels. It is for this reason that the individual movements must be isolated from the full recorded signal.

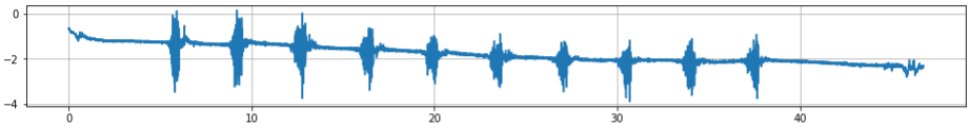


Figure 3.7: Raw signal

The main idea used to isolate the waves representing individual movement is to use a general approach to peak identification within the whole signal. As the rest position does not induce any biosignal, the peaks would hence each be part of a movement which can in turn be used to detect each signal motion individually. Nonetheless, before this process can be applied, the first step is to remove the edges. In fact, when turning the recording instrument on and off, it is usual for the subjects to have unwanted tension in their arm muscle which creates high peaks which would be problematic considering the approach of peak identification for the identification of the waves representing the movements. The technique used to bypass this issue involves a five-second wait before and after the start of the motion process. As mentioned in the description of the data recording process, prior to the first motion and after the last motion, a wait of approximately five seconds performed. This used to create 'flat' signal areas before and after the segment of interest. Hence the first step to remove the edges of the raw data signal to obtain 'flat' starts and ends to the signal as can be seen in fig. 3.8 which illustrates

the raw signal after the removal of its edges. After this first step, the signal still contains the ten motion waves but now has 'flat' regions prior to and following those motions.

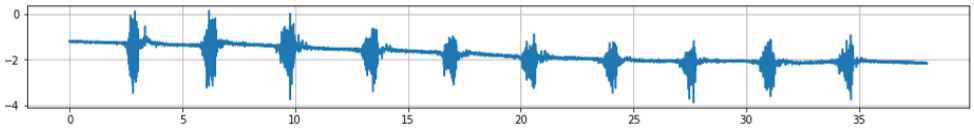


Figure 3.8: Signal after edge-removal

The second main step is to identify the peaks within the signals and to ensure that each wave only receives one wave. The EMG and the IMU signals each followed the same process. However, as the four EMG channels all had the same time domain, only one of the four channels used to extract the segment, usually channel 1, unless the result not concluding, then the channel performing best applied. This also ensures that the starting and ending times of each individual segment would coincide. The same approach also used for the IMU signals, only one channel used to extract the individual motion segments, usually the channel of $x$-acceleration used.

To identify the peaks within the signal, the following approach followed. The first step is to apply a bandpass filter on the signal, this will remove excessive noise and clarify the signal, which will in turn make the identification of the peaks more precise and simple. The cutoff frequencies are fixed to 20Hz and 250Hz, as well for the EMG as for the IMU process. This fixation is inspired by the suggested filters from past research and adapted for the purpose of this research (summarised in table 2.1). The signal is also normalised, enabling an adjustment of the amplitude or range of the signal to a standardised scale. This adds consistency and facilitates a more effective analysis towards peak identification. The implementation of the bandpass filtering in Python performed by using the *scipy* library and the *butter* function which allows the creation of the required bandpass filter easily and effectively (Scipy, 2024b). An example of a resulting filtered and normalised

signal is shown in fig. 3.9

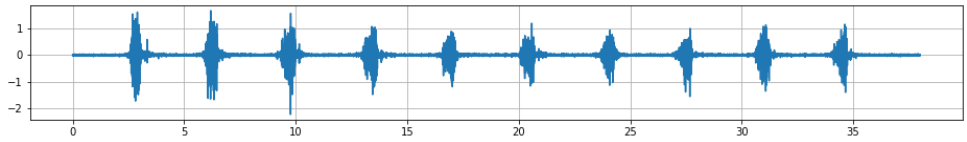


Figure 3.9: Signal after the application of the band-pass filter and normalisation

Following the filtering and normalisation, the waves representing single motions already appear more clearly. Nonetheless, by squaring the signal, those waves will come out even more clearly and the signal will be entirely positive which will make it especially easier to extract maximums. Hence, the signal is squared. This is performed in Python by defining a squaring function that squares the signal value by value. An example of a signal following the application of the squaring function is shown in fig. 3.10.

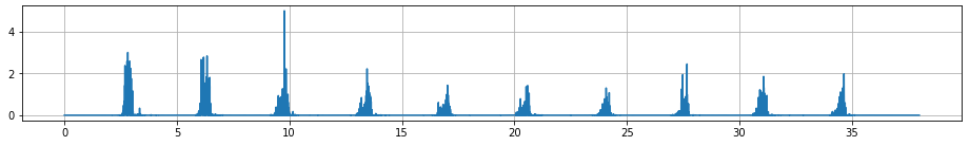


Figure 3.10: Filtered signal after the application of the squaring

The following step is to identify a peak for each motion wave that is now clearly identifiable in the squared signal as shown in fig. 3.10. To do this, a threshold defined manually. Each time the signal crosses the value of the threshold, the algorithm defines an area of 1.5 seconds before and 1.5 seconds after the threshold crossing is established. The index of the maximum value within this region is saved. It corresponds to the index of the peak of the wave representing one of the ten motions. The algorithm then moves on by skipping all values in a range of 1.5 seconds from the firstly found threshold crossing. This process iteratively goes over the entire squared signal and extracts the indexes of the ten peaks. Each peak representing the peak of a wave, in turn representing each single

motion. This algorithmic approach is provided in alg. 3.1. The resulting identified peaks are shown in fig. 3.11. It can be seen that each wave representing a single motion has a single peak.

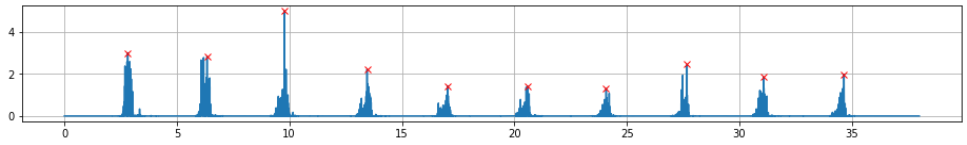


Figure 3.11: Filtered and squared signals with the identified peaks

The following step consists of extracting the individual motions from the overall signal. To do so, the previously identified peaks are used. Around each peak, a segment of 1.5 seconds before and 1.5 seconds after each peak is extracted. This time section is based on the fact that each motion performed around one second and hence ensures to cover the activation and relaxation of the muscles. The defined algorithm hence cut segments of three seconds around each of the identified peaks. Those segments can be visualised in fig. 3.12, where the segments extracted from the raw signal are shown in red.

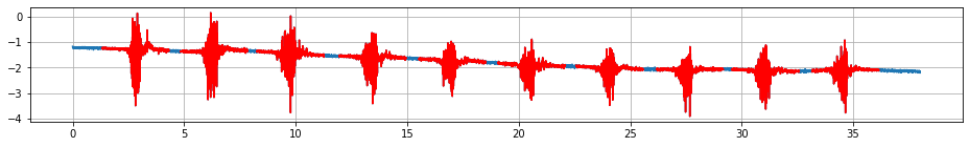


Figure 3.12: Signal with edge-removal, with the identified motion segments highlighted in red

The result is an individual signal for each single wave representing an individual movement. An example of such a single wave is shown in fig. 3.13.

The whole signal of the isolation of single waves representing individual motions is summarised in fig. 3.14. In conclusion, it can be summarised that the main steps of this

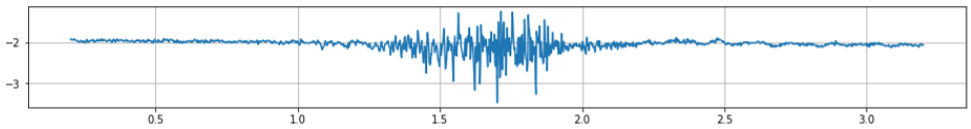


Figure 3.13: One the the ten single movement segments as extracted directly from the raw signal

process are firstly the removal of the edges, secondly, the detection of the peaks, and thirdly the extraction of the segments around each peak. As mentioned earlier, the same identified peaks from one channel are used to extract the individual waves from all the channels of a single signal (IMU or EMG).

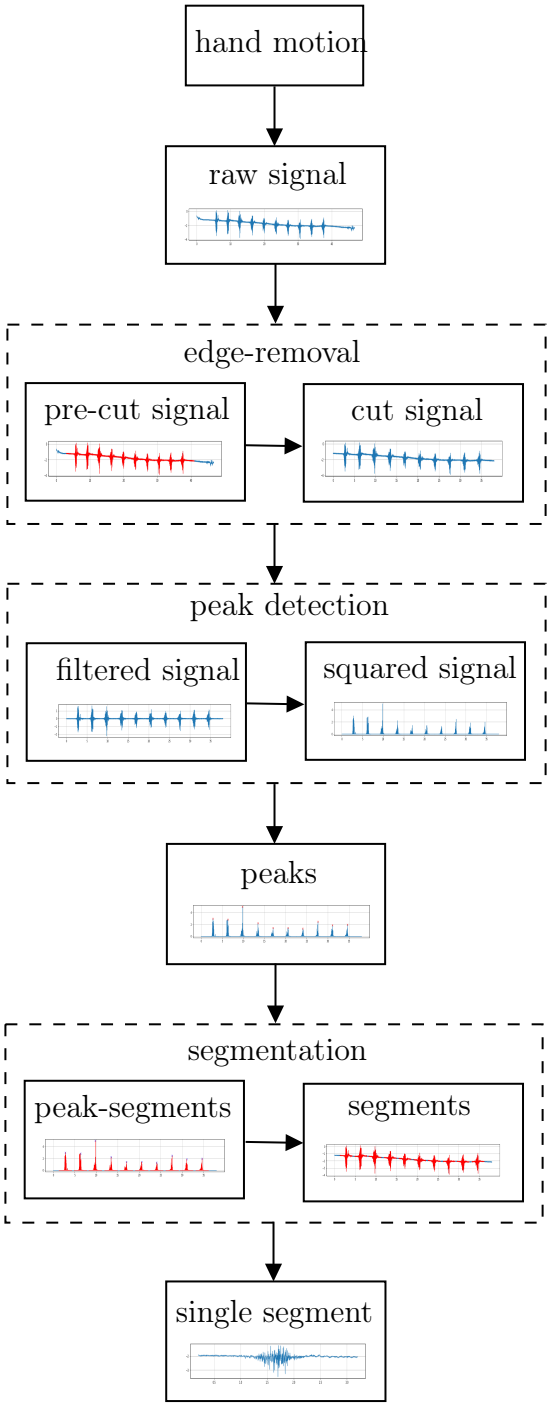


Figure 3.14: Acquisition and isolation of wave signals

**Algorithm 3.1:** Peaks extraction

**Input:** signal, threshold, fs

**Output:** peak_index : list with the index of peaks

**foreach** *index in signal* **do**

  **if** *signal at index is greater than threshold* **then**

    local_maximal_index ← index

    **for** *local_index in range(index - round(1.5*fs), index + round(1.5*fs))* **do**

      Avoid having negative indexes **if** *local_index is less than 0* **then**
        local_index ← 0

      Avoid overshooting **if** *local_index is greater than len(signal) - 1* **then**
        local_index ← len(signal) - 1

      Find index of local maximum **if**

      *sig[loc_idx] is greater than signal[local_maximal_index]* **then**
        loc_max_idx ← loc_idx

    Ensure that no peak is saved twice: **if** *len(peak_index) is greater than 0*

    **then**

      **if**

       *local_maximal_index is not equal to peak_index[len(peak_index) - 1]*

       **then**
        peak_idx.append(local_maximal_index)

    Avoid having twice the same peak **if** *len(peak_index) is equal to 0* **then**
      peak_index.append(local_maximal_index)

    Check that next index will not go too far **if**

    *Next segment will not overshoot* **then**
      index ← index + round(1.5*fs)

  **else**
    index ← index + 1

**return** *peak_index*

# 4 Formulation and Implementation of the Process

## 4.1 Preprocessing models

This section gives an insight into the preprocessing methods that are used in the process. The main objective of the preprocess is to transform the raw signals into signals that will be easier to analyse and from which the extracted features will deliver better information. This allows the machine learning approaches to obtain better results when classifying the signals back to the original motion in a later step. The main elements included within raw signals which must be removed are the noise and any other unwanted signals. Further, the preprocessing must also include a normalisation of the signal which allows an adjustment of the amplitude or range of the signal to a standardised scale. This step is crucial to add consistency and facilitate a more effective analysis in a later step.

The main filters that are used are widely suggested in the literature. To increase the signal-to-noise ratio, it is usual to apply a bandpass filter (Samuel et al., 2019). Similarly to the isolation process, the bandpass filter is implemented using the *scipy* library and the *butter* function (Scipy, 2024b). The cutoff frequencies which are applied are directly inspired by the suggested cutoff in past research (as summarised in table 2.1), and are fixated to 20Hz and 250Hz, this allows the removal of the unwanted low frequencies as suggested in literature, and the high-cutoff is chosen to ensure the respect of the Nyquist theorem based on the sample frequency of 512Hz and to so avoid aliasing.

Furthermore, a notch filter is also suggested in past research with the objective of removing power-line interferences (Samuel et al., 2019). Hence, a notch filter is implemented using a cutoff at 50Hz. The chosen cutoff frequency is based on the results obtained in past research, as several independent studies have illustrated that the power-line interferences usually occurred around this frequency, and hence using a notch filter at this

level of cutoff has proven to increase the reliability and precision of the obtained measurements. The notch filter is implemented in Python using the *scipy* library and the *iirnotch* function (Scipy, 2024a). This function is a simple, effective and robust approach for the implementation of a notch filter.

If this filtering approach is specifically designed for EMG signals, it is decided to also apply it to the IMU signal. This decision is mainly motivated by the noisy aspect of the recorded IMU which would also need to be filtered using a bandpass filter to increase the SNR. Further, it is observed that the IMU also seems to be affected by power-line interferences. This can be explained by the lab environment which is rich in electronic material and devices. Hence the use of the analogous notch filter is further justified. And lastly, the use of a single pre-processing method for all the signals made the general approach easier, faster and more robust, allowing an individual function to be used and hence reducing the computational requirements.

To conclude, it can be said that the preprocessing is rather simple and basic with a single bandpass filter and a notch filter. This approach is, within others, motivated by the observation that the raw signals obtained generally appear only minimally affected by interferences, and could already be analysed visually. Hence, the preprocessing is rather used mainly as a mean of normalisation and in a further objective to idealise the SNR of the obtained signals.

## 4.2 Features extraction

The objective at this stage is to develop a system that enables the extraction of a diversity of features from the desired signals. In fact, several tests should be run to allow the tuning of the systems of pattern recognition that would in turn predict which motion of hand is

performed by the subject based on the provided features extracted from its signals. This section details the approach used to extract the wanted features from the dataset. One of the main challenges of the feature extraction for this research is to establish a robust method which would allow swift testing based on an editable range of features and number of signals within the dataset. This approach of feature extraction is provided visually in the form of a block diagram in fig. 4.1.

The first step in the process of extraction of features in a logical and sensible way is to keep the structure of the dataset of signals in mind. Hence, building up on the understanding obtained from the data recording, the dataset is a data frame which includes a list of $N$ signals. Each single wave for each type of motion for each single subject has a different signal. In this context, the use of wave represents the number of the motion within the recording process. As the data is recorded by performing ten consecutive repetitions of a single motion, each single individual movement is extracted as an independent signal and labelled as a 'wave'. The format used in fig. 4.1 for illustration purposes is the same as the format in which the signals are labelled: $s_{X_1}\underline{\mathrm{m}}_{X_2}\underline{\mathrm{w}}_{X_3}$. This figure illustrates the process of data recording. $X_1$ is the number of the subject, $X_2$ shows the number of the specific type of motion that is performed, and lastly, $X_3$ is the number of the wave which is extracted within a set of ten movements.

Following a thorough understanding of the formatting of the dataset, the format of a single signal must also be understood. In fact, a single signal contains a total of $n$ channels. A total of seven channels are recorded for each signal: four EMG and three IMU channels. Nonetheless, the system of feature extraction allows choosing which channels must be used for the extraction of features. This is implemented within Python by using a dataframe formatting which in turn allows to use of the name of the desired channels to extract them from the frame.

At this stage, the feature extraction process extracts the manually desired channels from each signal of the database. The following step would hence be to extract the feature from each single channel of each single signal. The wanted features are all defined individually as functions receiving a list of data and returning the required feature. It can be mentioned that the used features are summarised and detailed in the following section.

The iteration used to extract the features is performed as follows. For each single signal, the wanted channels are extracted. Then, for those channels, the features are extracted one by one and stored within lists. Each list is hence storing the values of a single feature for all the channels of a single signal. Once this first iteration is performed, a total of $m$ lists of extracted features, representing the $m$ desired features, are obtained. These lists are then stored separately within a large data frame, feature by feature. The final format of the overall data frame storing the entirety of the extracted features has an individual column for each feature of each channel. In other words, if $m$ features must be extracted from signals with $n$ channels, the number of feature columns of the final data frame will be the product of $m \cdot n$.

This approach has the benefit of being very tuneable and allows the precise extraction of the desired features based on the desired channels from the data signals. This ability to easily decide which features are being obtained and from which channels is crucial for the following steps and tests of the research.

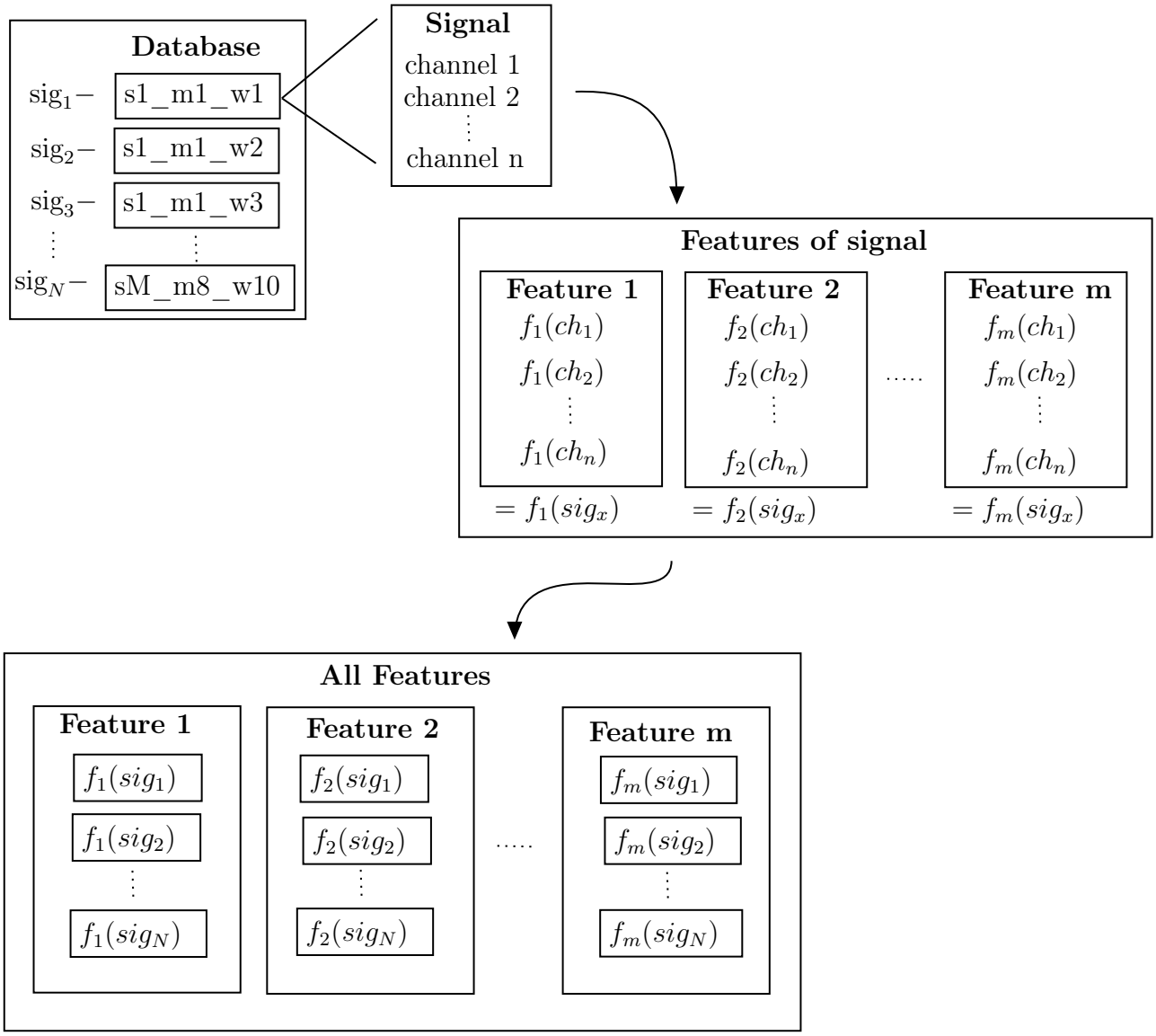


Figure 4.1: Process of feature extraction

## 4.3 k-Nearest-Neighbour

The following sections present a variety of machine-learning approaches which are used to classify the recorded data back to its original type of motion. Each section gives a brief introduction to the method and explains its functioning and interest towards the objectives of this study. Each section also details how the machine learning approach is implemented and used for the purpose of this research. The results of the methods are

then provided in the following chapters as they are highly dependent on the features used.

### 4.3.1 Introduction to the kNN-method

The k-nearest-neighbours method (kNN) is usually described as one of the simplest and most important classification methods and is within the first classification approaches ever developed as the first report suggesting the method is published in 1951 (Peterson, 2009). The K-nearest-neighbours algorithm is a supervised machine learning algorithm, which means that it receives labelled data from which it can learn and recognise patterns and in turn predict the label of unlabelled data based on its previous learning. A label represents the "family" or "group" to which the data element belongs.

The main idea of the kNN classification is to consider the closeness of data points (Steinbach and P.-N. Tan, 2009). The closeness in this context represents similarities between various objects. A simple understanding of the process can be obtained through the algorithmic representation of the kNN process given in alg. 4.1 (Steinbach and P.-N. Tan, 2009). This algorithm can be described as follows. The k-Nearest Neighbors method takes a set of training data ($D$), a test object ($\boldsymbol{z}$), and a set of labels ($L$) as input. For each training object in $D$, the algorithm computes the distance between the test object $\boldsymbol{z}$ and each training object. It then selects the k closest training objects to the test object, forming a neighbourhood $N$. Finally, the procedure assigns a class ($c_z$) to the test object by determining the class that maximises the sum of indicator values for each class in the neighbourhood N. The indicator function $I(x)$ returns 1 if the argument is true (i.e., the class of the current training object matches the considered class), and 0 otherwise. The result is an effective classification of the test object based on its proximity to the k neighbours in the training set.

**Algorithm 4.1:** kNN Algorithm (adapted from Steinbach and P.-N. Tan, 2009)

**procedure** kNN($D, \boldsymbol{z}, L$)

**Input:** $D$, the set of training objects; $\boldsymbol{z}$, the test objects; $L$, the set of classes

**Output:** $c_z \in L$, the class of $z$ **forall** $\boldsymbol{y} \in D$ **do**

Compute $d(\boldsymbol{z}, \boldsymbol{y})$, the distance between $\boldsymbol{z}$ and $\boldsymbol{y}$

Select $N \subseteq D$, the set (neighborhood) of $k$ closest training objects for $z$;

$c_z = \arg\max_{v \in L} \sum_{y \in N} I(v = \text{class}(c_y))$ ;

where the incator function $I(x)$ is introduced and returns 1 if the argument is true and 0 otherwise

**end procedure**

The distance can be computed via a wide range of different approaches. Nonetheless, the most commonly used methods are the Euclidian distance given in eq. (4.1), and the Manhattan distance given in eq. (4.2) (Steinbach and P.-N. Tan, 2009).

In a two-dimensional environment, the Euclidian distance can be understood as the distance described by a direct line between both points. Mathematically, this is obtained by calculating the square root of the sum of the squared differences of the coordinates of the two points. Extended to a n-dimensional space, the Euclidian distance can then be described as in eq. (4.1) (Steinbach and P.-N. Tan, 2009).

$$\text{Euclidian distance: } d(\mathbf{x}, \mathbf{y}) = \sqrt{\sum_{k=1}^{n} (x_k - y_k)^2} \tag{4.1}$$

The Manhattan distance can be visually understood as the shortest path between two points within a two-dimensional grid only using vertical and horizontal motion, and never

moving diagonally. This is mathematically obtained by computing the sum of the absolute coordinate differences within an axis of two points. Extended to an n-dimensional space, the Manhattan distance is described as in eq. (4.2) (Steinbach and P.-N. Tan, 2009).

$$\text{Manhattan distance: } d(\mathbf{x}, \mathbf{y}) = \sqrt{\sum_{k=1}^{n} |x_k - y_k|} \tag{4.2}$$

The main tuning possibility for the kNN classification method is the value of the k-parameter. In fact, the value of k is the key variable that will influence the process of classification and have a major impact on the accuracy of the algorithm. A great illustration for the choice of the value of k is provided in fig. 4.2. It shows how the value of k should be optimised to fit the characteristics of the dataset and labels. Indeed, if k is too small, the process will not be able to recognise sufficient similar points and hence the learning will not be able to occur satisfactorily. If the value of k is too large, too many points which are not of the same label will still be taken into account to understand the relationship between the features and the label. Consequently the learning will be mixed up, resulting in unsatisfying result (Steinbach and P.-N. Tan, 2009). For this reason, it is crucial to test a range of values of k to ensure an optimisation of the process and obtain the best possible results, ideally adapted to the available dataset.

One of the strengths of the k-Nearest-Neighbours algorithm is its simplicity and the fact that it does not make assumptions about the distribution of the data which is especially interesting when the dataset describes complex relationships. This makes the process effective for a wide range of different types of data and further in contexts of dynamic changes. Its main weaknesses however are the expensive computational requirements which may occur, especially for large datasets. The algorithm is also sensitive to

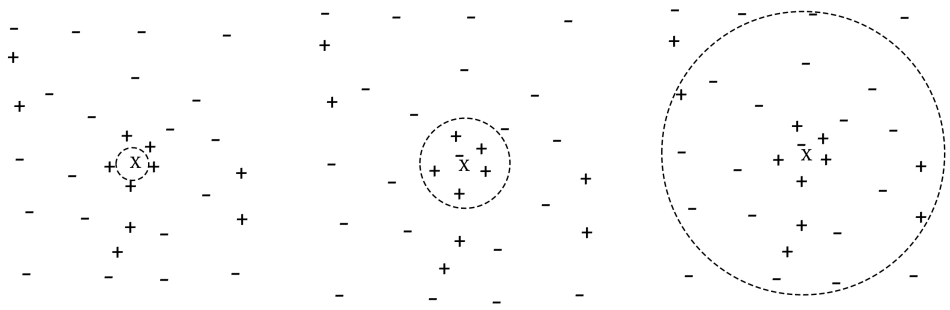


Figure 4.2: Illustration of the importance of optimising the value of k (adapted from Steinbach and P.-N. Tan, 2009)

irrelevant or inaccurate features, and further, wrongly labelled data points and outliers may have a great impact on the results. However, the kNN approach remains one of the major and most robust methods of classification within machine learning, which is why it is chosen to include it in this research.

### 4.3.2 Implementation of the kNN-method

The implementation of the kNN algorithm in Python is performed using the *scikit* library. And more precisely the *KNeighborsClassifier* function which is included within this library (Scikit-Learn, 2023). The use of this predefined function is considered sufficient for the purpose of this study as it allows the tuning of the parameters of interest which are the value of $k$ and the method of calculation of the distance. Hence, using the function provided by the *scikit* library appears satisfying.

For the method of distance calculation, the previously detailed approach of the Euclidian distance is preferred. This decision is motivated by the first observation of the dataset appearing to be rather random. Therefore, it aims to fulfil a spatially isotropic distribution rather than an axis-specific distribution. In addition, for the purpose of even-

tually adding more motion or features to the overall dataset, the Euclidian distance is more versatile and accepts more variation compared to the Manhattan distance as the distance is not calculated on an axis-specific basis, which in turn would make the process more robust towards change in the used features.

For each simulation, a range of values of $k$ is tested to obtain the best-suited value of $k$. The following section illustrates the ran tests for $k = 1, \ldots, 50$.

## 4.4 Gaussian Naive Bayes

### 4.4.1 Introduction to the Gaussian Naives Bayes method

The Gaussian Naive Bayes (GNB) algorithm is another probabilistic classification method. The approach bases itself on the Bayes theorem given in eq. (4.3) (Reddy et al., 2022). The naive aspect of the algorithm describes the assumption that the features are independent from each other given the class label. This signifies that the process will not try to find relations between the features, but rather treat each feature independently to find patterns and classify the data. This process allows a simplification which in turn makes the computing easier and faster.

$$P(A|B) = \frac{P(B|A)P(A)}{P(B)} \tag{4.3}$$

The GNB algorithm makes use of the Gaussian distribution to classify data. The Gaussian distribution is given in eq. (4.4), where $\mu$ represents the mean and $\sigma$ represents the standard deviation which characterise the Gaussian distribution (adapted from citereddy).

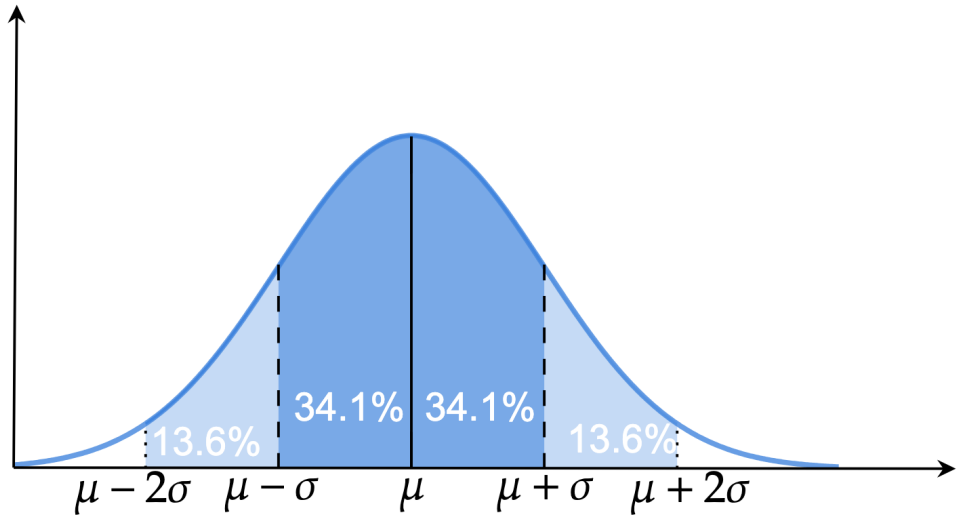


Figure 4.3: Illustration of the Gaussian distribution based on eq. (4.4)

$$f(x) = \frac{1}{\sigma\sqrt{2\pi}e^{-\frac{1}{2}(\frac{x-\mu}{\sigma})^2}} \tag{4.4}$$

This distribution also known as normal distribution is illustrated in fig. 4.3. It can be seen that the mean value is in the centre and that the remaining distribution occurs symmetrically around it. Further, a typical characteristic of the Gaussian distribution is that 68.2% of the area is contained in a range from $\mu - \sigma$ to $\mu - \sigma$, and that 95.4% of the area comprised is in the range from $\mu - 2\sigma$ to $\mu - 2\sigma$.

The algorithm processes by computing the mean value and the standard deviation for each of the provided labels following the definitions given in eq. (4.5) and eq. (4.6) (adapted from citereddy). Where $n_i$ is the number of instances in class $i$, and $x_{k,j}$ is the $j$-th feature value of the $k$-th instance in class $i$.

$$\mu_{i,j} = \frac{1}{n_i}\sum_{k=1}^{n_i} x_{k,j} \tag{4.5}$$

$$\sigma_{i,j} = \sqrt{\frac{1}{n_i}\sum_{k=1}^{n_i}(x_{k,j} - \mu i, j)^2} \tag{4.6}$$

The main reason for using this algorithm as an approach to data classification is to analyse the available datasets for potential Gaussian distribution which would in turn result in great accuracy using this method. Further, the naive aspect of the algorithm would in turn also have an impact on the accuracy of the classification if there is great dependency between the features and could indicate and motivate deeper analysis on data independence which is indeed performed.

Overall, it can be concluded that the GNB algorithm is especially interesting due to its simplicity and ease of implementation. Further, it is usually described as a computationally efficient process, especially with high-dimensional data. Due to its nature, this process would work best when the features approximatively describe a normal distribution. Nonetheless, the assumption of independence due to the naive aspect can lead to inaccuracies in cases where this assumption is not fulfilled by the data. In this same idea, for datasets not describing a Gaussian distribution, the algorithm may not lead to satisfying results. And lastly, this process has shown to be sensible to irrelevant features, which are features that do contribute to the labels targeted by the classification process.

Despite the unlikeliness of obtaining great results, as it is not expected to observe normal distribution within the features of the recorded dataset, trying the GNB approach for this classification problem would confirm the assumption and contribute to the analysis and research.

### 4.4.2 Implementation of the Gaussian Naives Bayes method

The implementation of the Gaussian Naive Bayes algorithm in Python is performed using the *scikit learn* library (Scikit-learn, 2023). Using the function *GaussianNB*, a GNB model is initiated and trained using the given train data. Using this library to implement the algorithm appears widely sufficient to fulfil the objective of this research, as the method does not require the tuning of parameters it seems satisfying to perform the classification using a library.

## 4.5 Logic Regression (One Vs Rest)

### 4.5.1 Introduction to the One Vs Rest method

Regression is another common method that can be used for classification problems. Regression is a statistical method that models relationships between variables using a mathematical function which can in turn be used to describe the analysed relationship (Freund, Wilson, and Sa, 2006). Regression is designed to obtain mathematical functions describing patterns between variables and is hence not designed for classification in the first place. Nonetheless, methods have been established to allow the use of this powerful algorithm for classification problems. The usual procedure used to apply regression to two-label classification, which describes classification problems where only two outcomes are possible, such as e.g. 'sick or 'healthy', consists of converting the labels into numerical labels such as $-1$ for 'sick' and 1 for 'healthy', and then using a threshold, usually 0. The regression process will then result in a mathematical function based on the provided features. When predicting the label of unlabelled data, if the resulting value of the mathematical function is below the threshold, the first label will be chosen, and the second label will be preferred if the resulting value of the regression is above the threshold. So in the previously mentioned example, if the mathematical expression results in a value below 0, the regression algorithm will conclude that the provided set of features corresponds to a 'sick'

person, and if the result is a value above 0, the algorithm will conclude that the set of features is measured on a 'healthy' subject. This method can be summarised by making the binary output into numerical values and then using a threshold to apply regression as classification (Freund, Wilson, and Sa, 2006).

While this method is usually considered as rather effective, it has the significant drawback that it is only applicable to binary classification, meaning that it can handle only two possible outcomes. In the case of this research, however, the number of possible outcomes is greater than two, given that a total of eight different types of motion are recorded. For this reason, the regression algorithm had to be expanded to allow more possible outcomes. The first method that is applied is known as the *One-Versus-Rest* (OVR) regression method (Vogiatzis et al., 2021).

The OVR regression approach consists of training a regression model for each label class, each model will then decide whether the dataset belongs rather to the specific class or any other class. This allows to obtain binary classification, which enables the application of the regression method for classification. To then decide to which class the set of features belongs, the algorithm will run each model and try the set for each possible outcome. In the end, the class which receives the highest score is chosen by the algorithm as a final answer (Vogiatzis et al., 2021).

In the case of this study, where eight possible outcomes referring to the eight different types of motion are available, the OVR process will train eight different regression classifiers. Each classifier will predict the likelihood of the set of features belonging to one of the motions rather than any other. And the motion receiving the highest fit will be chosen as the predicted motion for the given dataset.

The OVR regression approach for classification is usually described as a simple and intuitive method for multi-label classification. The problem is simplified by having a unique and independent classifier for each different class, which in turn makes the entire algorithm robust and allows it to handle imbalanced class distribution (Brownlee, 2021). Nonetheless, the OVR method may not be ideal for tasks with strong label dependencies as it assumes independence between the labels. This may also lead to issues in the presence of rare classes which would in turn not be treated as such. Further, the algorithm appears to be sensitive to outliers which may have a great impact on the individual binary classifiers.

### 4.5.2 Implementation of the One Vs Rest method

The implementation of the OVR regression within the Python environment is done through the use of the *Scikit-Learn* library. Firstly, a model of linear regression is initiated using the sublibrary *linear_model* and the function *LogicRegression* (Scikit-Learn, 2024b). This defines a classifier which uses logic regression. To settle the initiated model of linear regression into the specific model using the OVR approach, the sublibrary of *multiclass* is used. The function *OneVsRestClassifier* is in turn used to parameter the previously defined model as OVR (Scikit-Learn, 2024d).

This approach provides the exact need for the establishment of a multi-label classifier for the purpose of this research and is hence considered widely sufficient.

## 4.6 Logic Regression (One Vs One)

### 4.6.1 Introduction to the One Vs One method

Another approach to adapt regression to classification problems including more than two possible outcomes is the *One-Versus-One* approach. This approach treats each pair of labels as a separate regression problem by computing an independent prediction system for each pair (Brownlee, 2021). In other words, each pair of labels will be treated as a binary classification problem. This approach hence requires computing a large number of binary classifiers. In fact, for a problem including $k$ different classes a total of $\frac{k\cdot(k-1)}{2}$ different classifiers need to be computed. To predict which class is most likely to be the class of the given set of features, the algorithm will then process through each one versus one by going over each binary classification and the class receiving the majority of votes would then be chosen as the most likely to be the class of the given set of features.

In the case of this study, a total of $\frac{8\cdot7}{2} = 28$ binary classifiers must be modelled to allow the classification of the datasets to the eight possible types of motions that are recorded previously.

This process has several advantages. In fact, it is a simple approach that allows to use of regressive classification for more possible outcomes than simple binary problems. Further, it handles multi-label classification without explicitly considering the possible dependency of the labels. Further, as more regression problems are being run compared to the *One-Versus-Rest* approach, the OVO approach can be expected to provide better classification results. Nonetheless, analogously to the OVR, this approach is very sensitive to outliers and to label dependencies. Furthermore, the large number of systems that need to be computed can quickly become an issue considering the computing capacities. In fact, the number of required classifiers increases with the square of the number of classes.

Nonetheless, for this current research, the number of classifiers that must be computed remains acceptable and hence the OVO regressive classification approach is implemented and tested for the classification problem of the research.

### 4.6.2 Implementation of the One Vs One method

The implementation of the OVO regression within the Python environment is done in a similar way as the OVR approach through the use of the *Scikit-Learn* library. Firstly, a model of linear regression is initiated using the sublibrary *linear_ model* and the analogous function *LogicRegression* (Scikit-Learn, 2024b). This defines a classifier which uses logic regression. To adapt the initiated model of linear regression into the specific model using the OVO approach, the sublibrary of *multiclass* is used. Secondly, the function *OneVsOneClassifier* is used to parameter the previously defined model as OVO (Scikit-Learn, 2024c).

The use of this predefined function allowed the generation classifiers fitting to the exact requirements for the objectives of this study. Hence, the result of the use of the library functions is considered widely sufficient and satisfying.

## 4.7 Random Forest

### 4.7.1 Introduction to the Random Forest method

A classification approach that has been described as getting more and more popular by the days within the research community is the *Random Forest* (RF) classification method (Parmar, Katariya, and Patel, 2019). RF is an ensemble pattern recognition method for classification that proceeds by building a multitude of decision trees during the training phase. In the prediction phase, each tree returns a 'vote' on the predicted class of the

provided set of features. In the end, the algorithm will use the class having received the majority of votes as its final prediction (Parmar, Katariya, and Patel, 2019).

To generate an RF classifier, the following process is followed. Firstly, the training dataset is randomly divided into subsets. Secondly, decision trees are trained using subsets of the training features. For each subgroup within the training data, a decision tree is created. This process is repeated for each multiple feature subset until decision trees have been created for each subset of the training features. (Parmar, Katariya, and Patel, 2019) .

To generate the prediction trees, the algorithm proceeds through bootstrapped sampling. Bootstrapped sampling is a statistical method which draws random subsets of the data repeatedly. This allows some data points to be included multiple times which leads to enhancing the characteristics of the dataset and further, obtaining a more robust model of classification. Using the bootstrapped sampling approach, the RF algorithm trains each single tree based on a unique subset of the data (Parmar, Katariya, and Patel, 2019). Nonetheless, the RF classification algorithm is known to be a 'black box' model, which means that the internal workings of the system cannot easily be interpreted or understood.

The main positive aspects of RF for classification problems are its high accuracy and its robustness towards noise. It is usually described as a great algorithm to avoid overfitting (Parmar, Katariya, and Patel, 2019). Nonetheless, the RF approach can quickly become complex with a larger number of trees which in turn would impact the computational cost. This would especially be an issue for large datasets. Further, the algorithm can also tend to show a bias towards the most represented class, which would result in low performance for the classification of the minority classes.

### 4.7.2 Implementation of the Random Forest method

The implementation of the Random Forest classification within the Python environment is performed using the *Scikit-Learn* library. To establish such a model of RF, the function RandomForestClassifier, from the *ensemble* sublibrary is used (Scikit-Learn, 2024a). This function allows a wide options of parameterising the machine learning model making it highly versatile and adaptable to a wide range of individual situations. Hence, for the purpose of this research, using the function predefined in the *Scikit-Learn* environment appears as widely satisfying and sufficient.

## 4.8 Neural Network

### 4.8.1 Introduction to Neural Networks

Another approach to solving classification problems that has been gaining popularity over the past few years is the neural network. The neural network is a type of machine learning method that is directly inspired by the structure of the human brain (Y.-c. Wu and Feng, 2018). It consists of interconnected nodes which are organised in layers. The first layer receives the input data, which is then processed within the inside layers more commonly called *hidden layers*, and finally, the output layer provides the end prediction. An example of a structure of a neural network is shown in fig. 4.4. This example illustrates a neural network with an input layer (in red), two hidden layers (in blue) and an output layer (in green).

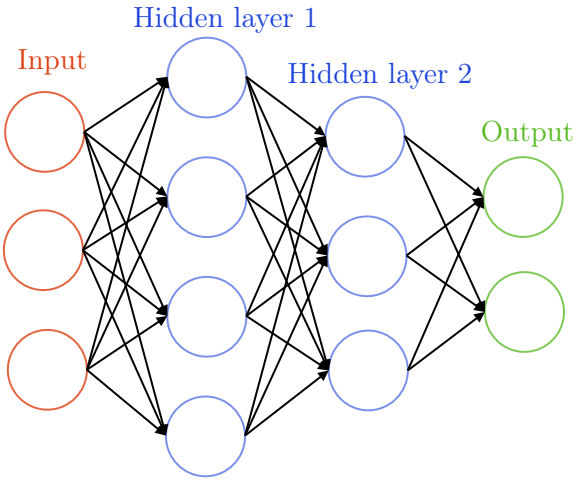


Figure 4.4: Illustration of a neural network with two hidden layers (adapted from Y.-c. Wu and Feng, 2018)

Each node of the neural network can be pictured as a neurone which passes its input through a weighted activation function to produce an output. A commonly used activation function is the sigmoid function provided in eq. (4.7). During the training phase, the weights of the nodes are adjusted based on the error between the predicted and the actual outcomes.

$$\sigma(x) = \frac{1}{1 + e^{-x}} \tag{4.7}$$

Neural networks often include hidden layers between the input and the output. This flexibility in structure makes the neural network a great approach for complex classification problems in a wide range of industries and applications such as information, medicine, economy, control, transportation and psychology (Y.-c. Wu and Feng, 2018). This versatility and adaptability are some of the major strengths of neural networks. Further, other benefits consist in the concept of parallel processing which allows the network to process different tasks simultaneously as the main classification task is being divided within a

multitude of smaller sub-tasks. This enables faster computation.

Nonetheless, the approach of neural networks for classification remains a method demanding computational resources which can sometimes take a consequential amount of time. Further, neural networks are prone to overfitting, which means that the produced model of classification will work very well on the training data without representing the phenomenon from which the data is extracted. Which in turn leads to non-satisfying results in testing. Furthermore, due to its hidden layers, the neural network is a black box method which means that it is not possible to interpret the inner functioning of the system once established. This can be an issue when trying to understand correlation or build an understanding of a physical process.

The neural network approach is a powerful classification method which has shown to be very effective in many applications. Nonetheless, for the purpose of classifying hand motions based on EMG and IMU recordings, no previous study could be found in which neural networks have been used. Hence, it is interesting and crucial to implement the approach and observe its results for this study.

### 4.7.2 Implementation of the Neural Network

The implementation of the Neural Network Method within the Python environment is done differently from the implementations of the previously presented methods. Indeed, Neural Network can become very complex and it is nonetheless crucial to follow the parameters that occur within the process. Hence, the Neural Network is manually defined in Python to ensure that each parameter fulfils the needs and requirements of the purposes of this study.

Overall, one main function is defined. This Python function is used to generate the

adequate Neural Network with the adapted number of neurons and to then train the so-defined model to the available training dataset. The function takes the number of wished training epochs as input and returns the weights of the neural network after its training as output. The epoch is a concept which refers to the number of passes through the entire training dataset that occurs in the training process. Two independent neural networks are defined. A first one with one hidden layer and a second one with two hidden layers, where the two-layer model is used to try to add complexity and eventual accuracy to the classification.

The function initializes the weights with random values and then iterates through the specified number of epochs. Being able to parameterise the number of epochs allows the testing phase to try out a range of parameters and obtain statements on which epoch is best suited for the classification problem given the specific training dataset. Within each epoch, the function goes through each training sample and performs a forward pass to obtain a classification output. It then computes the error and updates the weights using backpropagation. To obtain the values of backpropagation, the previously presented sigmoid function given in eq. (4.7), is implemented within the Python environment. After having gone through all the epochs, the final weights defining the neural network are returned. This neural network can then directly be used for prediction using the testing dataset.

This implementation is straightforward and simple, yet offers the possibility to control with precision each parameter as well as the functioning of the generation of the Neural Network, enabling customisation to best fit the objectives of this research.

## 4.9 Techniques of result analysis

Following the establishment of the general procedures of pre-processing and extraction of features, and the presentations of all the used machine learning approaches and how those are implemented, the tools which will be utilised to obtain information on the results obtained during the process of pattern recognition and classification must be presented.

The general approach to identify and graduate the result of a classification procedure is based on the visual method of the confusion matrix. A confusion matrix is a table that compares the real labels of the dataset to the labels that the machine learning method predicted for the dataset. The most basic and standard way to visualise a confusion matrix is in a two-dimensional state where the classification only has two possible outcomes, positive or negative. Such a two-dimensional confusion matrix is given in fig. 4.5. This illustration can easily be understood with the example of trying to predict if a patient suffers from a sickness. In this case, the real labels state whether the patient is *positive* or negative to the sickness. The classification process predicts the health status of the patient based on other features and provides its prediction. The true positives (TP) are subjects who are positives and are predicted correctly as positives by the classification process. The true negatives (TN) represent the subjects who are negative to the sickness and are identified as such by the classifier. These two categories correspond to the true categories, which indicate the datasets which the classifier correctly predicted. On the opposite, the false positives (FP) are subjects who are negatives but are labelled as positives by the classifier. The false negatives (FN) are subjects who are positive but are predicted to be negative. The FP and the FN are categories which represent cases in which the classifier wrongly attributed the subject, i.e. the set of features of the subject to the wrong label. The concepts of TP, TN, FP, and FN are the bases on which all the analyses of the performance of the classification process are set.

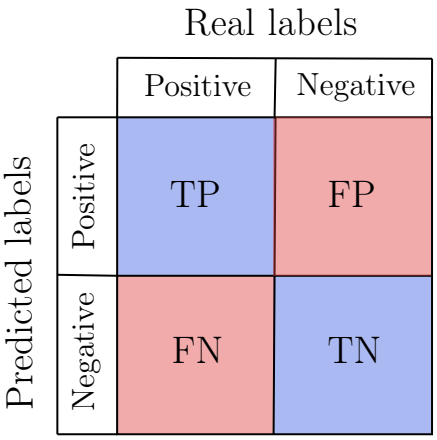


Figure 4.5: Basic confusion matrix (adapted from Mohajon, 2020)

The general confusion matrix represents cases where only two labels are available as outcomes. Nonetheless, in certain cases such as in this study, the possible outcomes are more numerous than two. Hence, in order to obtain an analysis of the performance of the classification, the basic concept of a two-dimensional confusion matrix can be expanded into an $n$-dimensionality as follows. The illustration of such an extended $n$-dimensional confusion matrix is shown in fig. 4.6 (Mohajon, 2020). In this case, it can be seen that the labels 1 to $n$ are displayed within a square matrix. The diagonal represents all the labels that are correctly predicted by the classifier. The other entries however represent the datasets where the classifier predicted the wrong label for the provided data element. The first column for example shows all the elements that are in truth from the first label, however only the elements which are in the first row and have been predicted correctly.

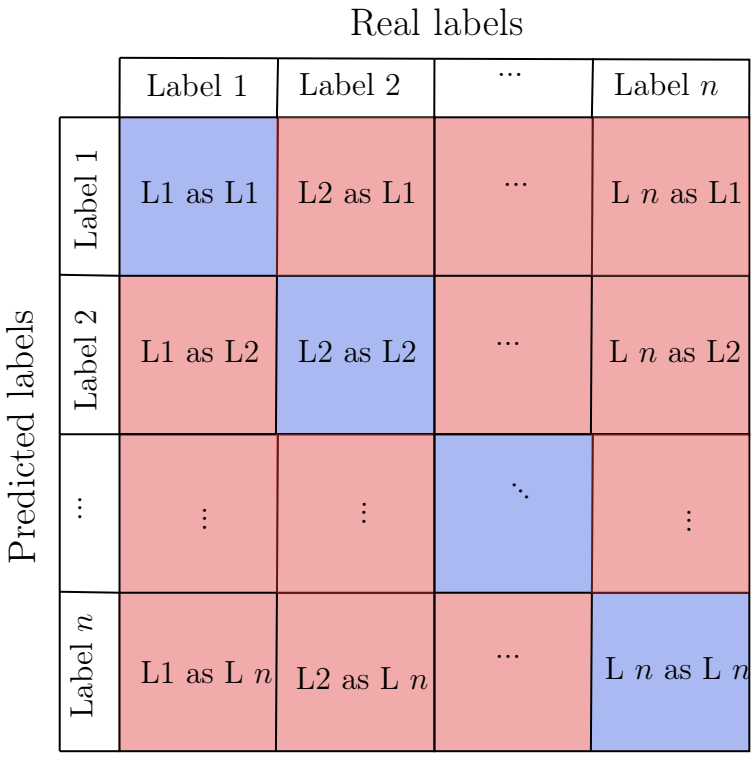


Figure 4.6: Illustration of an $n$-dimensional confusion matrix

In an $n$-dimensional confusion matrix, the concept of positive and negative that is detailed previously can also be applied. This can be done by considering each label individually. By taking into account the label $x$ as positive, any other label would become negative. In this case, a binary classification can be seen, and the previously introduced concepts of TP, TN, FP, and FN can be adapted. This adaptation is especially interesting and necessary for further analysis which relies on features that will be detailed in the following section. To extend these concepts to the $n$ dimension, each label is considered individually, which means that the TP, TN, FP and FN will vary depending on which label is considered (Mohajon, 2020). For the $x$ label, the TPs are the elements from label $x$ which are correctly classified as label $x$. The TNs are all the elements which are not from $x$ and are labelled as not being from label $x$. The FPs are the elements which are not from label $x$ but are classified as label $x$. And lastly, the FNs are elements which are not labelled as $x$ but are in fact labelled $x$. An illustration of this adaptation to the $n$-dimension is shown in fig. 4.7. In this example, the second label is picked out and the

TPs, TNs, FPs, and FNs are shown in the confusion matrix.

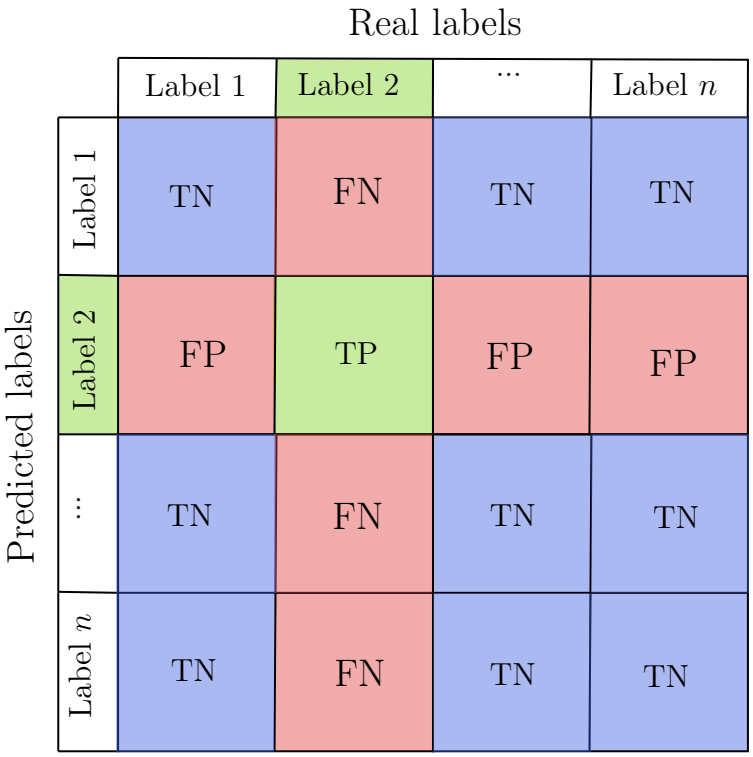


Figure 4.7: Illustration of an $n$-dimensional confusion matrix

In the following segments, the specific analysis features that can be obtained from a confusion matrix are explained and detailed. The main feature that can be obtained from a confusion matrix is the overall accuracy. It describes how well an $n$-dimensional classification is performed by giving the quotient of the sum of all correctly attributed elements (the diagonal shown in fig. 4.6) and all the elements that are classified, hence the global accuracy is defined in eq. (4.8).

$$\text{Accuracy} = \frac{\text{Correctly classified elements}}{\text{All classified elements}} \tag{4.8}$$

The next features that can be extracted from the confusion matrix are, for the case of a confusion matrix of n-order for $n$ label, dependent on the label that is being analysed as has been previously illustrated in fig. 4.7. The first feature that can be extracted is the label-specific accuracy. It is defined as the quotient of the true positives (TP) and the sum of all the elements available that have been classified. The label-specific accuracy is defined in eq. (4.9) (Mohajon, 2020).

$$\text{Label Accuracy} = \frac{TP + TN}{TP + TN + FP + FN} \tag{4.9}$$

The next feature that can be extracted from the $n$- dimensional confusion matrix is precision. The precision is a feature that indicates the proportion of elements that are classified as the label of interest that are actually from this label. The label precision is obtained by dividing the number of TPs by the sum of TPs and FPs, as shown in eq. (4.10) (Mohajon, 2020).

$$\text{Label Precision} = \frac{TP}{TP + FP} \tag{4.10}$$

Following, the next feature that can be extracted is the label-specific recall rate. It indicates the proportion of elements from the label of interest that is classified correctly as the label being analysed. The label-specific recall rate is obtained by dividing the TPs by the sum of TPs and FNs, as shown in eq. (4.11) (Mohajon, 2020).

$$\text{Label Recall} = \frac{TP}{TP + FN} \tag{4.11}$$

Lastly, the last feature that can be extracted from the confusion matrix that is used in this case study is the F1 rate. It can be mentioned that more features can also be extracted such as the misclassification rate or the specificity, nonetheless, those are not as informative in this case and are hence not extracted in the analysis process to ensure a better readability of the results. The label-specific F1-rate combines the precision and the recall rate into a single feature and can be calculated as defined in eq. (4.12) (Mohajon, 2020).

$$\text{Label F1-Rate} = \frac{\text{Precision} \cdot \text{Recall}}{\text{Precision} + \text{Recall}} = \frac{2TP}{2TP + FP + FN} \tag{4.12}$$

To conclude, the analysis of the results obtained from the classification processes will mainly be performed through the concept of the confusion matrix. The confusion matrix is usually defined as a two-dimensional concept but is expanded to fit the classification problem of higher dimensions. Various features which can be extracted from confusion matrices of $n$ order are defined. The main feature is the overall accuracy which delivers information on the accuracy of the classification process.

# 5 Models Implementation

This section details several individual models that are designed to classify the recorded data back to the type of motion. In this context, a model is defined by the use of certain specific features. In fact, for each mode approach, several pattern recognition methods that have been presented in the previous section are used. Nonetheless, it is the level of features that impacts the resulting classification. The objective of this section is henceforth to develop various models, each with various objectives as to create knowledge towards the main objective of this research. It can be reminded at this point that the main target is to obtain a statement on the feasibility of a control scheme based on pattern recognition that would classify hand motions from the forearm, and ideally wrist area.

## 5.1 First Model: Basic Time Features

### 5.1.1 Model Definition

The first model approach uses the most standard and common features provided by the literature research. Past studies have in fact mainly concluded that the best features to use when studying EMG signals and trying to classify the signals back to a previously defined motion for varied applications are time-domain features. In particular, the most commonly encountered features and those usually described as the most information-carrying as shown in table 2.3.Those features are the mean absolute value (MAV), the waveform length (WL), the root mean square (RMS) and the zero crossing rate (ZCR). Those features have all also been defined in eq. (2.5) to eq. (2.9).

Therefore, it is reasonable to use those four features as a first base to test the implemented methods of pattern recognition. The definition of the first model is hence given in model 5.1.

**Model 5.1:** Basic Time Features

**Input signals:**

- **EMG:** ch1, ch2, ch3, ch4
- **IMU:** $a_x$, $a_y$, $a_z$

**Preprocessing:**

- Normalisation
- Bandpassfilter (20Hz, 250Hz) & Notch-filter (50Hz)

**Features:**

- **Time-Domain:** MAV, WL, RMS, ZCR
- **Frequency-Domain:** /

### 5.1.2 Model Results

The previously defined model approach is then applied to each of the presented machine learning algorithms that have been detailed in the previous section.

For the kNN algorithm, a range of values of k is tested from $k = 1, \ldots, 50$. The resulting accuracies for each value of k within this range are shown in fig. 5.1. Overall, although a brief increase can be observed at the start for small values of k, the accuracy swiftly drops with an increasing value of k. This phenomenon can be understood due to the limited number of data representing each motion. Hence, a maximum in accuracy is reached at 0.69 for $k = 4$.

Another classification method for which the main parameter is tested and adapted iteratively as a range of values is the neural network approach. In this case, the parameter that is tested is the epoch value, or the number of passes through the entire training

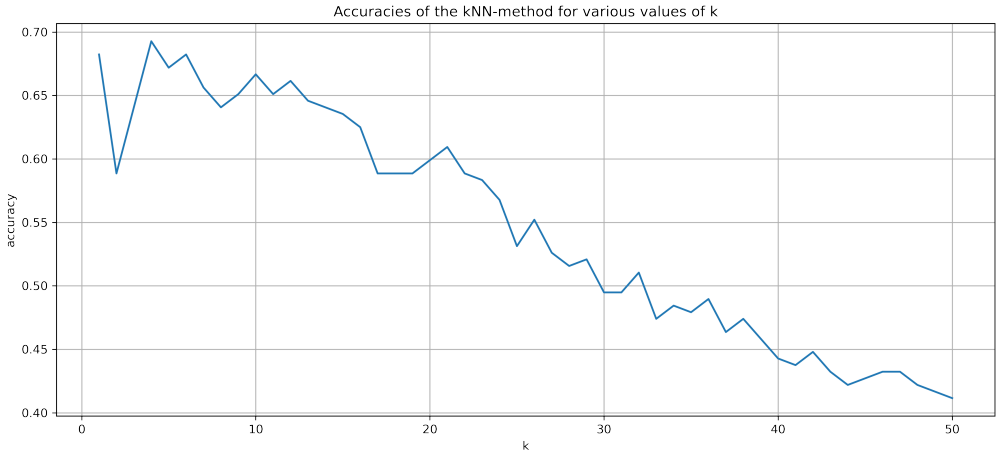


Figure 5.1: Accuracy of the classification over the value of k for the kNN algorithm using the pattern of Model 1

dataset that occurs in the training process. Values from 100 to 5000 with a step of 100 are tried out. The resulting accuracies are shown in fig. 5.2. It can be seen that for values from 100 to around 1500, the accuracy gradually increases. After this, it reaches a maximum accuracy of around 0.53, a value around which the increase in the number of epochs only has a small impact. This random 'noise' around this value of accuracy despite the increase in the epoch value can be understood by the concept of the neural network. Indeed, the process always starts by setting the weights of the neural network at random values. Hence, from a certain level of epoch, or passes through the dataset, the weights reach a maximal adaptability over which an increase in passes only has a small influence. And further, the random set of the starting weights also impacts the end results as running the same process twice will never return the exact same accuracy. Nonetheless, it can be seen that the maximal accuracy is reached for a value of 4000 epochs and this accuracy is at 0.57.

The overall accuracies of each of the classification methods for the first model are summarised in table 5.1. This overall accuracy expresses the proportion of motions that

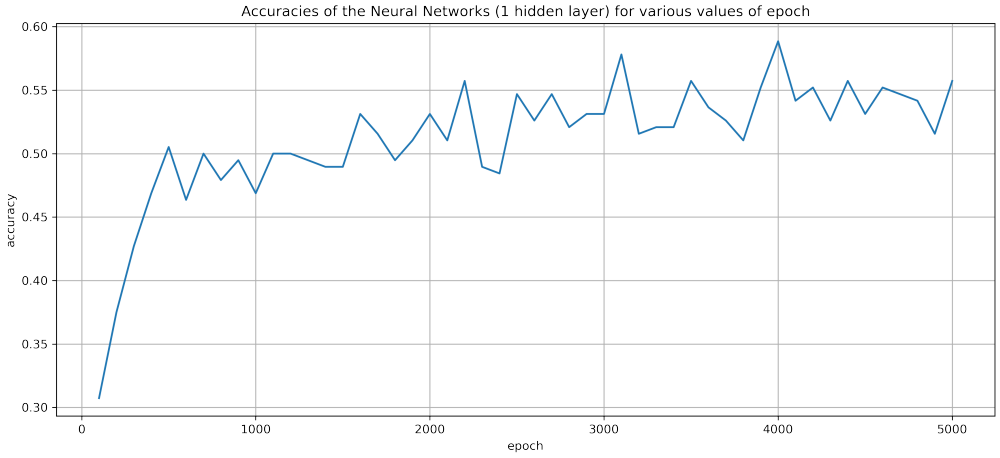


Figure 5.2: Accuracy of the classification over the value of epoch for the Neural Network algorithm with 1 hidden layer using the pattern of Model 1

are identified correctly by the classifier within the testing dataset regardless of the type of motion. The higher the accuracy, the more motions have been identified correctly. The threshold of randomness is at 0.125, as a total of eight motions are possible and hence, the classifiers have the choice between eight individual outcomes. Therefore, a classifier that would predict the motion on a total random base would have an expected accuracy of 0.125.

It can be seen that most methods have an accuracy that ranges between 0.6 and 0.7, which can already be considered satisfying, taking into account that no optimisation has been done at this point and that only the most basic and common features have been implemented within the model. The machine learning algorithm that provides the best accuracy is the one-versus-one regression with an accuracy of 0.71.

Nonetheless, an exception occurs with the case of the Gaussian-Naïve-Bayes which has an accuracy significantly lower than the other approaches with a value of 0.39. This worse result can be explained by the nature of the GNB method, which is based on

| Pattern Recognition Method | Accuracy |
|---|---|
| kNN | 0.69, k=4 |
| GNB | 0.39 |
| OVR | 0.69 |
| OVO | 0.71 |
| RF | 0.68 |
| NN-1 | 0.57, p=4000 |
| NN-2 | 0.57 |

Table 5.1: Summary of the accuracies obtained for the process for the model 1

Gaussian distribution. Hence, this classifier is not very effective in cases where the data distribution does not follow such a Gaussian distribution. Therefore, it is likely that the provided dataset of features does not follow such a distribution and hence the result of the classification is not ideal.

Two different neural network methods have been implemented for the first model. A first one with a single hidden layer (NN-1) and a second one with two hidden layers (NN-2). The neural network with a single hidden layer is tested on various values of the epoch, and the best resulting accuracy is obtained for $p = 4000$. Due to computational limitations, such an iteration could not be performed with two hidden layers, hence the epoch is set at p=1000, which is the value of epochs observed in the one hidden layer model, from which accuracy starts to settle, and minimal increase follows. The resulting accuracies of both neural networks are slightly lower than the other well-performing methods, both with results of respectively 0.57.

The accuracies provided and summarised in table 5.1 are obtained using the confusion matrices of each method. Those confusion matrices are shown in fig. 5.3. It can be

mentioned that for visual reasons and purposes of consistency, the confusion matrix of the neural network with two hidden layers is not provided. For most of the confusion matrices, a clear diagonal of correctly classified motions can be observed. The confusion matrix that most comes out and differs from the other is the confusion matrix for the GNB approach shown in fig. 5.3b. This indicates the lesser performance of the GNB approach for the purpose of this research.

From these confusion matrices, a broad observation can be made that certain motions have sometimes been mistakenly identified as another more recurrently. For instance, motion number 8 has repeatedly been wrongly identified as motion number 3 by all the classifiers. This may eventually be explained by the closeness and similarity of those two motions, yet this observation cannot be made in the other way. In fact, motion 3 has rarely been identified as motion 8.

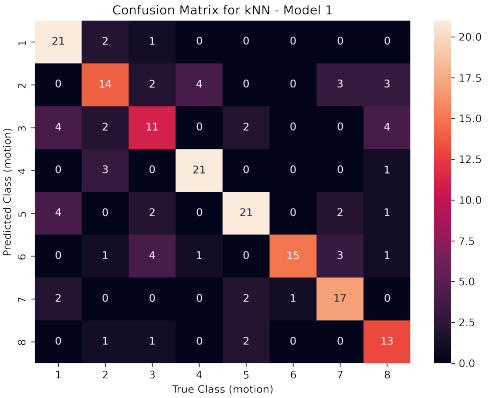


(a)

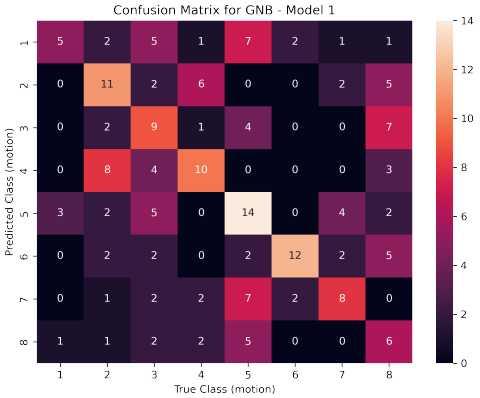


(b)

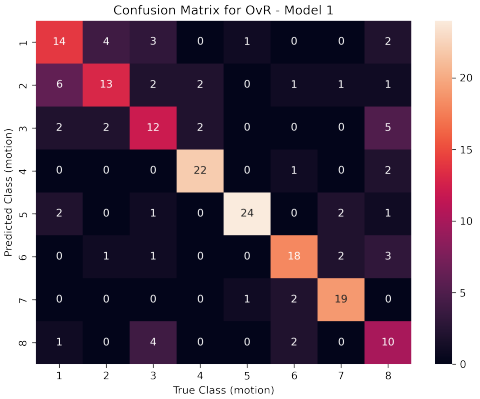


(c)

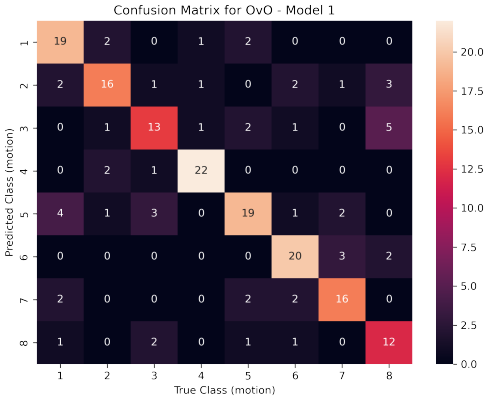


(d)

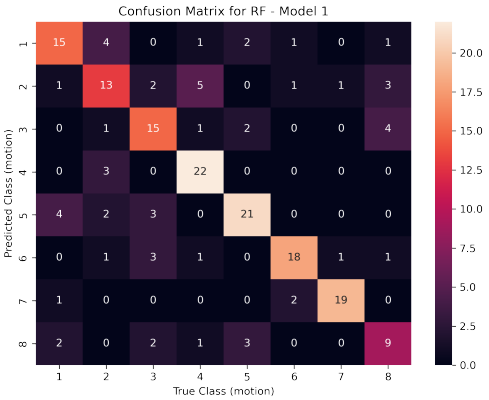


(e)

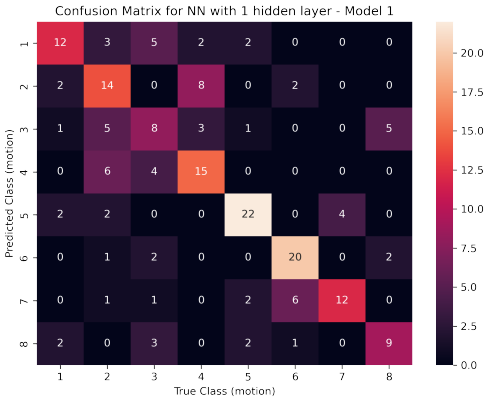


(f)

Figure 5.3: Confusions matrices for Model 1, for classification methods : (a) kNN ; (b) GNB ; (c) OVR ; (d) OVO ; (e) RF ; (f) NN with 1 hidden layer

## 5.2 Second Model: Basic Time and Frequency Features

### 5.2.1 Model Presentation

A surprising statement that has come up during this research is the fact that past studies claimed features from the frequency domain did not lead to any improvement when trying to recognise patterns within EMG signals being recorded on similar motions (Simao et al., 2019 & Samuel et al., 2019). Despite this claim, the second model aims to improve the results obtained by the first model by expanding the basic set of features from the time domain with the most common feature from the frequency domain: the mean frequency $f_{mean}$.

Hence the second model can be defined as in model 5.2. The input signals and the preprocessing are the same as in the first model. Further, the features from the time domain are also kept identical. The only expansion is that the second model now has a new feature, from the frequency domain: $f_{mean}$.

---

**Model 5.2:** Basic Time and Frequency Features

---

**Input signals:**

- **EMG:** ch1, ch2, ch3, ch4
- **IMU:** $a_x$, $a_y$, $a_z$

**Preprocessing:**

- Normalisation
- Bandpassfilter (20Hz, 250Hz) & Notch-filter (50Hz)

**Features:**

- **Time-Domain:** MAV, WL, RMS, ZCR
- **Frequency-Domain:** $f_{mean}$

---

### 5.2.2 Model Results

This subsection now details the results of the classification performed by the pattern recognition algorithms based on the second model.

Analogously to the previous model, the value of k is also iteratively tested for the kNN model. Similarly, a range of values from $k = 1, \ldots, 50$ is tested. The best value of k is found at $k = 7$ with a best accuracy of 0.71. Similarly to the observation made for model 1, a slight increase in accuracy can be observed at the beginning of the increase in the value of k, but from a certain value around 7 or 8, a linear decrease in accuracy can be seen. Analogously, this phenomenon can be explained by the limited number of elements of the same motion available within the dataset and hence in the test set. This has as a consequence that from a certain value of k, the neighbours that are taken into consideration to predict which motion the element comes from are not from the same motion anymore as too many non-relevant items are being considered.

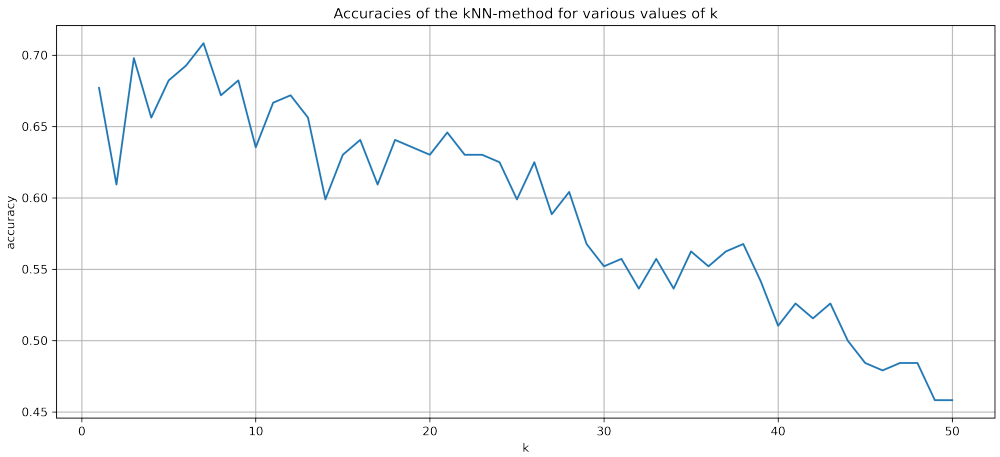


Figure 5.4: Accuracy of the classification over the value of k for the kNN algorithm using the pattern of Model 2

Furthermore, the process of iteration to determine an adequate value of epoch for the

neural network with a single hidden layer is also performed, with an epoch value ranging from $p = 100, \ldots, 5000$ in steps of 100. The resulting value of accuracy over the set value of the epoch is shown in fig. 5.5. A quick increase can be observed at the start as the accuracy ascents rapidly from around 0.25 to around 0.55 within the first few increases. From a value of $p = 700$, the accuracy remains around 0.55 with a noisy behaviour around that value. A maximal value is reached at $p = 4900$, with an accuracy of 0.57. Nonetheless, this maximal value is different every time the classification is reset. This can be understood by the fact that the initial weights are set randomly and that the final result is very dependent on those. This phenomenon has already been observed for the first model but is especially clear in this example.

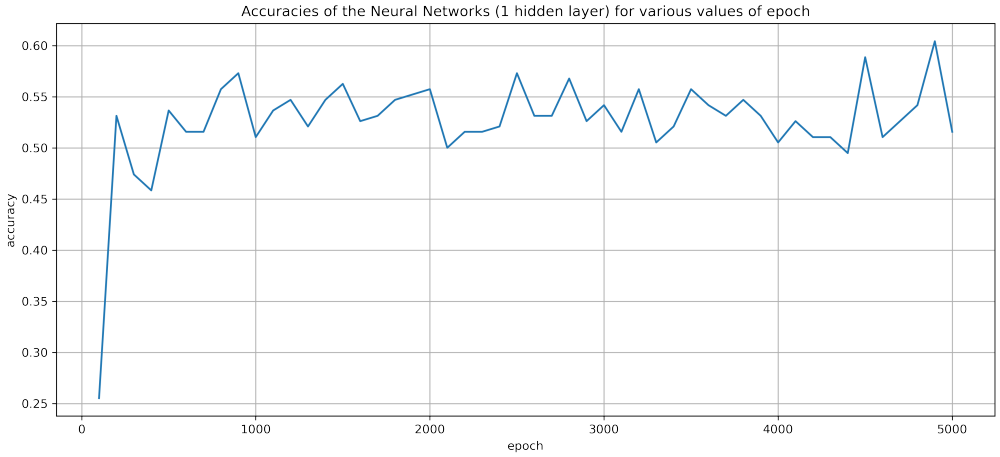


Figure 5.5: Accuracy of the classification over the value of epoch for the Neural Network algorithm with 1 hidden layer using the pattern of Model 2

All the overall accuracies obtained by each of the machine learning methods for the second model are summarised in table 5.2. The first observation that can be made is that each individual accuracy is higher compared to the accuracies obtained for the first model. Most methods have an accuracy that ranges between 0.7 and 0.8, with a minimal accuracy anew set by the GNB method at 0.46. This again remains the lowest result,

illustrating that no clear Gaussian distribution is included within the recorded dataset.

The highest accuracy is reached by the one-versus-one regression method with a value of 0.81. Such a level of accuracy can already be considered very satisfying. All the results despite the GNB approach can be considered satisfying at this stage. Naturally, the bad results of the GNB can also be related to the likely non-gaussian distribution of the dataset. Hence, it can be summarised that a clear increase in accuracy, regardless of the use method of pattern recognition, can be observed when adding a basic feature from the frequency domain. However, this increase is considerably higher for certain methods compared to others. For instance, the accuracy of the OVO method increases by 0.1, while the accuracy of the kNN approach only rises by 0.02. Hence, it can be concluded that the observation and derived statements made in previous research claiming that features from the frequency domain only have minimal impact on pattern recognition for EMG signals (Samuel et al., 2019) do not exactly meet the observation that can be made in this current study. It can be mentioned that this increase is highly dependent on the method and approach of machine learning used in the process. And additionally, it must be kept in mind that the current research is further using IMU signals and extracting features from those, which is not performed in the past research and may hence be an additional explanation for the difference in observation. Nonetheless, this result illustrates the impact that frequency domain features can have in the melioration of accuracy.

The confusion matrices resulting from the classifications of the second model are given in fig. 5.6. Similarly to the results of the first model, clear diagonals are visible representing the correctly recognised motions. The analogous observation made previously about the recurring confusion between certain motions can be made in this case, too. In fact, motions 2 and 4 are usually mixed up, this is especially visible for the RF prediction in fig. 5.6e. And the motions 3 and 8 are also confounded on several predictions.

| Pattern Recognition Method | Accuracy |
|---|---|
| kNN | 0.71, k=7 |
| GNB | 0.46 |
| OVR | 0.76 |
| OVO | 0.81 |
| RF | 0.74 |
| NN-1 | 0.67, p=4900 |
| NN-2 | 0.64 |

Table 5.2: Summary of the accuracies obtained for the process for the model 2

This is especially to be seen in the predictions of the OVO in fig. 5.6d and OVR in fig. 5.6c.

## 5.3 Third Model: Dimensionality Reduction

### 5.3.1 Introduction to dimensionality reduction

At this point, a model that delivers satisfying results has been obtained. Nonetheless, this model includes a total of 5 features for each signal which may eventually deliver analogous information to the classifiers. This can be investigated through a feature correlation analysis. A correlation score is a measure that describes the degree to which two variables change together. A positive correlation suggests that as one variable increases, the other tends to increase, while a negative correlation indicates that as one variable increases, the other tends to decrease.

The relevance of such an examination is to attempt to reduce the number of features used in the model while keeping similar accuracy levels in the classifications. By reducing the number of features, the model would become more robust and would further require

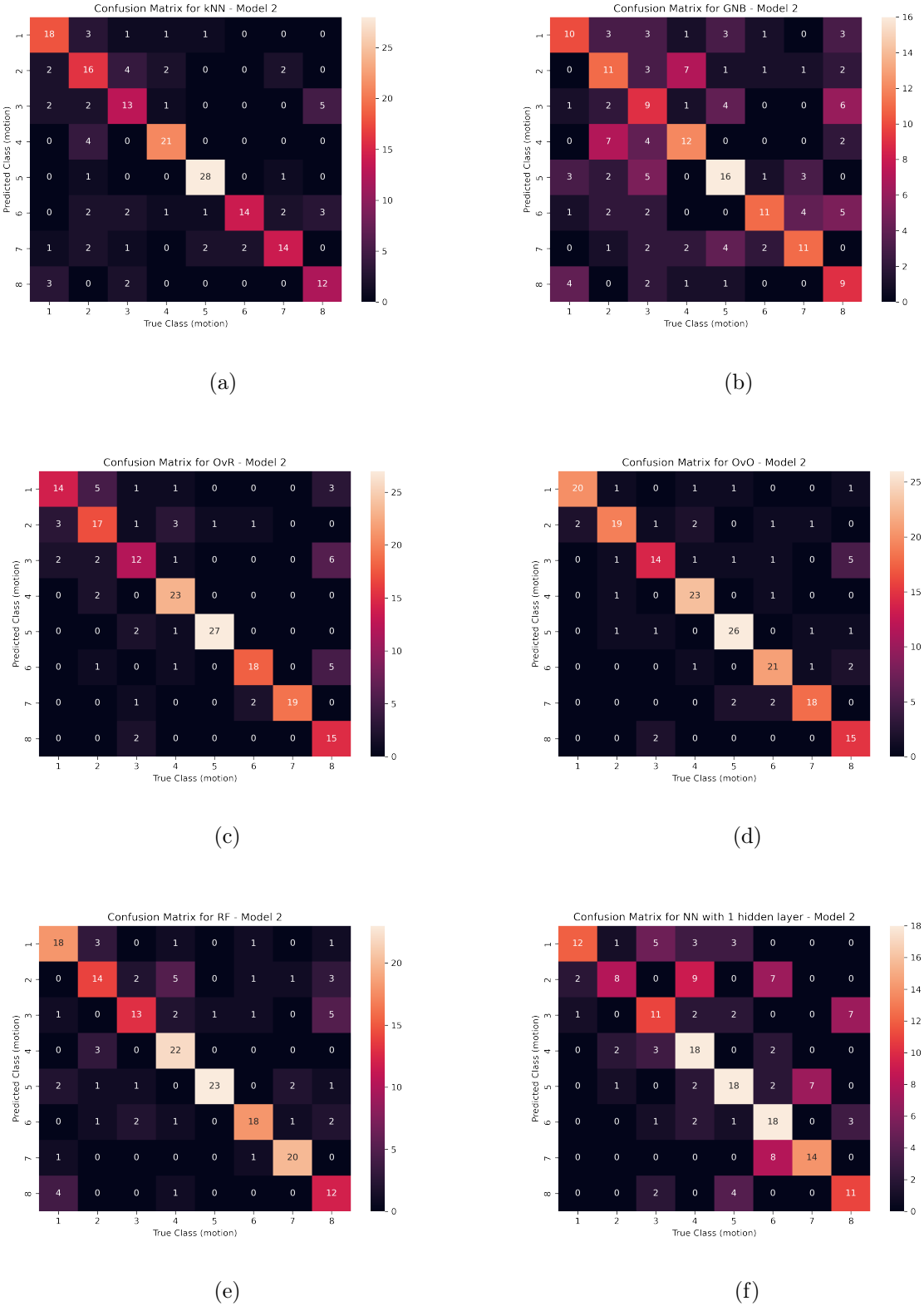


Figure 5.6: Confusions matrices for Model 2, for classification methods : (a) kNN ; (b) GNB ; (c) OVR ; (d) OVO ; (e) RF ; (f) NN with 1 hidden layer

less computation time. Which in case of a real-time implementation of the model would be highly beneficial and required. In fact, simpler models are less prone to lagging and hence of great importance when considering the quality of the final system.

Hence, a correlation analysis is performed on the features that are extracted on model 2. To do so, the *.corr()* Python function for pandas Dataframe is used (pandas, 2024). The result is a square matrix that gives the correlation score between all the provided features. The correlation scores are then rounded for clarification purposes and transcribed as a heat map, to allow a better visualisation of the result of the analysis. The result is given in fig. 5.7.

The first element that can distinctively be observed is the diagonal of one. This diagonal is characteristic of a correlation matrix as it represents the correlation between a feature and the feature itself, which is hence always one. The next obvious element that can be noticed is the three-by-three squares of high correlation score that appear clearly thanks to the heatmap. Those squares hence emerge as bright areas. These squares represent areas of very high correlation with at least 0.8 for the top left areas and 0.6 for the bottom right squares. These squares illustrate the assumption that within a kind of signal (EMG or IMU), the features MAV, RMS and WL have a high to very high linear correlation.

These observations linked to the definition of the MAV and RMS would suggest that the different channels of EMG display proportional variations in magnitude. In fact, MAV and RMS measure signal magnitude, and are features based on the average absolute magnitude and root mean square magnitude, respectively. The same observation can be made for the various channels of the IMU. Further based on the definitions of those features, considering the high correlation with the WL, it can be suggested that the signals exhibit

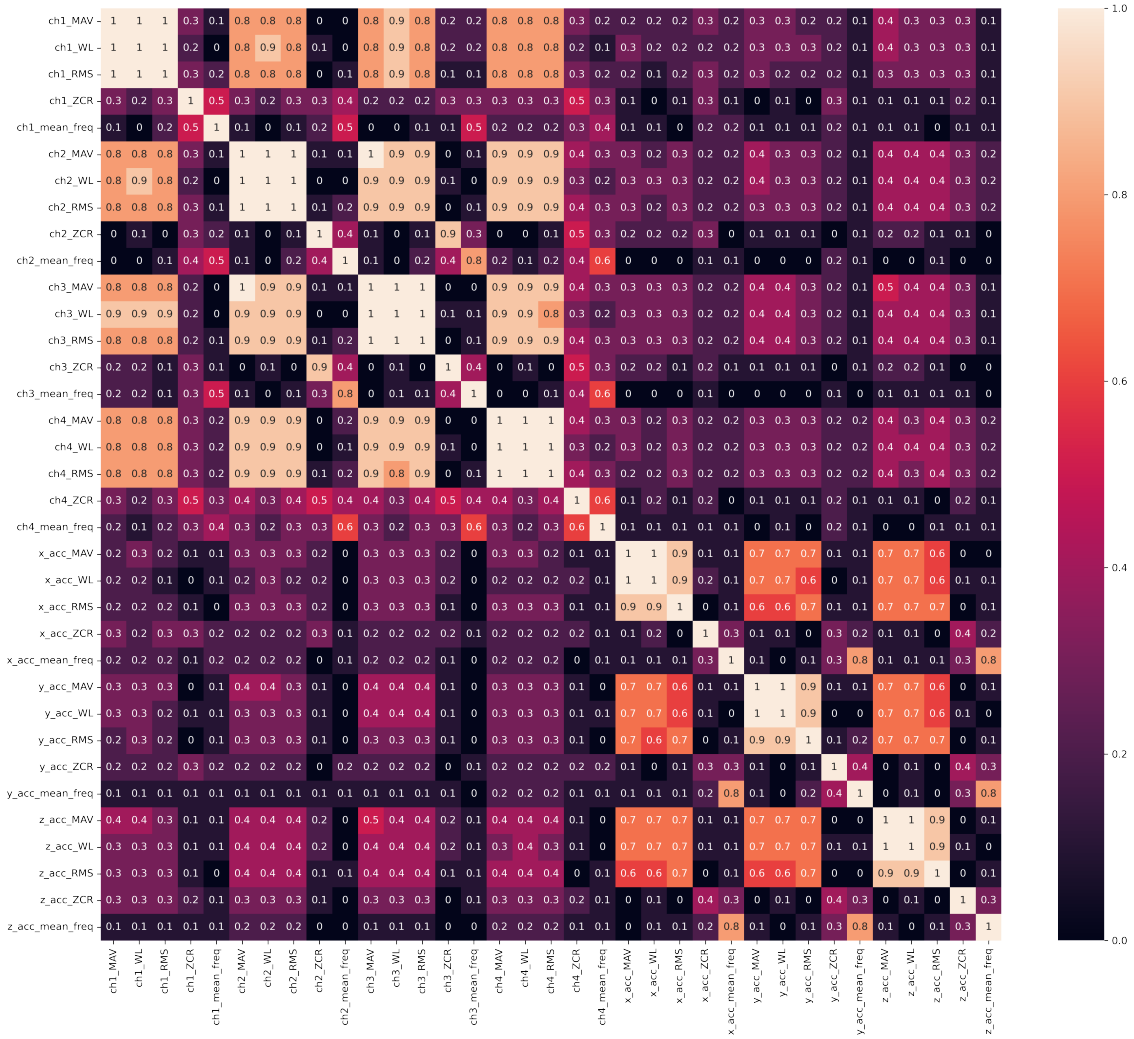


Figure 5.7: Correlation Matrix for the features extracted in model 2.

consistent patterns of both magnitude and variation.

On the opposite, no such observation can be made for the results of the correlation analysis for the ZCR and the mean frequency. Indeed, those two features show low to very low levels of correlation towards any other features, and towards the same feature applied on other channels or signals.

Henceforth, keeping in mind the idea of reducing the dimension of the list of features that is being fed to the classifying algorithms, the following statements can be made. The high level of correlations between the MAV, the RMS and the WL suggests that those features deliver analogous information or at least very correlated information. Following this conclusion, it appears possible to proceed to the dimensionality reduction by keeping only one of those three features. It would then be assumed that the resulting accuracy would remain analogous regardless of which of these features are kept, and that the overall accuracy would only slightly be affected by dropping two of those.

Accordingly, three tests are run by defining three test models based on model two, with the specificity that each test only includes one of the three features from MAV, RMS and WL. All the other parameters of the previously presented second model are kept analogous. The resulting accuracies of the outcoming classifications are given in table 5.3.

Overall, the first assumption that using either of the features would result in a similar accuracy can be confirmed. Indeed, for each machine learning method, the resulting accuracy is relatively close for each of the dimensional reduction approaches. However, comparing these results with the original results of the second model illustrates that the accuracy of the classification has been affected negatively by the dimensional reduction despite having removed features that are highly to very highly correlated with each other.

Some possible explanations can eventually be suggested for the observation of the drop in accuracy. Firstly, it is clear that by removing features, even if highly correlated with remaining features, a loss in information occurs. Despite the strong bond some features have shown with each other, certain data might in truth come up as complementary and have a positive impact on the classification process. The positive impact that is lost

| | kNN | GNB | OVR | OVO | RF | NN-1 | NN-2 |
|---|---|---|---|---|---|---|---|
| Model 2 (reference) | 0.71 | 0.46 | 0.76 | 0.81 | 0.74 | 0.57 | 0.64 |
| MAV only | 0.65 | 0.47 | 0.67 | 0.71 | 0.73 | 0.57 | 0.57 |
| RMS only | 0.62 | 0.52 | 0.71 | 0.74 | 0.72 | 0.58 | 0.64 |
| WL only | 0.65 | 0.48 | 0.67 | 0.73 | 0.70 | 0.55 | 0.64 |

Table 5.3: Summary of the accuracies obtained while testing the different possible approaches of dimensional reduction based on Model 2.

through their removal and hence followed by the drop in accuracy. Secondly, the additional data may better highlight certain redundant aspects of patterns that come up for similar types of motions. The dimensionality reduction would then lead to a loss of this emphasising, which could be compared with a picture becoming blurrier and hence harder to recognise. Thirdly, the stability of the model may also have been impacted. It can be kept in mind that the number of data available is limited and hence having a greater number of features is a possible tool that can be used to make changes more obvious for the model that gains in robustness. On the other hand, reducing the number of features may destabilise the model and eventually support the loss in resulting accuracy. Fourthly, by reducing the number of available features on which the pattern recognition algorithms can base themselves, the risk of overfitting is increased. Further, past research has shown that including correlated features within pattern recognition applications reduces overfitting issues (Subramanian and Simon, 2013). This can be understood through the idea that correlated data can act as a regularisation that transcribes major trends more clearly.

These various suggestions of explanations support the observation that a slight decrease in accuracy occurs when removing highly to highly correlated features and suggests that keeping such features is beneficial for the final result of the model and classification.

### 5.3.2 Model Definition

As it has been shown that the removal of either RMS, MAV and WL deliver the same resulting accuracy, the definition of the third model is established using a random feature out of those, and as the RMS seems to have very slightly higher resulting accuracies, the third model is defined using the RMS. The model definition is provided in Model 5.4. The model definition is analogous to the definition of the second model, with the difference that the MAV and the WL are now dropped.

---

**Model 5.3:** Dimensionality Reduction

---

**Input signals:**

- **EMG:** ch1, ch2, ch3, ch4
- **IMU:** $a_x$, $a_y$, $a_z$

**Preprocessing:**

- Normalisation
- Bandpassfilter (20Hz, 250Hz) & Notch-filter (50Hz)

**Features:**

- **Time-Domain:** RMS, ZCR
- **Frequency-Domain:** $f_{mean}$

---

### 5.3.3 Model Results

The detailed resulting accuracies that the third model returns upon classification are summarised in table 5.4. A brief observation can be made that the overall resulting accuracies are indeed lower than the ones obtained with the classification process using the second model. Nonetheless, not all machine learning methods suffer from the same loss.

In fact, if the loss is considerable for the kNN (from 0.71 to 0.62), or for the OVO (0.81 to 0.74), certain classifiers have in truth a slight increase in the resulting accuracy. For example, when comparing the reduced model to the original one, the GNB increases its accuracy from 0.46 to 0.52, and the neural network with one hidden layer improves it from 0.57 to 0.58. This observation shows that the overall result of the model of dimensionality reduction has on average lower results, but that this statement can only be fully applied to specific machine learning methods as for certain approaches, the accuracy has in truth been improved. This allows to conclude that the dimensionality reduction is a great methodology to improve the simplicity and robustness of systems and reduce their computational requirements while overall keeping great accuracy.

| Pattern Recognition Method | Accuracy |
|---|---|
| kNN | 0.62, k=9 |
| GNB | 0.52 |
| OVR | 0.71 |
| OVO | 0.74 |
| RF | 0.72 |
| NN-1 | 0.58, p=800 |
| NN-2 | 0.64 |

Table 5.4: Summary of the accuracies obtained for the process for the model 3

The confusion matrices obtained from the results of the classifications of the main machine learning methods using the third model are shown in fig. 5.8. These support the observation made previously, that the overall accuracy has dropped as more misplaced motions are now clearly visible within the matrices.

An element of high interest in those matrices is again the fact that certain motions

are recurrently identified as the same wrong other motion. This recurrent confusion is especially visible for motion type 8, being identified as motion type 3. This particular case occurs for all the different machine learning approaches which illustrates again that the classifier is not the main element that justifies such recurring misclassification but suggests rather that similar motions may induce similar features. This is supported by the fact that this phenomenon is even more visible in the model of dimensionality reduction which includes a very reduced number of features. Hence, feature similarity would play a bigger role, and in turn, the increase misclassification supports the theory that similar motions induce similar features.

## 5.4 Fourth Model: Expansion model

### 5.4.1 Introduction to the model reduction

The previous model illustrated that a dimensional reduction can be performed without a considerable loss in accuracy but with a great increase in model simplicity. Nonetheless, at this stage, only the basic and most commonly used features from the time and the frequency domain have been implemented and used in the development of the models. However, many other features can be added to this, from which certain have been described in certain studies to be of high relevance when addressing EMG-related classification problems as is shown in table 2.3. For this purpose, the model that is introduced in the following section is an expansion of the reduced model presented previously. The aim is to study how the addition of a selection of further features from the time and the frequency domain can have an impact on the accuracy of the resulting classification.

The following subsection introduces the further added features and provides some general information on those and their characteristics. The added features from the time domain are the WAMP, the SSC, and the VAR. From the frequency domain, the PSD is

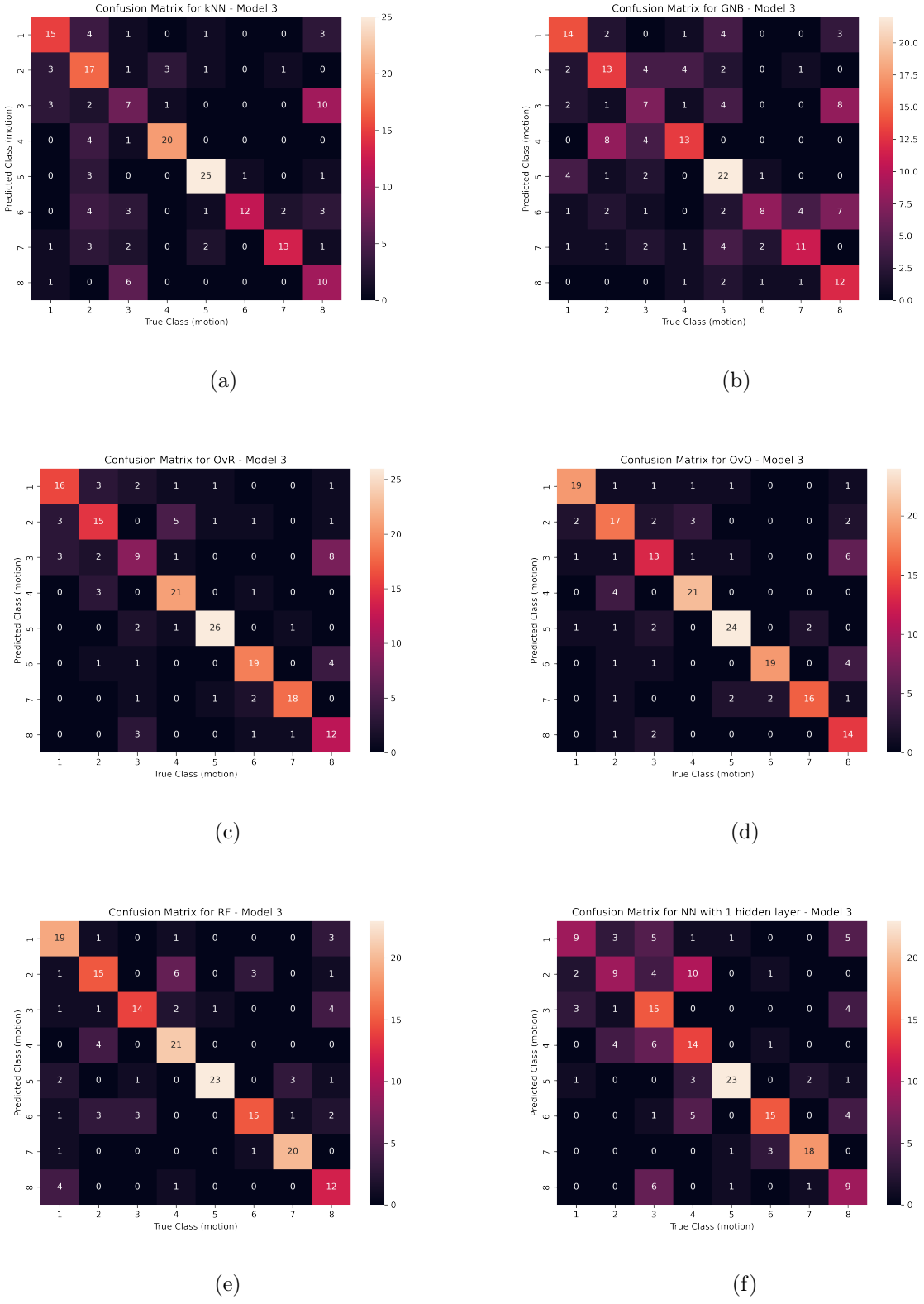


Figure 5.8: Confusions matrices for Model 3, for classification methods : (a) kNN ; (b) GNB ; (c) OVR ; (d) OVO ; (e) RF ; (f) NN with 1 hidden layer

implemented.

The Willison amplitude (WAMP) describes a measure of the changes within the signal and is obtained by establishing the number of times that the difference of two consecutive points exceeds a certain threshold (Xi et al., 2017). The slope sign changes (SSC) is a count of the number of times that the sign of the slope of the EMG signal changes (Torres-Garcıa et al., 2022). The variance (VAR) is the measure of the average power of the signal (Xi et al., 2017). And lastly, the power spectral density (PSD) describes the power held within the signal for each frequency (Maral, 2003).

The additional consideration of those features is expected to provide additional information which should in turn allow the classifiers to recognise the patterns within the data to a more extensive degree and hence provide an improved accuracy compared to the model that did not consider those features.

The model of feature expansion is defined in Model 5.4

**Model 5.4:** Expansion Model

**Input signals:**

- **EMG:** ch1, ch2, ch3, ch4
- **IMU:** $a_x$, $a_y$, $a_z$

**Preprocessing:**

- Normalisation
- Bandpassfilter (20Hz, 250Hz) & Notch-filter (50Hz)

**Features:**

- **Time-Domain:** RMS, ZCR, WAMP, SSC, VAR
- **Frequency-Domain:** $f_{mean}$, PSD

### 5.4.2 Model Results

The resulting accuracies obtained from the classifications using the fourth model which includes the additional features are provided and summarised in table 5.5.

The first major observation that can be made is that despite the addition of selected features the overall accuracies have close to not been affected compared to the model of dimensionality reduction presented previously. For the neural network with a single hidden layer, the accuracy even dropped from 0.58 to 0.39, which is a very unsatisfying accuracy level. In the following, possible explanations for such an occurrence are provided.

Firstly, one of the most likely explanations for the previously made observation is that the increased complexity of the model made it harder for classifiers to identify the patterns within the datasets. The resulting computational inefficiencies might have a great negative impact on the classification. And in this same idea, the increase in the number

of features might also have induced an overfitting within the classification. Indeed, it is likely that the pattern recognition algorithms may have learned from the noise within the data rather than from the true patterns. This phenomenon is especially likely to occur in larger datasets and is hence a likely explanation for the observation.

Secondly, the additional data may lack quality. The new features are more complex to compute and hence it is likely that those may come up as noisier or even with a certain degree of error. The erroneous information would in turn affect the classification negatively. Additionally, the added features are added based on the expectation that they would deliver information relevant to the requirement of this research. Nonetheless, those may also have been irrelevant or redundant and in turn, provide only little information related to the motion. The possible deterioration of data quality and relevance is another likely element that supports the observation made previously.

And lastly, in addition to those possibilities, the additional features might even lack any underlying relationship with the concept of the different individual motions. This might also explain the poorer performances of the classifiers and hence lead to worse results.

Further, the confusion matrices that the fourth model classifications have produced are shown in fig. 5.9.

## 5.5 Fifth Model: Optimised model

### 5.5.1 Introduction to model optimisation

The results of the study on dimensional reduction and feature expansion illustrate a key concept in the establishment of systems and models, the idea of the Bias-Variance Trade-off. This concept is a visual method to understand that as the complexity of a model

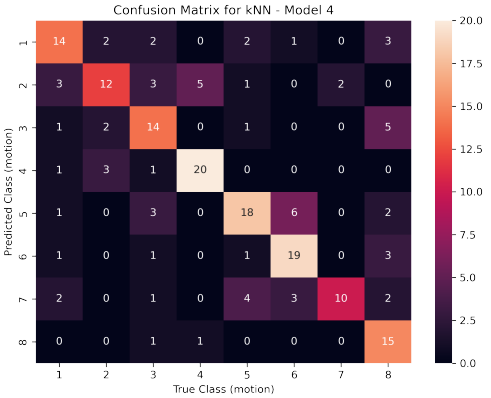


(a)

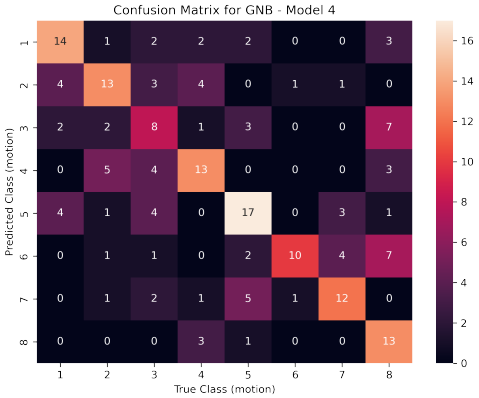


(b)

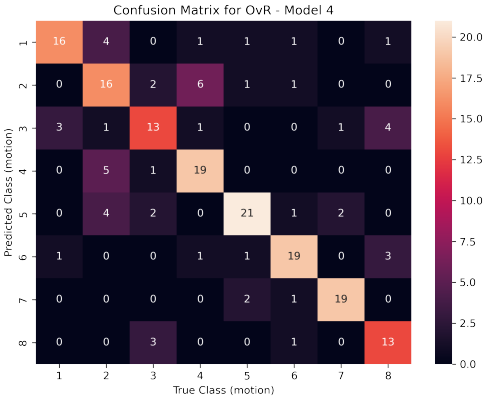


(c)

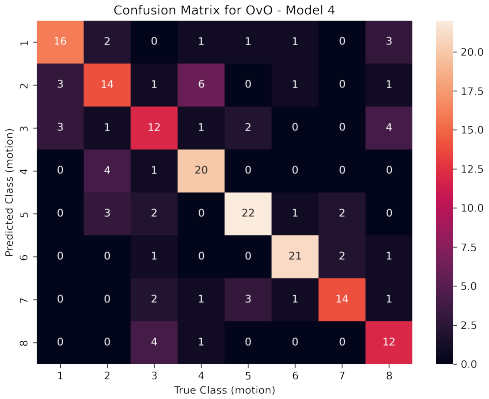


(d)

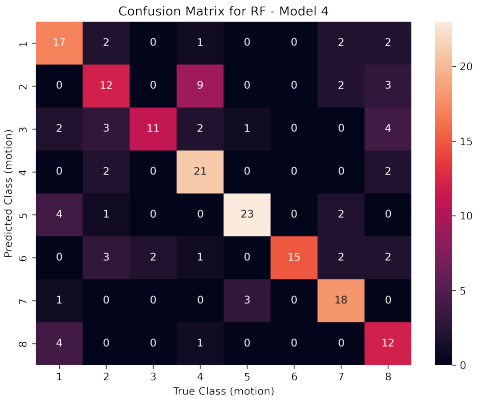


(e)

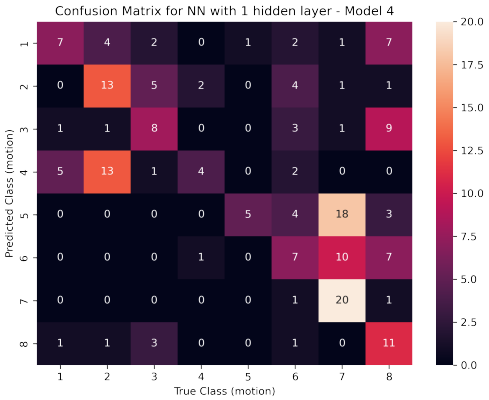


(f)

Figure 5.9: Confusions matrices for Model 4, for classification methods : (a) kNN ; (b) GNB ; (c) OVR ; (d) OVO ; (e) RF ; (f) NN with 1 hidden layer

| Pattern Recognition Method | Accuracy |
|---|---|
| kNN | 0.64, k=1 |
| GNB | 0.52 |
| OVR | 0.71 |
| OVO | 0.68 |
| RF | 0.67 |
| NN-1 | 0.39, p=3900 |
| NN-2 | 0.58 |

Table 5.5: Summary of the accuracies obtained for the process for the model 4

increases, the bias falls and the variance increases, which leads to a characteristic U-shaped error curve (Neal et al., 2018). In other terms, the Bias-Variance Tradeoff concept illustrates that there is a right balance between the simplicity and the flexibility of a model for which the error of the model would be minimal. In this context, the concept of bias can be understood as the degree of simplification of the model that is induced within the application. A higher bias would in turn signify that the problem has been very simplified. On the other hand, the variance increases with the sensitivity of the model, hence it is a measure to express the complexity of the model.

An illustration of the concept of the bias-variance tradeoff is provided in fig. 5.10. The relationship between the variance or complexity, and the bias or simplification is visible. The main idea of the concept is to visualise that there is a perfect balance between the complexity and simplicity of a model which leads to the optimised model, with a minimal error. This concept has been observed in the models of dimensional reduction and the model of feature expansion. Henceforth, to optimise the model, the balance between complexity and simplicity must be found.

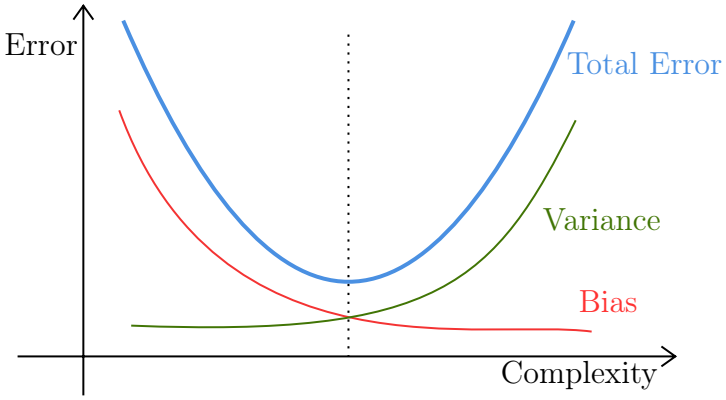


Figure 5.10: Illustration of the bias-variance tradeoff (adapted from Neal et al., 2018)

### 5.5.2 Optimisation Process

The key idea of the optimisation process is hence to find the optimal equilibrium between the simplicity and complexity of the model in order to reach the ideal point of minimal error, as suggested in the concept of the bias-variance tradeoff. To do so, several tests are run to try to obtain an overview of the influence of each feature on the resulting accuracies of the classifiers. The following subsection summarises these tests briefly and gives an explanation for each modification that is made between the tests.

The first test consists of analysing the role that the ZCR and the SSC may have on the resulting classification. For this purpose, four test models are created. At first, the MAV and the WL are reintroduced. Despite their high level of correlation with the RMS, it has been observed that correlated features can be a great support for classifiers. The four test models withhold as basic features the MAV, WL, RMS, VAR and mean frequency. Each test model will then also consider either the ZCR or SSC, or both, or neither. The results are summarised in table 6.1.

The first observation that can be made from table 6.1 is that most results are very similar, as the majority of the accuracies obtained for the same machine learning approach vary only lightly within the different test models. Nonetheless, it appears that the

| | ZCR | SSC | kNN | GNB | OVR | OVO | RF | NN-1 | NN-2 |
|---|---|---|---|---|---|---|---|---|---|
| Test 1 | | | 0.69 | 0.46 | 0.77 | 0.79 | 0.71 | 0.57 | 0.63 |
| Test 2 | x | | 0.71 | 0.48 | 0.76 | 0.82 | 0.69 | 0.48 | 0.68 |
| Test 3 | | x | 0.71 | 0.49 | 0.73 | 0.79 | 0.71 | 0.51 | 0.68 |
| Test 4 | x | x | 0.70 | 0.49 | 0.73 | 0.78 | 0.71 | 0.55 | 0.57 |

Table 5.6: Summary of all the accuracies obtained for the test models and all the machine learning approaches.

test models that only include either the SSC or the ZCR, hence the tests two and three, have slightly higher average accuracies than the two other models. This can eventually be brought back to the bias-variance tradeoff, considering that those two features are so similar, that only a little additional information is added when considering both. Hence, following the illustration of the tradeoff phenomenon shown in fig. 5.10, when neither the ZCR nor the SSC is considered, the test model is too simple. On the other hand, when both are taken into account, the complexity is too high, and hence the resulting error also increases. However, when only one of them is considered, the right balance between complexity and simplicity is reached as the accuracies appear to be at the maximum.

Similar tests have been run for various possible combinations and have resulted in the establishment of an optimised model, which maximises the benefits learned from the bias-variance tradeoff. Those tests have suggested,among others, that the removals of the WAMP and the PSD are beneficial for the resulting accuracy. The resulting optimised system is presented in the following subsection.

### 5.5.3 Model Presentation

The definition of the optimised model is given in 5.5. It can be observed that this model and the model that resulted from the basic time and frequency features are very similar. The only major difference is the addition of the VAR. In fact, the tests made previously lead to the conclusion that including many more features does not conduct to any consequential improvement. Henceforth the model given in Model 5.5 appears to be the best model for the given available dataset and objectives of the research.

---

**Model 5.5:** Optimised Model

---

**Input signals:**

- **EMG:** ch1, ch2, ch3, ch4
- **IMU:** $a_x$, $a_y$, $a_z$

**Preprocessing:**

- Normalisation
- Bandpassfilter (20Hz, 250Hz) & Notch-filter (50Hz)

**Features:**

- **Time-Domain:** MAV, WL, RMS, ZCR, VAR
- **Frequency-Domain:** $f_{mean}$

---

### 5.5.3 Model Results

The results of the classifications are given in fig. 5.11. The main observation that can be made is the presence of clear diagonals for each machine learning approach. Nonetheless, it can further be said that no major difference would discern these confusion matrices from those obtained from the classifications made previously using the previously presented models.

Nonetheless, the great balance between complexity and error limitation suggests that this model is a great compromise which fits the understanding of the bias-variance trade-off and consequently, this model can be seen as the optimal model for the purposes and objectives of this research.

## 5.6 Sixth Model: Optimised model - Wrist Only

### 5.6.1 Motivation for the 'wrist only' application

The main objective of this research is to establish an understanding of the applicability of the use of the combination of EMG and IMU signals measured on the wrist to control systems. If the use of EMG and IMU signals has been analysed in the previous models, certain EMG channels have been measured outside of the wrist area. This is done to follow recommendations and learnings from past studies, which are also made easy to implement through the available channels of the EMG sensor. Nonetheless, to fulfil the purposes of the research it is imperative to run the optimised model without the external channels and limit the data recording to the wrist area.

This can be done by dropping the irrelevant channels from the optimised model. The EMG has four channels. The first two channels (ch1 and ch2) are placed on the inner side of the elbow also known as *anticubital fossa*. The two next channels (ch3 and ch4) are then placed on the wrist area. To fulfil the requirements of wrist limitation, the first two EMG channels must hence be dropped.

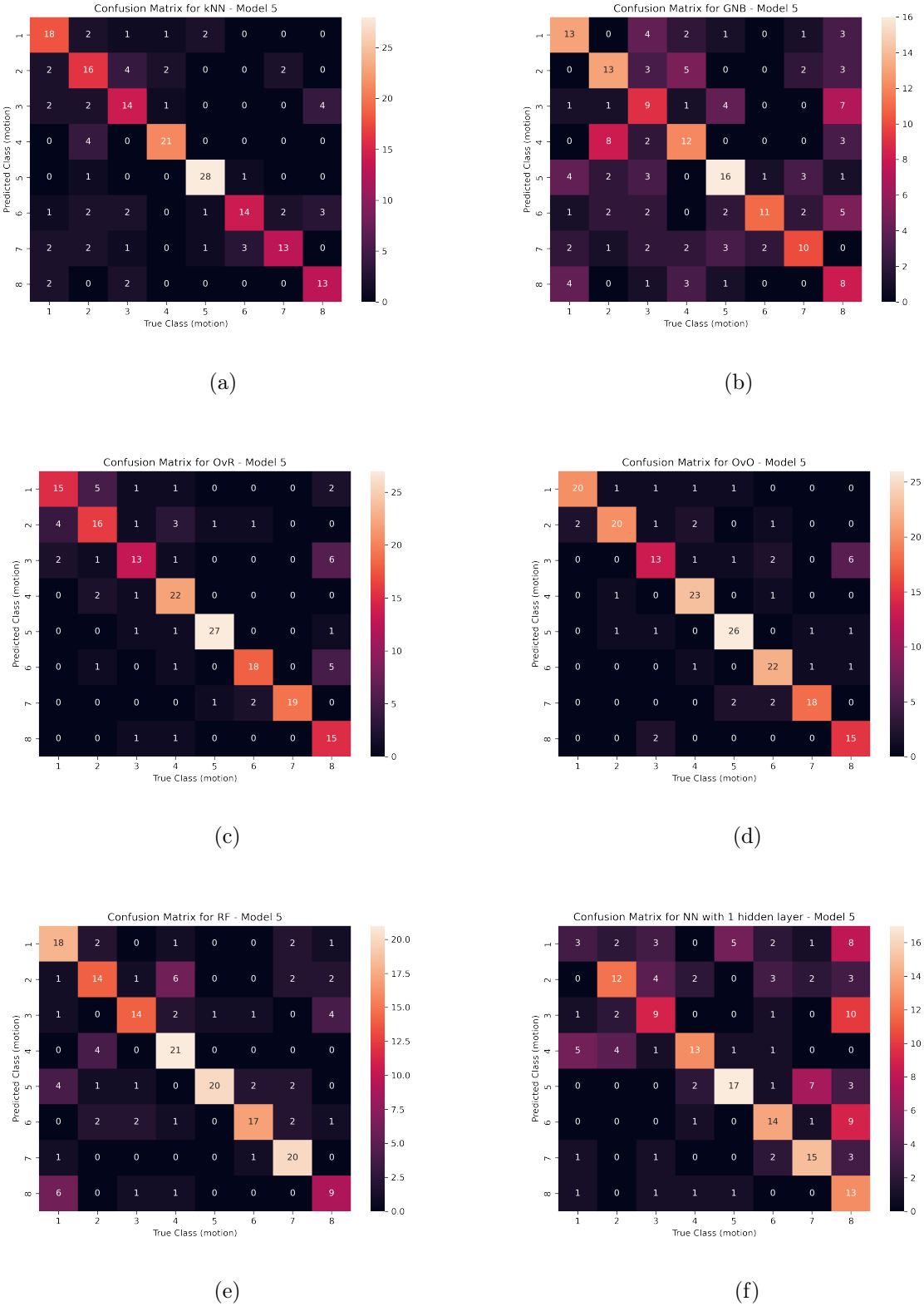


Figure 5.11: Confusions matrices for Model 5, for classification methods : (a) kNN ; (b) GNB ; (c) OVR ; (d) OVO ; (e) RF ; (f) NN with 1 hidden layer

### 5.6.2 Presentation of the 'wrist only' model

The optimised model settings are shown in Model 5.6. It can be seen that the only difference between this model and the optimised model that has been presented previously is that this model now only includes two out of the four EMG channels that are included previously. The only remaining channels are those measured from the wrist area (channel 3 and 4).

---

**Model 5.6:** Optimised Model

---

**Input signals:**

- **EMG:** ch3, ch4
- **IMU:** $a_x$, $a_y$, $a_z$

**Preprocessing:**

- Normalisation
- Bandpassfilter (20Hz, 250Hz) & Notch-filter (50Hz)

**Features:**

- **Time-Domain:** MAV, WL, RMS, ZCR, VAR
- **Frequency-Domain:** $f_{mean}$

---

### 5.6.3 Results of the 'wrist only' model

The resulting accuracies of the classifications made using the 'wrist only' model are given in table 5.7. It can directly be seen that the overall accuracies are considerably lower than those of the optimised model, which use the same features but including all the channels of the EMG. Several explanations can be brought up for this observation.

Firstly, a loss of information occurs by removing two input channels. It has been shown

| Pattern Recognition Method | Accuracy |
|---|---|
| kNN | 0.59, k=1 |
| GNB | 0.44 |
| OVR | 0.68 |
| OVO | 0.69 |
| RF | 0.64 |
| NN-1 | 0.47, p=600 |
| NN-2 | 0.56 |

Table 5.7: Summary of the accuracies obtained for the process for the model 6

that hand motions are intertwined with the forearm muscles (Rangayyan, 2015). Hence, it is very likely that removing the signals that are directly related to the activity of those muscles serves as a clear explanation for the observed loss in accuracy. The remaining signals may not describe the occurring motions as well or are not supported by highly motion-correlated signals.

Secondly, the previously suggested equilibrium between complexity and simplicity may be broken by removing those signals. In fact, the bias-variance tradeoff may not be ideal anymore hence leading to a reduced accuracy. In this same idea, the loss of EMG channels seems to have an influence on the differentiation of similar motions. Indeed, an observation is made with the previous models that similar types of motions tend to be mixed up by the classifiers, often ending up as having a great number of a certain motion wrongly recognised as another. The similar motions may in fact produce very similar IMU signals as the motions produce the same wrist acceleration, and the differenciation occurs in more subtile parts of the hands and fingers which can only be analysed through the recording of EMG signals. For this reason, it appears clear that reducing the number of EMG channels while keeping the same number of IMU channels reduces the influence

of the EMG data compared to the IMU. Hence, the signals that would allow identifying more subtle differences become a lesser proportion of the entire dataset. Consequently, it becomes harder for the classifier to differentiate between similar types of motions. This can be observed in the resulting confusion matrices provided in fig. 5.12.

Thirdly, with a limited number of inputs, it is likely that the model also lost some of its robustness. In fact, outliers may not be identified as well as previously, given that the amount of information on each motion is now reduced.

To conclude, the results obtained when using only the channels measured from the wrist area are slightly lower in accuracy of classification compared to those obtained when further considering measurements from the forearm area. Possible explanations for this observation can be the simple loss in information, the broken equilibrium between complexity and simplicity and between the IMU and EMG channels which makes it harder for classifiers to differentiate similar motions and the loss in robustness. Despite the loss in accuracy, it can be concluded that the results of the 'wrist only' model are sufficient and still reflect an overall successful classification and identification of the type of motion.

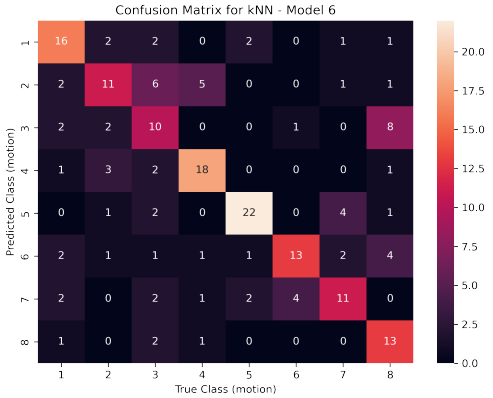


(a)

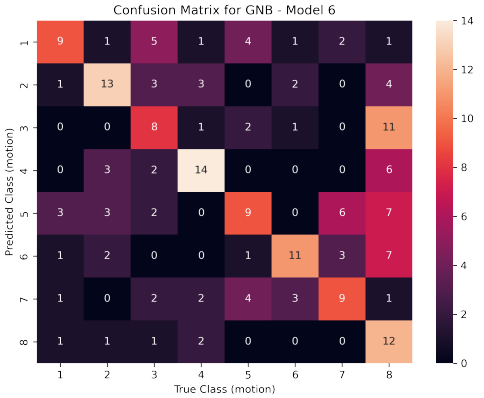


(b)

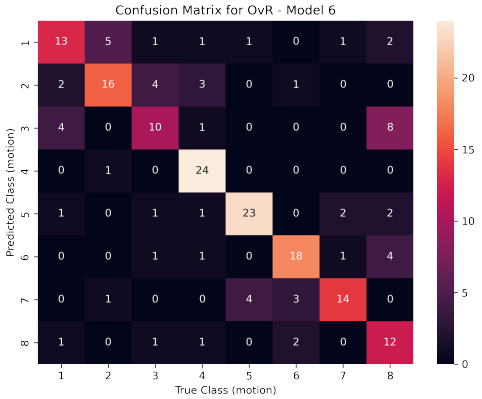


(c)

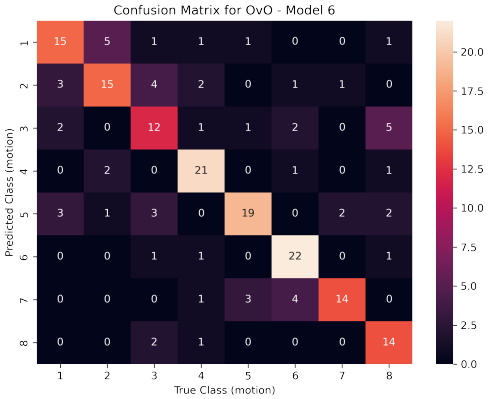


(d)

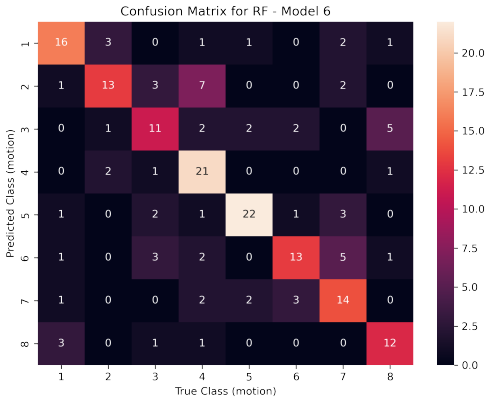


(e)

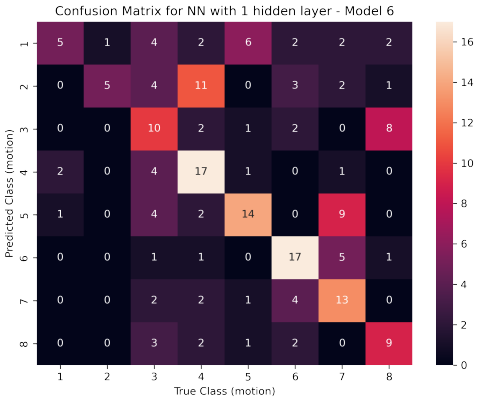


(f)

Figure 5.12: Confusions matrices for Model 6, for classification methods : (a) kNN ; (b) GNB ; (c) OVR ; (d) OVO ; (e) RF ; (f) NN with 1 hidden layer

# 6 Analysis

This section aims to summarise the general results obtained from the different models and the various accuracy levels obtained from the following classifications. Based on this analysis, a conclusion on implementability and suggestion of applicability of the introduced technology within the industry can be made. Finally, this section aims to suggest how future studies could expand the resulting suggestions to make its implementations wider and better suited to the probable future requirements of the society.

## 6.1 General Results

All the resulting accuracies obtained from the classifications are summarised in table 6.1. Each used model is mentioned by number and name, and the resulting accuracies for each of the different machine learning approaches are given. The main observation that can be made is that the accuracies do not strictly increase with the evolution of the model. In fact, the idea of this research has much more been to explore the possibilities of the utilisation of specific features for various signals and channels which in turn lead to the establishment of an optimised model.

Another major observation that can be made is that each machine learning approach reacts differently to each change in the specification of the models. This can be explained by the pre-made assumptions in the model design on which a specific machine learning approach might be based. As each classification method is defined using an assumption that the dataset describes a certain pattern, the change in used features impacts the resulting pattern that the dataset describes. This explains the different impact that the feature change has on the various pattern recognition algorithms.

A further important observation that can be made is that the utilisation of the basic

features from the time domain already provides a high level of accuracy. Further improvement and tests that enhance these basic features with further features also including some from the frequency domain allow to increase in the resulting accuracies. Nonetheless, the fact that basic time domain features provide such great results suggests that the data may include a certain level of consistency and distinctive patterns. This is an element that supports the suggestion that each motion has produced unique sequences within the recorded signals which could in turn be identified by the classifiers. This distinctiveness within the patterns can however be limited by the further observation that the additional consideration of frequency domain features has a positive impact on the resulting accuracies. Nonetheless, the increase in correctness is only little, yet non-neglectable.

A further observation is the fact that neural networks do not provide the best levels of accuracy through the research. If no past study using neural networks for any kind of similar application is found, great hope had been set in their implementation for this research. Certain possible explanations can be made to suggest the observed lesser levels of accuracy of the resulting classifications. Firstly, neural networks usually require a consequential amount of data to become effective. Hence, it might be that the provided limited dataset did not allow the neural networks to recognise the correct patterns. This is especially possible considering the likely complexity of the data combined with the limitation of data which in turn might encourage overfitting. Further, the nature of the recorded data which comes from human-based reproduction of motions is very prone to lack of exactitude which can be compared to a high level of noise. This is a further element that can be considered to explain the lesser results of the neural network. A possible way to increase the resulting accuracies of the neural network would hence be to record further datasets and increase the available data from which the neural networks can learn.

Another main observation that can be made from table 6.1 is the fact that the re-

| | kNN | GNB | OVR | OVO | RF | NN-1 | NN-2 |
|---|---|---|---|---|---|---|---|
| Model 1 (basic t) | 0.69 | 0.39 | 0.69 | 0.71 | 0.68 | 0.57 | 0.57 |
| Model 2 (basic t & f) | 0.71 | 0.46 | 0.76 | 0.81 | 0.74 | 0.57 | 0.64 |
| Model 3 (dim. reduction) | 0.62 | 0.52 | 0.71 | 0.74 | 0.71 | 0.58 | 0.64 |
| Model 4 (dim. expansion) | 0.64 | 0.52 | 0.71 | 0.68 | 0.67 | 0.39 | 0.58 |
| Model 5 (optimised) | 0.71 | 0.48 | 0.76 | 0.82 | 0.69 | 0.48 | 0.68 |
| Model 6 (opt. - wrist only) | 0.59 | 0.44 | 0.68 | 0.69 | 0.64 | 0.47 | 0.56 |

Table 6.1: Summary of all the accuracies obtained for all the models and all the machine learning approaches.

sulting accuracies obtained from the classifications made with the sixth model, the model using only the channels that measured signals directly in the wrist area do not meet the high levels obtained by the previous models. The accuracies can still be considered satisfying with highs at almost 0.7, yet the observation is made that this is considerably lower than for the previous models. The suggested possible explanations for this can be the simple loss in information, the broken equilibrium between complexity and simplicity and between the IMU and EMG channels which makes it harder for classifiers to differentiate similar motions and the loss in robustness. Nonetheless, despite this loss in accuracy, the results of the model solely using the channels measured from the wrist area still reflect a reasonable accuracy which suggests that patterns can be identified from EMG and IMU signals measured from the wrist which in turn allows the recognition of the kind of motion that is performed by the subject.

## 6.2 Analysis of the results

The main conclusion that can be made based on the previously presented results is that the classification of hand motions based on forearm and wrist EMG and IMU measurements is possible. The previously acquired results allow to conclude that hand motions generate specific EMG and IMU signals which can in turn be measured, recorded and analysed to obtain information on the performed motion.

This concept is especially visible in the several confusion matrices that are provided throughout the research. In fact, motions that show similar attributes when being performed tend to generate similar signals. Which in this case means the type or way that the motion is performed such as a similar arm extension or finger movement induces similar features within its recorded data. This can especially be observed in the confusion matrices that are provided for the resulting classification of each of the models. The misclassification rate for certain motions as a specific other motion is recurrently similar for the same motions. Indeed, the most striking example is motion type eight being classified as motion type three. When comparing the actual motion that is being performed, the similarity between the motions is striking and supports the conception that similar motions induce similar signals with similar features.

This resulting observation appears especially encouraging for the further expansion of the technology. In fact, if being able to classify eight different pre-defined motions based on wrist EMG and IMU recordings is a great first step, an ideal control approach would be to expand this classification to a total recognition of any performed hand motion based on those similar signals. The observation that similar motions induce similar signals with similar features suggests that one possible way to widen the scope of motion recognition may be through a tree-based approach. This approach could then in a first step recognise the characteristic attributes of a general type of motion such as an arm extension or wrist

flexion and go into more detail by analysing further details of the signal and its features. Such an approach would require a wider dataset and additional data recording but would in turn allow a better understanding of the relationship between the wrist-recorded EMG and IMU signals and the performed hand motion. For such an approach, straightforward basic classification would not be sufficient as the idea would not be to simply reassess predefined motions to a dataset but to predict the motion of the hand in general. For which the implementation of a neural network seems best suited.

A further element that can be mentioned is that the number of channels used for this research is limited to availability and functionality. This is the reason that only two EMG signals could be used in the wrist area, and only the three-dimensional accelerometer of the IMU sensor could be used properly. Nonetheless, it can be expected that adding more channels based on more sensors could allow to eventually cover more subtle details of the hand motions, hence making the classification even more accurate.

## 6.3 Usability within the industry

The results of this research allow to conclude that predefined hand motions can be identified with great accuracy based on EMG and IMU recording based solely on wrist measurements. The results even allow to conclude that further research and analysis would in turn allow the development and implementation of a control method which could, based on these forearm measurements, obtain detailed information on the entire and detailed motion performed by the hand of the subject.

This conclusion can now be used to suggest an implementation which would fit the current needs of the control industry. It is shown that the current remote control methods based on hand motions are all drastically limited by either the need for an external

device, such as a remote controller, or by the need for a consistent and constant camera recording to allow visual motion recognition which in turn is a clear limiting factor to the possibilities and implementations of the technology. On the opposite, adapting the newly introduced approach of utilising a combination of EMG and IMU recordings from the forearm area would allow suppression of the need to hold a remote controller, as the hands of the subject would remain completely free. This approach does further not rely on the need for visual confirmation or recording, hence no need to be in visual connection to a camera as is required for the current motion recognition.

If the positive aspects of the suggestion based on the learnings from the research are clear, the way that such an innovation could be implemented is still open. A possible product suggestion that can be made is to implement the required EMG and IMU sensing on the wrist area in the form of a new product which could be designed similarly to some kind of wristband. This suggestion has the benefit that the product can then be designed in an optimal way to maximise the signal obtention and comfort of the subject. The wristband could easily implement surface EMG electrodes, which in contact with the skin, would in turn be able to record the muscular electrical activity in the wrist area. With the further implementation of an IMU sensor, the full possibilities of the conclusion of this research can be obtained. Hence, the suggested product would be a wristband which combines EMG and IMU sensors in the same way as performed during the scope of the study.

Another possibility to implement this technology would be to include it within an object that most people are already rather familiar with wearing around the wrist such as a watch or smartwatch. Most smartwatches already include a PPG sensor (photoplethysmogram) which allows the measurement of the heartbeat using a non-invasive approach. Hence, the use of biosignals-measuring devices within smartwatches is not a new idea and

has proven to be effective and accepted within society.

Whether as an independent device or as an extension of smartwatches, the implementation of this new approach to controlling systems could allow a range of breakthroughs and innovations in control methods within the industrial world and society in general. In fact, several examples from basic gesture-based interactions to more complex virtual reality approaches can be suggested, and the range of implementations quickly appears endless.

Gesture-based implementation could be widely changed. In fact, in everyday life, this could translate through controlling the lighting of the house, or the thermostats via simple hand motions. For the automotive industry, an implementation of such technology could for example be used to reduce volume or answer calls with simple finger motions which would allow the driver to keep the hand on the steering wheel. If those could also be done via speech recognition, hand motion recognition has the benefit of being more reliable in loud environments and does not require the driver to redirect some of its focus, as a simple finger shake could be sufficient to answer a call, when full sentences are currently required for it.

In the industrial world, the implementation of gesture-based controlling could allow workers to steer machinery from a distance with high precision. This would make it possible to control systems without any physical contact, and in theory, from any distance. This could in turn allow for a drastic increase the security as well for the workers and for the company as the risk of incident suddenly decreases while the precision of the work becomes greater.

Such an implementation can also be visualised in the medical world where the need for

precision is rising. Further, the pandemic showed how dangerous contamination can be, and implementing remote control based on the non-invasive and non-hindering approach of motion recognition based on biosignals analysis would allow medical workers to perform many tasks from a distance. This would significantly reduce the risk of contamination for patients as well as for the doctors and nurses themselves.

Applications related to virtual reality (VR) are also thinkable. In fact, no more external controllers would be required and the simple implementation of the technology based on the hand/arm motions could allow many new implementations. Virtual creation would become much more versatile and accessible. For example, architects could easily immerse themselves within their creations and move objects, walls or furniture and reach more complex designs while directly having the impression of seeing those become reality in front of them. Another idea could have been virtual sculpting, where art students could then easily train their techniques in a virtual world while using their hands, and hence being in conditions as close as possible to reality. Such virtual training could also be implemented in medical schools where students could train complex operations while using their hands in the most natural way possible, while their motions would be recorded using this non-hindering approach. All these suggestions show how well this technology would adapt to the current needs of virtual reality.

Further examples such as extended control within the gaming industry or more basic implementations such as controlling a presentation during a conference are also possible. There is in fact close to no limitation to the possibilities of this technology. Hence, to conclude, it appears that the method of controlling a system based on forearm EMG and IMU sensing is very promising and would allow a great range of breakthroughs within a great diversity of applications.

## 6.4 Suggestion of further studies

A great range of future research based on the findings and limitations of this study appears to be possible. Indeed, the first suggestion that can be made is simply the extension of the results obtained within the scope of this research. Time and capacity limitations restricted the scope of the research. However, future studies could build on the presented findings to improve the obtained results by capturing additional data, and running more feature-based tests. Further possibilities in that sense would also include trying out different electrode placements in the wrist area or running tests for more than two electrodes.

A further suggestion would be to attempt predicting a wider range of types of motion and ideally train a neural network which could even be capable of predicting a motion on which it has not explicitly trained. To generate such a neural network, it would be necessary to divide each hand motion into a range of details, such as which finger is extended and which is retracted for which motion, the status of the arm, or the whole rotation of the hand. By cutting each motion into its components, it would in turn allow the neural network to create connections between the evolution of specific features of certain channels and the specific status of each finger or the angle of the arm, etc. Making each motion more detailed would then in turn allow the neural network to predict the specific motion that is performed by the subject, even if this motion has never been provided within the training dataset. This would then allow the creation of a virtual image of the hand and would provide total liberty for any kind of implementation. Indeed, if any motion, even those that have not been provided to the artificial intelligence can be used to control a system, then the scope of possible implementation is endless.

Another possible research area would be within the implementation of this technology as a control for a system. Suggestions for this could be to first try sending pre-recorded signals to a classifier which predicts the original motion and to each of those. Each mo-

tion would then have a task to which it would be connected, for example, if motion one is detected then a robotic arm is lifted and so on. From a basic control, further expansion could then be made until a more complex system could fully be controlled based on this technology.

Lastly, when further tests have been run, a suggestion would be to actually transform and implement the technology within the armband device that has been suggested previously. Many options for this are open, a possible way to do this would be to have a flexible semi-elastic bracelet which would ensure that the EMG contact electrodes are on the skin of the subject at all times. With the additional implementation of an IMU, the device could then be programmed using the trained algorithms and hence be connected to the system to be controlled and used as an actual control method. Yet, many steps remain open to reach this final objective, which is why further research on the subject appears to be challenging yet captivating. The potential final goal could fundamentally change the way people interact with their surroundings.

# 7 Conclusion

Innovations in means of control have always been the first step towards major breakthroughs. Whether the introduction of the keyboard, touch-sensitive screens or wireless technologies, each advancement has been a step towards a more subtle control of systems which would become always less hindering or constraining means of process regulation. In that sense, recent inventions have led towards the idea of using the hand as the main means of control, recognising the performed motion and allowing people to steer systems by simply moving their hand. However, the currently implemented technologies all included some down points. Whether the requirement of an external camera of visual motion recognition approaches, the need to carry a remote controller or the requirement to cover the hand in an assortment of sensors, no solution is currently able to provide a total non-hindering and versatile approach to control systems using hand motion.

Past research has shown that there is a consequential link that can be made between the hand and arm motion performed by a subject and the muscular electrical activity emitted by the muscles (Jarque-Bou, Sancho-Bru, and Vergara, 2021). The recorded signal of this muscular activity is known as electromyograph (EMG). Henceforth, the idea that is suggested in this thesis research is to take EMG measurings in the forearm area of various subjects while they are performing predefined hand motions, and use machine learning algorithms to, based on those recordings, predict which motion has been performed by the subject. It is further suggested to expand the EMG recordings with an accelerometer sensor (IMU) which allows recording of the movement of the wrist. By further limiting the position of the recording electrodes and sensors to the sole wrist area, the following conclusions allow a reflection on the implementability of this technology as an innovative control method which could be non-hindering as limited to the wrist area.

Therefore, this research consists of several steps to reach consequential conclusions.

Firstly, eight distinct motions are defined. Then, for each subject, the Shimmer3 IMU and Shimmer3 EMG sensors are used to record the resulting biosignals from the wrist and forearm areas. A total of ten recordings are performed for each single motion for each subject and on each side. In total, 640 single motions are recorded.

Following the motion recording, the datasets are segmented, normalised, and filtered. The main filters that are used are a bandpass filter with cutoffs at 20Hz and 250Hz, and a Notch filter at 50Hz. The next step is the establishment of a complete model. The concept of 'model' that is introduced in this research consists of a specific combination of used input signals, preprocessing methods and used features. Each model is a unique mixture which results in different results. The use of different and well-defined models allows versatile testing and facilitates the analysis, making the impact of changes clear.

Each model is then used as an input to the classification processes. A classifier consists of an algorithm of machine learning which receives a dataset composed of a wide number of data elements, the features extracted from the signals by the model, each representing a motion. The first dataset that is received by the classifier, known as the training dataset, contains the number of motions linked to the features. This allows the classifier to learn and recognise patterns within the data. The second dataset that is then given to the classifier, the testing dataset, consists of data that has not yet been provided to the classifier. The type of motion is now hidden from the classifier which, based on its learning and the features makes predictions on the type of motion it believes induced the new data. The results of this classification allow observing how well the machine learning recognised patterns within the dataset. From these results, the main indication is the accuracy which transcripts the proportion of motions that have been classified correctly.

In total, seven machine learning approaches are used for each model. The k-Nearest-

Neighbours (kNN), the Gaussian Naïve Bayes (GNB), two multidimensional regression methods: the One-Versus-Rest (OVR) and One-Versus-One (OVO), the Random Forest method (RF), and lastly Neural Networks with one hidden layer (NN-1) and with two hidden layers (NN-2).

Based on these classifiers, several models are developed with the idea of studying various possibilities and with the goal of suggesting an optimised version which could in turn be used in future studies. The main findings of these tests are firstly the observation that the use of features from the frequency domain does increase the resulting accuracy of the classification. This observation occurs as a slight contradiction to past studies that claimed that no major improvement in accuracy can be reached when further considering the frequency domain in EMG motion recognition (Simao et al., 2019 & Samuel et al., 2019). An element that can be considered in this case is also the fact that IMU signals are also used which may have an impact on this observation.

The second main observation that is made is that, overall, the classifications deliver great accuracies of motion recognition. This signifies that there is a great possibility to analyse hand motion and obtain information on the performed movement of a subject by recording forearm EMG and IMU signals.

A third observation that is made is that the sole consideration of signals recorded in the wrist area, hence dropping any signal recorded in other areas such as the forearm, has a slight negative impact on the resulting accuracy. However, it still results in satisfying levels of classification. This results in an encouraging conclusion that the implementation of a technology of motion recognition based only on the wrist area is possible and thinkable.

Lastly, the final main observation that has been made is that motions that contain similar patterns tend to have a greater misclassification rate than motions that are considerably more different and unique. And this misclassification rate is even relatively high in certain cases. This observation allows the conclusion that certain specific motions within the hand induce similar signals which in turn leads to the suggestion that hand motions could be divided into all of their attributes, such as the movement of single fingers. This would allow the obtention of detailed information on the motion of the hand, and it is even suggested that a motion from which the artificial intelligence has not been learning could even be identified using this attribute division approach.

To conclude, this research conducts an experimental approach towards an innovative framework based on wrist EMG and IMU motion recognition. The obtained results are very promising and encouraging and translate into a real opportunity that can be exploited in further research and eventually have a considerable impact on the control methods used within the industrial world and society in general.

# Bibliography

adafruit (2023a). *Adafruit Micro Lipo - USB LiIon/LiPoly charger - v2*. URL: https://www.adafruit.com/product/1304 (visited on 05/09/2023).

— (2023b). *Lithium Ion Polymer Battery - 3.7v 500mAh*. URL: https://www.adafruit.com/product/1578 (visited on 05/09/2023).

Afsharipour, Babak et al. (2016). "Spatial distribution of surface EMG on trapezius and lumbar muscles of violin and cello players in single note playing". In: *Journal of Electromyography and Kinesiology* 31, pp. 144–153.

Andren, Peter (2006). "Power spectral density approximations of longitudinal road profiles". In: *International Journal of Vehicle Design* 40.1-3, pp. 2–14.

Bangaru, Srikanth Sagar, Chao Wang, and Fereydoun Aghazadeh (2022). "Automated and Continuous Fatigue Monitoring in Construction Workers Using Forearm EMG and IMU Wearable Sensors and Recurrent Neural Network". In: *Sensors* 22.24, p. 9729.

Botter, Alberto and Taian M Vieira (2015). "Filtered virtual reference: A new method for the reduction of power line interference with minimal distortion of monopolar surface EMG". In: *IEEE Transactions on Biomedical Engineering* 62.11, pp. 2638–2647.

Bremer, Anne K et al. (2006). "Moment arms of forearm rotators". In: *Clinical Biomechanics* 21.7, pp. 683–691.

Bretherton, Christopher S. (2014). *Lecture 15: Spectral Filtering*. URL: https://atmos.washington.edu/~breth/classes/AM582/lect/lect12-notes.pdf (visited on 10/22/2023).

Brownlee, Jason (2021). *One-vs-Rest and One-vs-One for Multi-Class Classification*. URL: https://machinelearningmastery.com/one-vs-rest-and-one-vs-one-for-multi-class-classification/ (visited on 12/20/2023).

Calabrese, Barbara (2019). "Data Reduction". In: *Encyclopedia of Bioinformatics and Computational Biology*. Ed. by Shoba Ranganathan et al. Oxford: Academic Press, pp. 480–485. ISBN: 978-0-12-811432-2. DOI: https://doi.org/10.1016/B978-0-12-

809633-8.20460-3. URL: https://www.sciencedirect.com/science/article/pii/B9780128096338204603.

Chan, Bunseng et al. (2021). "A review of surface EMG in clinical rehabilitation care systems design". In: *2021 IEEE 19th Student Conference on Research and Development (SCOReD)*. IEEE, pp. 371–376.

Constant, Nicholas et al. (2021). "Data analytics for wearable IoT-based telemedicine". In: *Wearable sensors*. Elsevier, pp. 357–378.

Davis, P.D., G.D. Parbrook, and G.N.C. Kenny (1995). "CHAPTER 15 - Biological Electrical Potentials: Their Display and Recording". In: *Basic Physics and Measurement in Anaesthesia (Fourth Edition)*. Ed. by P.D. Davis, G.D. Parbrook, and G.N.C. Kenny. Fourth Edition. Butterworth-Heinemann, pp. 189–207. ISBN: 978-0-7506-1713-0. DOI: https://doi.org/10.1016/B978-0-7506-1713-0.50020-2. URL: https://www.sciencedirect.com/science/article/pii/B9780750617130500202.

Dicker, Lee H (2014). "Variance estimation in high-dimensional linear models". In: *Biometrika* 101.2, pp. 269–284.

DigiKey (2023a). *Gravitiy analog EMG sensor*. URL: https://www.digikey.fi/fi/products/detail/dfrobot/SEN0240/8019061 (visited on 05/09/2023).

— (2023b). *Grove EMG detector*. URL: https://www.digikey.fi/en/products/detail/seeed-technology-co-ltd/101020058/5482548 (visited on 05/09/2023).

dji (2024). *SPARK series*. URL: https://www.dji.com/fi/products/spark (visited on 02/26/2024).

Edmunds, Michael (2024). *Antikythera mechanism*. URL: https://www.britannica.com/topic/Antikythera-mechanism (visited on 02/18/2024).

Englehart, Kevin and Bernard Hudgins (2003). "A robust, real-time control scheme for multifunction myoelectric control". In: *IEEE transactions on biomedical engineering* 50.7, pp. 848–854.

*Ethical review in medical research* (2023). URL: https://www.utu.fi/en/research/ethics/medical-research-assessment (visited on 10/16/2023).

Felici, Francesco and Alessandro Del Vecchio (2020). "Surface electromyography: what limits its use in exercise and sport physiology?" In: *Frontiers in neurology* 11, p. 578504.

Freund, Rudolf J, William J Wilson, and Ping Sa (2006). *Regression analysis*. Elsevier.

fruugo (2023). *Muscle Signal Sensor EMG Sensor Controller*. URL: https://www.fruugo.fi/muscle-signal-sensor-emg-sensor-controller-detects-muscle-activity-%20for-development-board-for-wearab/p-136726244-288506391?language=en (visited on 05/09/2023).

Giannini, Paolo et al. (2020). "Wearable sensor network for biomechanical overload assessment in manual material handling". In: *Sensors* 20.14, p. 3877.

González-Mendoza, Arturo et al. (2018). "Validation of an EMG Sensor for Internet of Things and Robotics". In: *15th International Conference on Electrical Engineering, Computing Science and Automatic Control (CCE)*. IEEE, pp. 1–5.

Grover, Abhishek and Brejesh Lall (2020). "A novel method for removing baseline drifts in multivariate chemical sensor". In: *IEEE Transactions on Instrumentation and Measurement* 69.9, pp. 7306–7316.

Hasegawa-Johnson, Mark (2021). *Lecture 6: Sampling and Aliasing, ECE 401: Signal and Image Analysis*. URL: https://courses.engr.illinois.edu/ece401/fa2021/lectures/lec06.pdf (visited on 10/21/2023).

Hellmers, Hendrik et al. (2013). "An IMU/magnetometer-based indoor positioning system using Kalman filtering". In: *International Conference on Indoor Positioning and Indoor Navigation*. IEEE, pp. 1–9.

Heydarian, Mohammadreza, Thomas E Doyle, and Reza Samavi (2022). "MLCM: Multi-label confusion matrix". In: *IEEE Access* 10, pp. 19083–19095.

Jamal, Muhammad Zahak (2012). "Signal acquisition using surface EMG and circuit design considerations for robotic prosthesis". In: *Computational Intelligence in Elec-*

*tromyography Analysis-A Perspective on Current Applications and Future Challenges* 18, pp. 427–448.

Jarque-Bou, Néstor J, Joaquin L Sancho-Bru, and Margarita Vergara (2021). "A systematic review of emg applications for the characterization of forearm and hand muscle activity during activities of daily living: results, challenges, and open issues". In: *Sensors* 21.9, p. 3035.

Jaskot, Krzysztof and Artur Babiarz (2010). "The inertial measurement unit for detection of position". In: *Przeglad Elektrotechniczny* 86.11A, pp. 323–333.

Kim, Jonghwa, Stephan Mastnik, and Elisabeth André (2008). "EMG-based hand gesture recognition for realtime biosignal interfacing". In: *Proceedings of the 13th international conference on Intelligent user interfaces*, pp. 30–39.

Lee, Helen A. (2023). *This is why Microsoft Kinect was a complete failure*. URL: `https://www.svg.com/301470/this-is-why-microsoft-kinect-was-a-complete-failure/` (visited on 12/16/2023).

Li, Xiangxin et al. (2017). "Increasing the robustness against force variation in EMG motion classification by common spatial patterns". In: *2017 39th Annual International Conference of the IEEE Engineering in Medicine and Biology Society (EMBC)*. IEEE, pp. 406–409.

Liu, Wenzhao and Frede Blaabjerg (2021). "Phase-locked loops and their design". In: *Control of Power Electronic Converters and Systems*. Elsevier, pp. 269–301.

Malwade, Chandrakant R et al. (2013). "Chemometrics for analytical data mining in separation process design for recovery of artemisinin from Artemisia annua". In: *Computer Aided Chemical Engineering*. Vol. 32. Elsevier, pp. 49–54.

Maral, G (2003). *VSAT Networks, John Wiley & Sons*.

"Medical Research Act" (n.d.). In: *Ministry of Social Affairs and Health, Finland* (). URL: `https://finlex.fi/en/laki/kaannokset/1999/en19990488.pdf`.

Mendez, Irene et al. (2017). "Evaluation of the Myo armband for the classification of hand motions". In: *International Conference on Rehabilitation Robotics (ICORR)*. IEEE, pp. 1211–1214.

Mewett, David T, Homer Nazeran, and Karen J Reynolds (2001). "Removing power line noise from recorded EMG". In: *2001 conference proceedings of the 23rd annual international conference of the IEEE Engineering in Medicine and Biology Society*. Vol. 3. IEEE, pp. 2190–2193.

Mohajon, Joydwip (2020). *Confusion Matrix for Your Multi-Class Machine Learning Model*. URL: `https://towardsdatascience.com/confusion-matrix-for-your-multi-class-machine-learning-model-ff9aa3bf7826` (visited on 01/05/2024).

Morrow, Melissa MB et al. (2017). "Validation of inertial measurement units for upper body kinematics". In: *Journal of applied biomechanics* 33.3, pp. 227–232.

Nadipally, Manasa (2019). "Optimization of methods for image-texture segmentation using ant colony optimization". In: *Intelligent data analysis for biomedical applications*. Elsevier, pp. 21–47.

Navathale, Trupti J, Anand A Paralkar, and Vijaykumar S Ghorade (2017). "Design and analysis of centrifugal governor: a review". In: *International Research Journal of Engineering and Technology (IRJET)* 4.1, pp. 1058–1062.

Neal, Brady et al. (2018). "A modern take on the bias-variance tradeoff in neural networks". In: *arXiv preprint arXiv:1810.08591*.

Niegowski, Maciej et al. (2015). "Unsupervised learning technique for surface electromyogram denoising from power line interference and baseline wander". In: *2015 37th Annual International Conference of the IEEE Engineering in Medicine and Biology Society (EMBC)*. IEEE, pp. 7274–7277.

OPEN-BCI (2023a). *All-in-one emotibit bundle*. URL: `https://shop.openbci.com/products/all-in-one-emotibit-bundle` (visited on 05/09/2023).

OPEN-BCI (2023b). *Low-cost biosensing starter bundle*. URL: https://shop.openbci.com/products/low-cost-biosensing-starter-bundle?_pos=1&_sid=6095768e6&_ss=r (visited on 10/01/2023).

Oudah, Munir, Ali Al-Naji, and Javaan Chahl (2020). "Hand gesture recognition based on computer vision: a review of techniques". In: *journal of Imaging* 6.8, p. 73.

pandas (2024). *Pandas DataFrame corr() Method*. URL: https://pandas.pydata.org/docs/reference/api/pandas.DataFrame.corr.html (visited on 02/01/2024).

Parajuli, Nawadita et al. (2019). "Real-time EMG based pattern recognition control for hand prostheses: A review on existing methods, challenges and future implementation". In: *Sensors* 19.20, p. 4596.

Parmar, Aakash, Rakesh Katariya, and Vatsal Patel (2019). "A review on random forest: An ensemble classifier". In: *International conference on intelligent data communication technologies and internet of things (ICICI) 2018*. Springer, pp. 758–763.

Pedregosa, F. et al. (2011). "Scikit-learn: Machine Learning in Python". In: *Journal of Machine Learning Research* 12, pp. 2825–2830.

Peterson, Leif E (2009). "K-nearest neighbor". In: *Scholarpedia* 4.2, p. 1883.

Phinyomark, Angkoon et al. (2014). "Feature extraction of the first difference of EMG time series for EMG pattern recognition". In: *Computer methods and programs in biomedicine* 117.2, pp. 247–256.

Pradhan, Ashirbad, Jiayuan He, and Ning Jiang (2022). "Multi-day dataset of forearm and wrist electromyogram for hand gesture recognition and biometrics". In: *Scientific Data* 9.1, p. 733.

Rangayyan, Rangaraj M (2015). *Biomedical signal analysis*. John Wiley & Sons.

Reddy, Eguturi Manjith Kumar et al. (2022). "Introduction to Naive Bayes and a Review on Its Subtypes with Applications". In: *Bayesian Reason. Gaussian Process. Mach. Learn. Appl*, pp. 1–14.

samsung (2022). *Control your Samsung TV with Gesture Interaction*. URL: https://www.samsung.com/ph/support/tv-audio-video/control-your-samsung-tv-with-gesture-interaction/ (visited on 02/26/2024).

Samuel, Oluwarotimi Williams et al. (2019). "Intelligent EMG pattern recognition control method for upper-limb multifunctional prostheses: advances, current challenges, and future prospects". In: *Ieee Access* 7, pp. 10150–10165.

Scikit-Learn (2024a). *sklearn.ensemble.RandomForestClassifier*. URL: https://scikit-learn.org/stable/modules/generated/sklearn.ensemble.RandomForestClassifier.html (visited on 01/12/2024).

— (2024b). *sklearn.linear$_m$odel.LogisticRegression*. URL: https://scikit-learn.org/stable/modules/generated/sklearn.linear_model.LogisticRegression.html (visited on 01/11/2024).

— (2024c). *sklearn.multiclass.OneVsOneClassifier*. URL: https://scikit-learn.org/stable/modules/generated/sklearn.multiclass.OneVsOneClassifier.html (visited on 01/11/2024).

— (2024d). *sklearn.multiclass.OneVsRestClassifier*. URL: https://scikit-learn.org/stable/modules/generated/sklearn.multiclass.OneVsRestClassifier.html (visited on 01/11/2024).

— (2023). *sklearn.neighbors.KNeighborsClassifier*. URL: https://scikit-learn.org/stable/modules/generated/sklearn.neighbors.KNeighborsClassifier.html (visited on 12/18/2023).

Scikit-learn (2023). *sklearn.naive$_b$ayes.GaussianNB*. URL: https://scikit-learn.org/stable/modules/generated/sklearn.naive_bayes.GaussianNB.html (visited on 12/19/2023).

Scipy (2024a). *scipy.signal.iirnotch*. URL: https://docs.scipy.org/doc/scipy/reference/generated/scipy.signal.iirnotch.html (visited on 01/11/2024).

Scipy (2024b). *scipy.signal.butter*. URL: https://docs.scipy.org/doc/scipy/reference/generated/scipy.signal.butter.html (visited on 01/08/2024).

Sell, John and Patrick O'Connor (2014). "The xbox one system on a chip and kinect sensor". In: *IEEE Micro* 34.2, pp. 44–53.

Shimmer (2023a). *Consensys EMG Development Kits*. URL: https://shimmersensing.com/product/consensys-emg-development-kits/ (visited on 09/01/2023).

— (2023b). *EMG User Guide Revision 1.12*. URL: https://shimmersensing.com/wp-content/docs/support/documentation/EMG_User_Guide_Rev1.12.pdf (visited on 10/31/2023).

— (2023c). *EMG/ECG Electrodes*. URL: https://shimmersensing.com/product/emg-ecg-electrodes/ (visited on 05/09/2023).

— (2023d). *IMU User Guide Revision 1.4*. URL: https://shimmersensing.com/wp-content/docs/support/documentation/IMU_User_Guide_rev1.4.pdf (visited on 10/30/2023).

— (2023e). *Shimmer Dock*. URL: https://shimmersensing.com/product/shimmer-dock/ (visited on 05/09/2023).

— (2023f). *Shimmer3 EMG Unit*. URL: https://shimmersensing.com/product/shimmer3-emg-unit/ (visited on 05/09/2023).

— (2023g). *Shimmer3 IMU Unit*. URL: https://shimmersensing.com/product/shimmer3-imu-unit/ (visited on 09/09/2023).

Shoemaker, Nate (2016). *SKELETAL MUSCLE: WHOLE MUSCLE PHYSIOLOGY*. URL: https://content.byui.edu/file/a236934c-3c60-4fe9-90aa-d343b3e3a640/1/module7/readings/muscle_twitches.html (visited on 02/19/2024).

Simao, Miguel et al. (2019). "A review on electromyography decoding and pattern recognition for human-machine interaction". In: *Ieee Access* 7, pp. 39564–39582.

Smith, Lauren H et al. (2010). "Determining the optimal window length for pattern recognition-based myoelectric control: balancing the competing effects of classification

error and controller delay". In: *IEEE transactions on neural systems and rehabilitation engineering* 19.2, pp. 186–192.

Sörnmo, Leif and Pablo Laguna (2005). "Chapter 4 - Evoked Potentials". In: *Bioelectrical Signal Processing in Cardiac and Neurological Applications*. Ed. by Leif Sörnmo and Pablo Laguna. Biomedical Engineering. Burlington: Academic Press, pp. 181–336. ISBN: 978-0-12-437552-9. DOI: https://doi.org/10.1016/B978-012437552-9/50004-0. URL: https://www.sciencedirect.com/science/article/pii/B9780124375529500040.

Steinbach, Michael and Pang-Ning Tan (2009). "kNN: k-nearest neighbors". In: *The top ten algorithms in data mining*, pp. 151–162.

Subramanian, Jyothi and Richard Simon (2013). "Overfitting in prediction models–is it a problem only in high dimensions?" In: *Contemporary clinical trials* 36.2, pp. 636–641.

Tan, Zhichao et al. (2020). "Incremental delta-sigma ADCs: A tutorial review". In: *IEEE Transactions on Circuits and Systems I: Regular Papers* 67.12, pp. 4161–4173.

Taranovich, Steve (2021). *Understanding EMI Filters: The Bare Essentials*. URL: https://www.electronicdesign.com/technologies/power/whitepaper/21168064/electronic-design-understanding-emi-filters-the-bare-essentials (visited on 11/05/2023).

Tekin, Bugra, Federica Bogo, and Marc Pollefeys (2019). "H+ o: Unified egocentric recognition of 3d hand-object poses and interactions". In: *Proceedings of the IEEE/CVF conference on computer vision and pattern recognition*, pp. 4511–4520.

Tkach, Dennis, He Huang, and Todd A Kuiken (2010). "Study of stability of time-domain features for electromyographic pattern recognition". In: *Journal of neuroengineering and rehabilitation* 7.1, pp. 1–13.

Torres-Garcıa, Alejandro A et al. (2022). "Pre-processing and feature extraction". In: *Biosignal processing and classification using computational learning and intelligence*. Elsevier, pp. 59–91.

Vignais, Nicolas et al. (2013). “Dynamic assessment of finger joint loads using kinetic and kinematic measurements”. In: *Digital Human Modeling Symposium*.

Vogiatzis, Antonios et al. (2021). “A Novel One-vs-Rest Classification Framework for Mutually Supported Decisions by Independent Parallel Classifiers”. In: *2021 IEEE International Conference on Imaging Systems and Techniques (IST)*. IEEE, pp. 1–6.

Wang, Robert Y and Jovan Popović (2009). “Real-time hand-tracking with a color glove”. In: *ACM transactions on graphics (TOG)* 28.3, pp. 1–8.

Waris, Asim and Ernest Nlandu Kamavuako (2018). “Effect of threshold values on the combination of EMG time domain features: Surface versus intramuscular EMG”. In: *Biomedical Signal Processing and Control* 45, pp. 267–273.

Wendong and Changjun Wang (2021). “Design and Realization of 3D Movie Animation Production Management System Based on Motion Capture Technology”. In: *2021 International Conference on Aviation Safety and Information Technology*, pp. 631–635.

Wu, Yu-chen and Jun-wen Feng (2018). “Development and application of artificial neural network”. In: *Wireless Personal Communications* 102, pp. 1645–1656.

Wu, Wei et al. (2014). “Probabilistic common spatial patterns for multichannel EEG analysis”. In: *IEEE transactions on pattern analysis and machine intelligence* 37.3, pp. 639–653.

Xi, Xugang et al. (2017). “Evaluation of feature extraction and recognition for activity monitoring and fall detection based on wearable sEMG sensors”. In: *Sensors* 17.6, p. 1229.

Yuan, Tongtong et al. (2019). “Signal-to-noise ratio: A robust distance metric for deep metric learning”. In: *Proceedings of the IEEE/CVF conference on computer vision and pattern recognition*, pp. 4815–4824.

Zhao, Jingdong (2018). “A review of wearable IMU (inertial-measurement-unit)-based pose estimation and drift reduction technologies”. In: *Journal of Physics: Conference Series*. Vol. 1087. IOP Publishing, p. 042003.

# Appendix

## Pictures

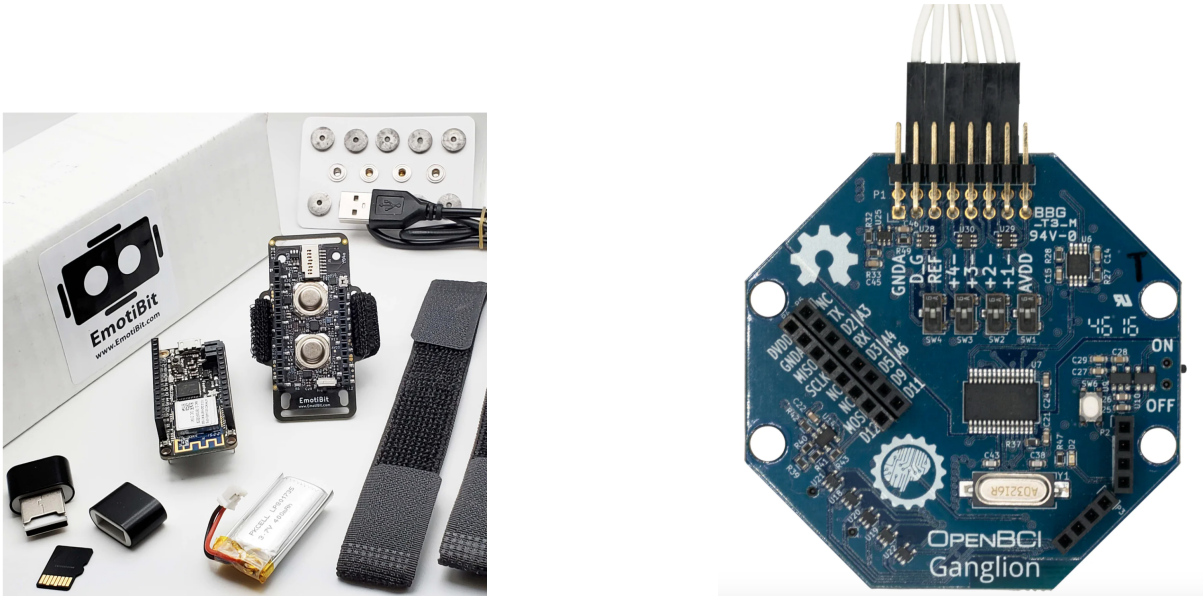


(a) (b)

(c) (d)

Figure A.1: (a) “All-in-one emotibit bundle”, (b) “Low-cost biosensing starter bundle”, (c) “Lithium Ion Rechargeable Battery (500mAh)”, (d) “USB LiIon/LiPoly charger”


(a) (b) (c)

Figure A.2: (a) “Grove EMG detector”, (b) “Gravitiy analog EMG sensor”, (c) “Muscle Signal Sensor EMG Sensor Controller”